Universidade do Minho

Escola de Ciências da Saúde

Bárbara Filipa Mendes Pinheiro

MESENCHYMAL STEM CELLS SECRETOME IN PARKINSON'S DISEASE REGENERATIVE MEDICINE

Dissertação de Mestrado

Mestrado em Ciências da Saúde

Trabalho efetuado sob a orientação do:

Doutor António José Braga Osório Gomes Salgado

e co-orientação do:

Doutor Fábio Gabriel Rodrigues Teixeira

Junho de 2016

DECLARAÇÃO

Nome: Bárbara Filipa Mendes Pinheiro

Endereço electrónico: barbaramp@ecsaude.uminho.pt

Telefone: 917663429

Número do Cartão de Cidadão: 14144198

Título da dissertação:

Mesenchymal stem cells secretome in Parkinson's disease regenerative medicine

Orientador:

Doutor António José Braga Osório Gomes Salgado

Co-Orientador:

Doutor Fábio Gabriel Rodrigues Teixeira

Ano de conclusão: 2016

Designação do Mestrado:

Ciências da Saúde

É AUTORIZADA A REPRODUÇÃO INTEGRAL DESTA DISSERTAÇÃO APENAS PARA EFEITOS DE INVESTIGAÇÃO, MEDIANTE DECLARAÇÃO ESCRITA DO INTERESSADO, QUE A TAL SE COMPROMETE.

Universidade do Minho, 8 de Junho de 2016

Assinatura:

Bárbara Pinheiro

Às pessoas mais importantes da minha vida: aos meus pais, ao Daniel e ao Eduardo

AGRADECIMENTOS

Estas limitadas páginas de agradecimentos, não me permitem agradecer, como devia, a todas as pessoas, que ao longo do meu Mestrado em Ciências da Saúde, direta ou indiretamente, me ajudaram a cumprir os meus objectivos e a realizar mais uma etapa da minha formação académica. Desta forma, deixo apenas algumas palavras, mas com um sincero e profundo sentimento de reconhecido agradecimento.

As minhas primeiras palavras de agradecimento vão para o meu orientador António Salgado. Agradeço o apoio, a partilha de saber, as oportunidades e as ferramentas necessárias para o desenvolvimento de todo o trabalho. Sem tudo isto, este trabalho não era possível. Um sentido obrigado por passares pelo laboratório todos os dias e perguntares: "Precisas de alguma coisa?"

Ao meu co-orientador Fábio Teixeira por acreditar em mim e por levar este projeto a bom rumo. Ensinaste-me quase tudo o que sei fazer, sempre com paciência e boa disposição. E não foi fácil, porque não há aluna mais stressada que eu, pois não? Obrigado pelas conversas, pelos conselhos, e por teres sempre um sorriso sincero para dar. Porque mais do que um orientador és uma pessoa com quem posso contar. O meu mais profundo obrigado, pois não tenho palavras para descrever tudo o que fizeste por mim. Esta tese devo-a em grande parte a ti.

Ao resto da equipa Tó Team, Sofia, Rita, Ana, Eduardo, Rui e Nuno, agradeço as sugestões, momentos de entreajuda e pelo bom ambiente de trabalho. Obrigado Eduardo por transmitires a calma que eu muitas vezes não tenho. Obrigado companheira de secretária, Sofia, pelas dicas práticas que em muitos momentos foram cruciais. Obrigado Ana por toda a ajuda, principalmente pela companhia nas horas intermináveis de comportamento no biotério.

Aos melhores colegas do mestrado do mundo, Ana, Leonor, Diana, Joana, Sara, Daniel e Margarida pelas partilhas e companheirismo nestes últimos dois anos. Quando decidi ingressar nesta instituição não achei que pudesse conhecer pessoas tão fantásticas como vós. Estão todos no meu coração. Um obrigado especial à Leonor pela amizade. Recebeste-me de braços abertos quando aqui cheguei, e isso eu nunca vou esquecer.

Expresso também a minha gratidão a todos os NERDs, principalmente às pessoas do I2.01, o melhor laboratório de Neurociências. Um obrigado especial à companheira da frente, Sónia Gomes, pela humanidade e sorriso doce.

À Carina, por ser ter disponibilizado para me ensinar e ajudar sempre que fosse preciso, no microscópio, que tanta dor de cabeça me deu.

Às "Pomposas" Rita Silva, Rita Santos, Joana e Patrícia. Obrigada pelos tantos almoços e lanches divertidos, cheios de boa disposição e gargalhadas. Gosto muito de todas vós.

À Cláudia, uma das melhores pessoas que tive oportunidade de conhecer. Obrigado pelas boleias, conversas, brincadeiras e jantares. Obrigado principalmente por me aturares todos os dias, tanto no trabalho como em casa sempre com boa disposição e cumplicidade.

À Ângela, a melhor colega de casa do mundo e a loira com mais estilo que eu conheço. Obrigado pela pessoa cheia de vida que és, e pelos serões cheios de confidências e partilhas.

Ao Pedro, Tiago, Marco, Dinis, Luís e Ângela, os meus amigos de sempre e para sempre. Obrigado por todos estes anos de amizade, pelos cafés ao sábado à noite, por partilharem comigo alegrias e inquietações. Obrigado por fazerem parte da minha vida, tenho a certeza que nunca mais irão sair dela.

À Joana, companheira de uma vida. Obrigado pelas conversas, desabafos e telefonemas e por estares presente em todos os momentos. Obrigado simplesmente por seres a melhor amiga do mundo.

À minha família, em especial aos meus Pais e ao meu irmão Daniel, um enorme obrigada por acreditarem sempre em mim e naquilo que faço. Obrigado por todo o carinho, apoio e dedicação que constantemente me oferecem. A vós devo tudo aquilo que sou hoje e a pessoa em que me tornei. Obrigado Dani, por me receberes sempre com um beijinho e um sorriso nos lábios e por dizeres: "Já tinha saudades tuas maninha". Amo-vos incondicionalmente, e dedico-vos todo este trabalho.

As minhas últimas palavras vão para o Eduardo. Obrigado por teres aparecido na minha vida e por me fazeres feliz todos os dias. Obrigada pela transmissão de confiança e de força em todos os momentos, e pelo encanto do teu sorriso que faz desaparecer todos as dúvidas. Obrigado pela paciência, pelo carinho e por todas as experiências que vivemos ao longo destes dois anos. Espero que o futuro nos sorria sempre, e que não saias nunca do meu lado.

ABSTRACT

Parkinson's disease (PD) represents the second most common neurodegenerative brain disorder, which is clinically characterized by the progressive degeneration of dopaminergic neurons (DAergic neurons), mainly in the nigrostriatal pathway, leading to the appearance of characteristic motor and non-motor symptoms. Currently, pharmacological and surgical treatments are the most common approaches for the treatment of PD. However, so far, all of these treatments are focused on reducing the symptoms. In fact, they do not slow down or reverse the degenerative process, imposing the need for innovative therapeutical approaches. The use of adult stem cells cell-based strategy has emerged as a potential alternative therapy for PD, in which, among a number of promising stem cell sources, human mesenchymal stem cells (hMSCs) and neural progenitors cells (hNPCs) have stand out as a valid therapeutic option. Indeed, over the last years, a substantial effort has been performed in order to address the impact of hMSCs and hNPCs in central nervous system repair. Recently, and from an application point of view, several studies have claimed that the therapeutical effects of stem cells is mainly mediated by their trophic action namely, through their capacity of secreting a wide panel of neuroregulatory molecules (e.g. neurotrophic factors, cytokines, vesicles), which is defined as secretome. Thus, based in all these concepts, in this thesis we aimed to: 1) Characterize the secretome of hMSCs and hNPCs through proteomic-based approaches; 2) Determine the role of hMSCs and hNPCs secretome as a modulator of neuronal differentiation and 3) Investigate the effects of the hMSCs and hNPCs secretome in a rat model of PD, in comparison with cell transplantation. *In vitro,* experiments revealed that the secretome of hMSCs induced a more robust neuronal differentiation when compared to the one obtained from hNPCs. Additionally, it was also possible to observe that the injection of the secretome of both hMSCs and hNPCs in a 6-hydroxydopamine (6-OHDA)-rat model of PD potentiated the recovery of DAergic neurons (estimated by neuronal densities in substantia nigra and striatum) when compared to the untreated group 6-OHDA, and those transplanted with cells (hMSCs and hNPCs). Similar outcomes were observed in the motor performance of these animals as assessed by the rotarod and staircase tests. Finally, proteomic characterization of hMSCs and hNPCs secretome revealed that these cells were able to secrete important molecules with neuroregulatory actions such as, Galectin-1, 14-3-3 proteins, PEDF, DJ-1, whereby may support the effects observed both *in vitro* and *in vivo.* Overall, we concluded that the use of secretome *per se* was able to partially revert the motor phenotype and the neuronal structure of PD animals, indicating that the secretome of stem cells could represent a novel therapeutic tool for the treatment of PD.

RESUMO

A doença de Parkinson (DP) é clinicamente caracterizada pela degeneração progressiva dos neurónios dopaminérgicos (ND), principalmente na via nigroestriatal, levando ao aparecimento dos sintomas motores e não motores da doença. Atualmente, os tratamentos farmacológicos e cirúrgicos representam a abordagem mais comum no tratamento da DP. Contudo, estes estão apenas focados na redução sintomática da doença, não retardando ou revertendo o processo degenerativo, sendo assim necessária a criação de abordagens terapêuticas inovadoras. O uso de células estaminais adultas tem emergido como uma potencial terapia alternativa para a DP. Dentro destas, as células humanas estaminais mesenquimatosas (hMSCs) e as células progenitoras neurais (hNPCs) têm emergido como uma válida opção terapêutica. Do ponto de vista de aplicação destas duas populações de células estaminais na DP, diversos estudos demonstraram que o seu efeito terapêutico é essencialmente mediado pela sua ação trófica, isto é, através da sua capacidade de segregar um vasto painel de moléculas neuroreguladoras (p.ex. fatores neurotróficos, citoquinas e vesículas), definido como secretoma. Assim, a presente tese teve como principais objetivos: 1) Caraterizar o secretoma de hMSCs e hNPCs através de análises de proteómica; 2) Determinar o efeito do secretoma de hMSCs e hNPCs como um modulador da diferenciação neuronal e 3) Investigar os efeitos do secretoma de hMSCs e hNPCs num modelo de rato da DP (6-OHDA), em comparação com a transplantação de células. *In vitro*, verificou–se uma maior diferenciação neuronal promovida pelo secretoma de hMSCs quando comparado com o das hNPCs. *In vivo*, observou-se que a injeção do secretoma quer de hMSCs quer de hNPCs num modelo de DP em ratos (6-OHDA) potenciou a recuperação dos ND (avaliado por densidades neuronais na substância negra e estriado) quando comparado com o grupo não tratado, e com os grupos transplantados com células (hMSCs e hNPCs). Resultados semelhantes foram observados no desempenho motor destes animais, avaliado pelos testes rotarod e staircase. Por último, a caracterização proteómica do secretoma de hMSCs e hNPCs revelou que estas células são capazes de segregar moléculas com importantes ações neuroreguladoras tais como, Galactina-1, proteínas 14-3-3, PEDF, DJ-1, suportando desta forma os efeitos observados tanto *in vitro* como *in vivo*. Em suma, podemos concluir que a utilização de secretoma por si só foi capaz de reverter parcialmente o fenótipo motor e a estrutura neuronal de animais parkinsonianos, indicando que o secretoma das células estaminais pode representar uma nova abordagem terapêutica para o tratamento da DP.

TABLE OF CONTENTS

LIST OF ABBREVIATIONS

#

6-OHDA - 6-hydroxydopamine

A

ACN - Acetonitrile

ALS - Amyotrophic lateral sclerosis

ASCs - Adipose stem cells

B

BDNF - Brain-derived neurotrophic factor

bFGF - Basic fibroblast growth factor

BM-MSCs - Bone marrow mesenchymal stem
cells

BrdU - 5-bromo-2-deoxyuridine

C

CES - Collision energy spread

cm - centimeter

CM - Conditioned medium

CNS - Central nervous system

CO_2 - Carbone dioxide

Cys C - Cystatin C

D

DA - Dopamine

DAergic - Dopaminergic

DAB - 3,3-diaminobenzidine

DAPI - 4-6-diamidino-2-phenylindole-
dhydrochloride

DAT - Dopamine transporter

DBS - Deep brain stimulation

DCX - Doublecortin

DG - Dentate gyrus

DMEM - Dulbecco's Modified Eagle Medium

E

EGF - Epidermal growth factor

ESCs - Embryonic stem cells

EVs - Extracellular vesicles

F

FA - Formic acid

FBS - Fetal bovine serum

FDR - False discovery rate

G

g - g-force

GBA - Glucocerebrosidase

GDN - Glia derived nexin

GDNF - Glial cell-derived neurotrophic factor

GPi - Globus pallidus internus

H

h - hours

H_2O_2 - Hydrogen peroxidase

HCl - Hydrochloric acid

HD - Huntington's disease

HGF - Hepatocyte growth factor

HUCPVCs - Human umbilical cord perivascular
cells

xiii

I

IDA - Information-dependent acquisition

IGF-1 - Insulin-like growth factor 1

IL-10 - Interleukin 10

IL-6 - Interleukin 6

i.p. - Intraperitoneally

iPSCs - Induced pluripotent stem cells

ISCT - International Society for Cellular Therapy

IV - Intravenous

K

kDA - kilo Daltons

L

LBs - Lewy bodies

LC - Liquid chromatography

LNs - Lewy neurites

LRRK2 - Leucine-rich repeat kinase 2

M

m - meter

M - Molar

m/z - mass-to-charge ratio

MAO - Monoamine oxidase

MAO-B - Monoamine oxidase-B

MAP-2 - Microtubule associated protein-2

MFB - Medial forebrain bundle

mg - milligram

mg/kg - milligram per kilo

mg/ml - milligram per milliliter

MHC-II - Major histocompatibility complex class II

MIF - Macrophage migration inhibitor factor

min - minutes

miRNAs - micro RNAs

ml - milliliter

mm - millimeter

MPTP - 1-methyl-4-phenyl-1,2,3,6-tetrahydropyridine

MS - Mass spectrometry

ms - millisecond

MS/MS - Tandem mass spectrometry

MSCs - Mesenchymal stem cells

N

NaCl - Sodium chloride

NBCS – Newborn calf serum

NGF - Nerve growth factor

NMS - Nonmotor symptoms

NPCs - Neural progenitor cells

NSCs - Neural stem cells

O

O.D. - Optical density

P

PBS - Phosphate buffered saline

PBS-T - Phosphate buffered saline-Triton

PD - Parkinson's disease

PEDF - Pigment epithelium-derived factor

PFA - Paraformaldehyde

PINK1 - PTEN-induced putative kinase 1

ppm - parts per million

Prdx1 - Peroxiredoxin 1

R

ROS - Reactive oxygen species

rpm - Rotations per minute

RT - Room temperature

S

s - seconds

SCF - Stem cell factor

SDF-1 - Stromal cell-derived factor 1

SEM - Standard error of the mean

SEM7A - Semaphorin-7A

SEZ - Subependymal zone

SGZ - Subgranular zone

SNpc - Substantia nigra pars compacta

SODC - Superoxidase dismutase-cytoplasmatic

SODM - Superoxidase dismutase-mitochondrial

STN - Subthalamic nucleus

SVZ - Subventricular zone

SWATH - Sequential Windowed data independent Acquisition of the Total High-resolution Mass Spectra

T

TCA - Trichloroacetic acid

TGF-β -Transforming growth factor beta

TH - Tyrosine hydroxylase

Tris-HCl - Tris-hydrochloride

TrxR1- Thioredoxin reductase 1

U

UHCL1 - Ubiquitin carboxyl-terminal hydrolase L1

μl - microliter

μm - micrometer

μl/min - microliter per minute

UPDRS – Unified Parkinson's disease rating scale

UPS - Ubiquitin proteasome system

V

V - Volts

VEGF - Vascular endothelial growth factor

VTA - Ventral tegmental area

W

W - Watts

WJ-MSCS - Wharton jelly mesenchymal stem cells

LIST OF FIGURES

LIST OF TABLES

CHAPTER 1
INTRODUCTION

1. INTRODUCTION

1.1. Parkinson's Disease

Originally described by James Parkinson in 1817, Parkinson's disease (PD) represents the second worldwide most common neurodegenerative disorder (de Lau and Breteler, 2006). Although an exact evaluation of PD epidemiological values is missing, studies have suggested that the prevalence in industrialized countries is generally estimated at 0.3% of the entire population, in which about 1% in people over 60 and 4% over 80 years of age are the most affected, demonstrating to be an aging-related disease (de Lau and Breteler, 2006; Dexter and Jenner, 2013; Pringsheim et al., 2014). Nowadays, the mean onset of PD has been established between 50-60 years. However, it has also been suggested that 10% of cases could occur between 20 and 50 years of age, being in this case classified as an young onset, which may represent a distinct disease group (Anisimov, 2009; Dexter and Jenner, 2013).

Clinically, PD is mainly characterized as a disease that affects the motor system. The diagnosis currently available depends on the identification of cardinal features namely, bradykinesia (slowness in the execution of voluntary movements), muscular rigidity (stiffness), postural instability (a tendency to fall even in the absence of weakness or cerebellar balance disturbance) and tremor at rest, with an asymmetric onset, which becomes bilateral with time (Gibb and Lees, 1988; Lees et al., 2009). Other motor signs such as akinesia (absence of normal unconscious movements like arm swing in walking), hypomimia (reduction of normal facial expression), speech and swallowing difficulties, decrease in size (micrographia) and speed of handwriting, as well as reduction of stride length during walking, have also been used in PD diagnosis (Dauer and Przedborski, 2003; Jankovic, 2008). Pathologically, these motor deficits are the result of the progressive loss of dopaminergic neurons (DAergic neurons) in the nigrostriatal pathway, particularly in the substantia nigra pars compacta (SNpc), leading, as consequence, to the reduction of dopamine (DA) levels in the striatum (i.e. putamen and caudate nucleus) (Figure 1) (Langston, 2006; Lees et al., 2009). In addition to DA, it has also been suggested that the content of norepinephrine and serotonin is also low. However, of the three biogenic amines, DA is the most drastically reduced (Shannak et al., 1994), being this loss the responsible mechanism that triggers the onset of the majority of motor signs (Chung et al., 2010; Kim et al., 2011). Another hallmark feature of PD is the presence of Lewy bodies (LBs) (Gibb and Lees, 1988), which are typically used as a post-mortem confirmation of PD (Olanow and Brundin, 2013). LBs are distinctive intracytoplasmatic inclusions, containing a variety of cellular proteins, being α–synuclein the most

abundant one (Benskey et al., 2016). The precise reason why LBs form and its role in pathogenesis of PD remains unclear (Dickson et al., 2009). However, in recent years, it has become clear that the initial sites displaying LBs are the dorsal motor nucleus of the vagus in the brainstem and the olfactory bulb (which is defined as stage I). This staging concept was firstly proposed by Braak and colleagues (Braak et al., 2003a), demonstrating that the disease most likely progresses in an upward direction via the pons (stage II) to the midbrain (stage III), followed by the basal prosencephalon and mesocortex (stage IV), and eventually reaching the temporal cortex and neocortex (stages V and VI) (Braak et al., 2003b). Therefore, it is only in stage III, when DAergic neuronal death exceeds a critical threshold (i.e. 70-80% of striatal nerve terminals and 50-60% of SNpc perikarya) that motor features of PD become evident, which means, that there is a substantive pre-symptomatic period of the disease that is hidden due to the existence of possible compensatory mechanisms (Bezard et al., 1999; Navntoft and Dreyer, 2016). Indeed, Zigmond and colleagues (Zigmond et al., 1990) proposed a model of compensatory changes, showing that the relationship between DAergic neuronal loss and functional impairments results from adaptive neurochemical changes that occur within the striatum. Recently, this dogma has been challenged, and several reports have shown that the classically accepted dopamine-mediated mechanisms are not the primarily involved in the initial compensation of DA depletion in PD, proposing a series of functional compensatory changes within and outside of the basal ganglia (Bezard et al., 2003; Obeso et al., 2004). In fact, it has been shown that the activation of the subthalamic nucleus (STN) increases the activity of SNpc DAergic neurons. Thus, the loss of DAergic projections and consequent decrease in DA concentration leads to an hyperactivity of the STN before the onset of functional changes in the putamen, suggesting that STN is implicated in the compensatory mechanisms in the initial phases of PD (Bezard et al., 1999; Hamani et al., 2004; Vila et al., 2000). Nevertheless, the precise nature of these compensatory mechanisms, and the reason for their ultimate failure has still been elusive.

To date, PD motor deficits are the main focus of the therapeutic interventions. However, there is a growing literature reporting that nonmotor symptoms (NMS) form an integral part of the clinical features of PD, suggesting that they could precede the manifestation of the characteristic motor symptoms, which could represent a new approach for its early prognosis (Khoo et al., 2013). Like motor signs, the NMS can be equally debilitating to PD patients, and include depression, anxiety, sensory abnormalities, autonomic dysfunctions and cognitive decline (Langston, 2006; Pantcheva et al., 2015). Moreover, although the real cause of NMS still remains poorly understood, the current strategies for treating PD are mainly effective against the motor symptoms but widely ineffective at addressing

4

NMS. Therefore, it is important to understand the molecular mechanisms that cause the appearance of motor signs, but also NMS, in order to establish the pathophysiology pattern of PD (Chaudhuri and Schapira, 2009).
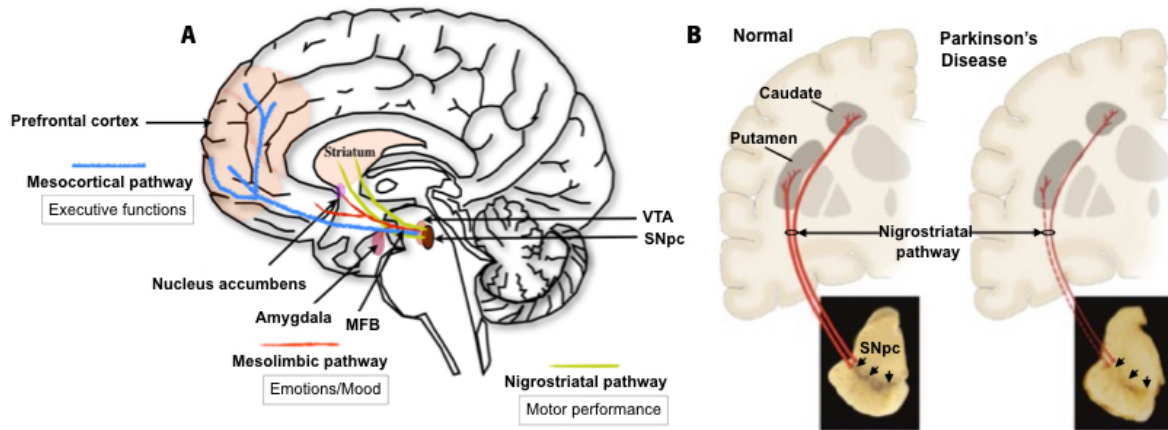
Figure 1. Neuropathology of Parkinson's disease.

A) DAergic network in the normal brain with main representative pathways: mesocortical, mesolimbic and nigrostriatal pathway. (B) When the disease occurs, the nigrostriatal pathway is the most affected, and is characterized by the progressive loss of DAergic neurons and consequent depigmentation of the SNpc. This neuronal loss leads to a DA deficiency in the striatum (i.e. putamen and caudate nucleus), which is responsible for characteristic motor symptoms. Adapted from (Dauer and Przedborski, 2003).

1.1.1. Etiology of Parkinson's disease

The majority of the cases of PD appear to be sporadic, and these probably represent an interaction between genetic and environmental factors (Warner and Schapira, 2003). Age represents the main predisposing factor, however, it remains unknown if it is the chronological age or the aging process the responsible for PD susceptibility (Dexter and Jenner, 2013). Familial cases of PD are rare, but in recent years the role of genetic factors has been intensely explored, showing significant outcomes from the molecular point of view (Bras and Singleton, 2009; Pagano et al., 2016). Recently, Pagano and colleagues (Pagano et al., 2016) explored clinical characteristics of PD at different ages in diagnosed patients with untreated PD, and found that 25% of the patients had a familiar history of the disease, raising the possibility that some of them were carriers of a genetic mutation. In fact, different reports on familial PD have revealed at least 17 autosomal dominant and autosomal recessive gene mutations namely, α-synuclein duplications and triplications, parkin, leucine-rich repeat kinase 2 (LRRK2), ubiquitin carboxyl-terminal hydrolase L1 (UCH-L1), DJ-1 (PARK7), PTEN-induced putative kinase 1 (PINK1), among others (Bras and Singleton, 2009; Dexter and Jenner, 2013). In addition,

although it has been suggested that familial forms of PD have distinct clinical and pathological phenotypes, many of these neurodegeneration mechanisms overlap with the mechanisms involved in sporadic PD such as oxidative stress, mitochondrial dysfunction and abnormal protein aggregation (Bras and Singleton, 2009; Dexter and Jenner, 2013).

Concerning environmental factors, studies have proposed that farming occupation, rural living and the consequent exposure to pesticides such as rotenone and paraquat [structurally similar to 1-methyl-4-phenyl-1,2,3,6-tetrahydropyridine (MPTP)] may have an impact in the appearance of the disease. Nowadays, all these chemicals are being used to create animal models of PD, exploring its effects on the pathophysiology of the disease. However, Noyce and colleagues (Noyce et al., 2016) have recently suggested that environmental toxins most likely play a minor role in PD risk. Furthermore, there also exists a consistent association between PD and lifestyle factors such as smoking and coffee consumption (de Lau and Breteler, 2006; Noyce et al., 2016). Indeed, many epidemiological studies have shown a reduced risk of developing PD among cigarette smokers. The most probable explanation involves nicotine, as this component may stimulate dopamine release and acts as antioxidant (Quik, 2004). Some studies also related PD with coffee consumption, showing a significantly decreased PD risk for coffee drinkers (de Lau and Breteler, 2006). These observations were based in the effects of caffeine, a known inhibitor of the adenosine A_2 receptor, which in turn has an important role in the regulation of dopamine release (Chen et al., 2001).

1.1.2. Mechanisms of Neurodegeneration

Where does PD begins at the cellular level? This is the key question that still remains to be answered. Evidences from the literature have suggested that the degeneration of DAergic neurons in PD starts in the axonal and synaptic terminals, retrogradely progressing to the cells bodies in SNpc (Burke and O'Malley, 2013). In fact, at the time of the onset of motor deficits, more than 70% of DA (Bernheimer et al., 1973; Dauer and Przedborski, 2003), and more than 50% of the tyrosine hydroxylase (TH) and DA transporter (DAT) have been lost in the striatum (Beach et al., 2008; Dauer and Przedborski, 2003; Nandhagopal et al., 2008). On the other hand, the SNpc presents a decrease of around 30% of DAergic cells at this time (Cheng et al., 2010; Ross et al., 2004). Little is known about the mechanisms underlying the early deterioration of synapses and axons of DAergic neurons in PD, but available data indicate that the retrograde degeneration implicates a decline of the axonal trafficking of proteins and mitochondrias, followed by the aggregation of α-synuclein and the formation of axonal spheroids (Chu et al., 2012; Chung et al., 2009; Coleman, 2005; Kim-Han et al., 2011). Surrounding

astrocytes and microglial cells have also been described as potential modulators of these axonal impairments (Privat, 2003; Shokouhi et al., 2010). However, the real influence of these cells on the degeneration and deterioration progress of nigral or striatal DAergic pathways is still poorly understood (Halliday and Stevens, 2011). Despite these issues, nowadays, it is well accepted that oxidative stress, mitochondrial dysfunction and abnormal protein aggregation are the key molecular mechanisms involved in PD neurodegeneration process (Figure 2) (Dauer and Przedborski, 2003; Dexter and Jenner, 2013).

The central nervous system (CNS) is particularly sensitive to oxidative stress due to different reasons, including its high oxygen consumption even under basal conditions, high production of reactive species from specific neurochemical reactions as well as increased deposition of metal ions in the brain with aging (Chiurchiu et al., 2016). Throughout the whole lifespan, DAergic neurons are exposed to reactive oxygen species (ROS) as a result of the metabolism of DA itself. In DAergic cells, ROS generation occurs by deamination (auto-oxidation process) of DA by the monoamine oxidase (MAO) activity. This results in significant amounts of hydrogen peroxidase (H_2O_2) that can further interact with metal ions (e.g. iron), leading to the origin of the reactive hydroxyl radical ($\bullet OH$), which is highly toxic to the neurons (Bhat et al., 2015; Datta and Bhonde, 2012). Indeed, post-mortem analysis has shown that significantly higher concentrations of iron, in SNpc region, were found in brain tissue of PD patients when compared to healthy individuals (Griffiths et al., 1999). Indeed, DAergic neurons are more susceptible to oxidative damage when compared to other neuronal cells mainly because of the dual presence of DA and high levels of iron. Mitochondrial dysfunction is also another origin of oxidative stress that has been widely associated with the pathogenesis of PD. Neurons are metabolically very active, and as such, they greatly depend on mitochondria for energy production. Any pathological situation that leads to mitochondrial dysfunction can cause a higher increase in ROS, inducing (for instance) the release of cytochrome c in the cytosol, and consequently apoptosis (Bhat et al., 2015; Moon and Paek, 2015). In addition, the decrease of complex I (of the mitochondrial respiratory chain) enzyme activity was also observed to be an important player of degeneration in the SNpc of parkinsonian patients (Parker et al., 1989). In fact this process in known to cause excitotoxicity and axonal damage, leading to the progression of PD (Chiurchiu et al., 2016).

Finally, the abnormal deposition of proteins in brain tissue has also been an important feature in the pathophysiology of PD. Although it remains unclear how misfolded proteins could directly cause toxicity or damage the cells via the formation of protein aggregates, the prevailing hypothesis is that the formation of the latter triggers a cascade of neurodegenerative events (Diack et al., 2016). Oxidative

damage, linked to mitochondrial dysfunction and an abnormal DA metabolism, may also promote or predispose misfolded proteins conformations. Nonetheless, these events are not mutually exclusive, and one of the aims of the current PD research is to elucidate the sequence in which they act and understand the interaction between these pathways (Dauer and Przedborski, 2003).
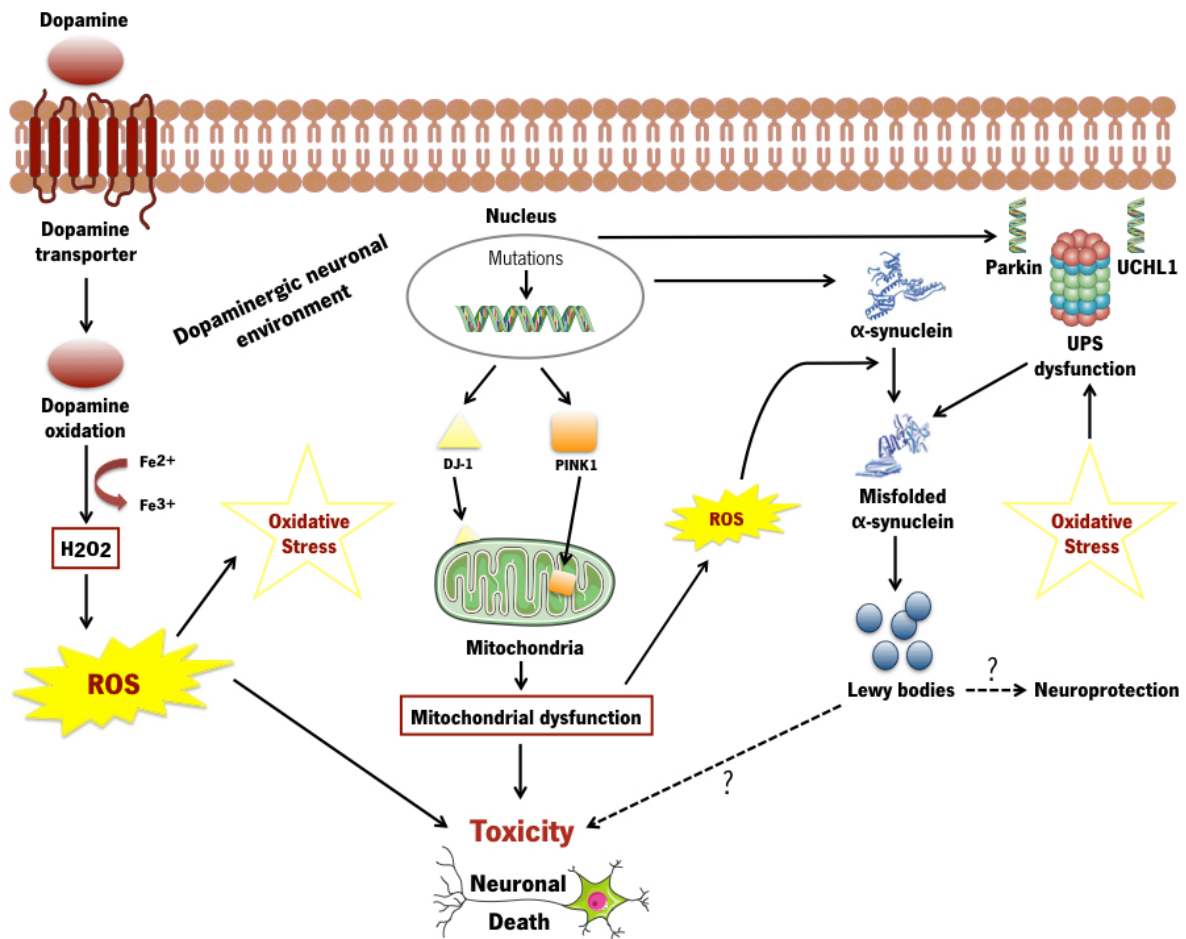
Figure 2. Key molecular mechanisms that contribute to the neurodegenerative process in dopaminergic neurons in Parkinson's disease.

Cell death may be caused by oxidative stress, mitochondrial and UPS dysfunction, and α-synuclein aggregation. Pathogenic mutations may directly induce mitochondrial dysfunction (DJ-1, PINK-1), abnormal protein conformations (as believed to be the case with α -synuclein) or damage the ability of the cellular machinery to detect and degrade misfolded proteins (Parkin, UCHL1). Controversy exists regarding whether LBs promote toxicity or protect the cells from harmful effects of misfolded proteins. ROS generation occurs by the auto-oxidation process of DA resulting in significant amounts of H_2O_2 that can further interact with metal ions like iron. Oxidative damage, linked to mitochondrial dysfunction and abnormal dopamine metabolism, may also promote misfolded protein conformations. ROS: Reactive oxygen species. UPS: Ubiquitin proteasome system.

1.2. Current therapeutic approaches in Parkinson's Disease: how far are we from the cure?

The treatment of PD has not significantly changed over the years, and the use of levodopa (L-DOPA) is still considered the *gold standard* treatment since its introduction in the early 1960s (LeWitt and Fahn, 2016). L-DOPA, is a naturally occurring aminoacid and is the immediate metabolic precursor for catecholamines like DA, and in contrast to DA, L-DOPA can readily cross the blood-brain barrier (BBB). This drug has revolutionized symptomatic treatment by providing improvement in activities of daily living and life quality. However, L-DOPA is just efficient during the first years of usage as its chronic administration has been associated with the appearance of undesirable side effects such as nausea, vomit, hypotension and long-term complications including motor fluctuations (loss of therapeutic effect benefit after each dose) and dyskinesias (excessive involuntary movements occurring at the peak of L-DOPA dosing) (Jankovic and Aguilar, 2008; Jimenez-Shahed, 2016; Rascol et al., 2003).

The use of DA agonists and enzyme inhibitors has been used as alternative to the above mentioned (Dexter and Jenner, 2013; Rascol et al., 2003). In the case of the DA agonists (e.g. pramipexole and ropinirole), studies have shown that they are efficient in controlling the cardinal motor symptoms of PD, particularly in early stages of the disease and in patients who have not been exposed to L-DOPA (Jankovic and Aguilar, 2008). For instance, the administration of pramipexole or ropinirole was found to significantly reduce the risk of motor complications compared to L-DOPA (Holloway et al., 2004; Rascol et al., 2000). However, the prolonged exposure to DA agonists also presents limiting features such as somnolence, sleep disturbances and impulse control disorders (Jankovic and Aguilar, 2008). On the other hand, the use of MAO-B inhibitors such as selegiline and rasagiline has attracted some attention (Dexter and Jenner, 2013). Safinamide, another MAO-B inhibitor compound, has recently been claimed as a promising agent for the treatment of PD. In Phase-III clinical trials, safinamide is a molecule with a dual mechanism of action based on the enhancement of the DAergic function and inhibition of the excessive release of glutamate. Indeed, safinamide was found to be a useful as a combinatory strategy to DA agonists in the early phases of PD, as well as to be able to reduce dyskinesias when used together with L-DOPA in patients with advanced PD (Kandadai et al., 2014; Onofrj et al., 2008). Despite these promising results, most of these treatments were not able to promote the total recovery of PD symptomatology, presenting long-term inefficiency as well as an inability to recover lost DAergic neurons or to protect the viability of the remaining ones.

Surgical treatments, such as deep brain stimulation (DBS) in the globus pallidus internus (GPi) or in the STN have been applied as an alternative in patients with significant motor complications where

the pharmacological treatment is no longer effective (Hariz et al., 2016; Hutchinson and Wick, 2016). Indeed, it has been reported that this surgical procedure is safe, leading to the lower consumption of anti-parkinsonian medications and dyskinesias (deSouza et al., 2013). However, DBS requires expertise in diagnosis, imaging and stereotaxic surgery, thereby limiting its widespread applicability (Rascol et al., 2003).

In addition to the conventional clinical treatments, some clinical trials based in the transplantation of human ventral mesencephalic tissues into the striatum of PD patients with advanced disease, were conducted in the late 1980s (Lindvall et al., 1990; Sawle et al., 1992). The results were quite promising, with patients displaying increased levels of DA, motor function amelioration as well as, reduction in the L-DOPA dosage requirement (Singh et al., 2007). Although these studies confirmed the relevance and feasibility of cell transplantation, the use of human tissue has some limitations associated with ethical and religion questions, as well as logistics of acquiring sufficient amount of fetal tissues (Kim et al., 2013; Suksuphew and Noisa, 2015).

In summary, all these interventions are not fully efficacious, and more importantly, the progression of the PD degenerative process is not avoided. Based on such limitations, cell-based strategies through the use of stem cells have been proposed as a possible therapeutic tool for the treatment of CNS disorders, including PD (Anisimov, 2009).

1.3. Stem cell-based therapeutic approaches

The low regeneration potential of CNS make it a challenge for the development of new protocols and strategies that could allow the generation of new functional neurons in response to injury (Williams, 2014). Endogenous stem cells are found in specific niches of human brain, which have the ability to differentiate and replace the damaged cells and secrete trophic factors required for tissue repair. However, this self-repair is not sufficient in most pathological processes, demanding external intervention (Buzhor et al., 2014). Recently, cell therapy has been proposed as an attractive option, and stem cells represent the most favorable cell source for such therapies, since these cells have the ability to renew themselves continuously, have high proliferation capability and are able to differentiate into different cell types (Kim et al., 2013; van der Kooy and Weiss, 2000). Over the years, several types of stem cells were investigated as potential agents for cellular therapy including embryonic stem cells (ESCs), neural stem cells (NSCs), mesenchymal stem cells (MSCs), or even induced pluripotent stem cells (iPSCs) from different sources, showing promising results in a wide panel of CNS disorders including PD (Goodarzi et al., 2015). From these, NSCs and MSCs have a number of interesting

properties that we will describe throughout this work. Indeed, it has been described that these cells display therapeutic effects of neuroprotection and immunomodulation, such as the capacity to protect and regenerate damaged DAergic neurons, as well as increase the motor function in PD animal models (Bonnamain et al., 2012; Drago et al., 2013; Kassem et al., 2004). Therefore, we focused our efforts in studying their potential use, as well as of its secretome, as a potential alternative therapy for PD.

1.3.1. Neural stem cells

NSCs are multipotent cells isolated from fetal and adult nervous system tissues, which have the ability to self-renew and differentiate into specialized functional neurons, astrocytes and oligodendrocytes (Buzhor et al., 2014; Fu et al., 2015), which makes them an interesting source of cells for neuronal repair after injury or disease (Bonnamain et al., 2012). It is known that NSCs exist not only in the developing brain but also in the adult brain (Palmer et al., 2001), particularly in the subgranular zone (SGZ) in the dentate gyrus (DG) of the hippocampus and the subependymal zone (SEZ) of the lateral ventricles (as reviewed by Salgado et al., 2015). These cells are commonly identified by the expression of the intermediate filament Nestin, GFAP, transcription factor Sox2, and the RNA binding protein Musashi1, together with absence of expression of the differentiated markers CD24, NeuN and O4 (Suksuphew and Noisa, 2015). NSCs are typically isolated from embryonic, fetal or adult nervous system tissue (Alvarez-Buylla and Garcia-Verdugo, 2002; Ogawa et al., 2009; Toma et al., 2001; Zhang et al., 2009), and can be cultured *in vitro* as neuroshperes, in the presence of growth factors such as basic fibroblast growth factor (FGF-2) and epidermal growth factor (EGF) (Bonnamain et al., 2012).

A growing number of studies have also highlighted NSCs as immunomodulatory agents and their capacity to reduce CNS inflammation (Ben-Hur, 2008; Kokaia et al., 2012). Although no reports have been presented regarding these effects of NSCs specifically in PD, it is known that inflammatory responses (e.g. T cell infiltration, increased expression cytokines, toxic mediators derived from activated glial cells) are prominent features of PD (Tufekci et al., 2012), and therefore, the immomodulation effects presented by these cells may be important for its use in cell transplantation.

Regarding the application of NSCs in PD, there are several examples of their impact on the reversion of the latter. For instance, Harrower *et al.* (Harrower et al., 2006) showed a reliable long-term survival and integration of transplanted NSCs in the striatum of rats lesioned with 6-hydroxydopamine (6-OHDA). According to the authors, an increase of DA fiber densities, as well as synapse formation was observed. Richardson and colleagues (Richardson et al., 2005) demonstrated that the transplantation of

adult NSCs (expanded from SEZ) in the striatum of 6-OHDA-lesioned rats led to a functional recovery in the animals, and the DAT immunoreactivity was restored in the host tissue. Using the same model (6-OHDA), Armstrong and colleagues (Armstrong et al., 2002) revealed that transplanted NPCs could differentiate into neurons, and indeed, a small number of TH-immunopositive neurons were present in both intrastriatal and intramesencephalic grafts. Yasuhara and co-workers (Yasuhara et al., 2006) also observed that by transplanting an immortalized NSC line (HB1.F3), functional improvements could be observed along with an evident preservation of TH immunoreactivity in the nigrostriatal pathway. Moreover, in other CNS related disorders, such as amyotrophic lateral sclerosis (ALS), Huntington's disease (HD) and ischemic stroke, the transplantation of NSCs was also effective in delaying disease progression, exert neuronal protection and enhance motor function, and led to the increase of dendritic plasticity and axonal rewiring (Andres et al., 2011; Ryu et al., 2004; Xu et al., 2006).

Although promising, it is important to note that the application of NSCs for transplantation is still limited. Tissue availability, ethical and logistical concerns linked to the fact that it is also challenging to maintain and expand these cells for long periods of time, represent important issues to overcome in the future before resuming it for clinical applications (Bonnamain et al., 2012; Fu et al., 2015). Besides that, NSCs have been described as a potential stem cell source for the treatment of neurological disorders not only because they may provide a (tissue-specific) cellular reservoir for the replacement of lost or damaged cells, but also because of other capabilities, such as tissue trophic support (Ben-Hur, 2008; Drago et al., 2013).

1.3.2. Mesenchymal Stem Cells

MSCs represent a non-hematopoietic and multipotent stem cell population with self-renewal capacity and multiple differentiation potential (Wang et al., 2011). According to the International Society for Cellular Therapy (ISCT), there are three minimal criteria to define MSCs, namely: (1) the adherence to plastic surfaces when maintained in standard culture conditions; (2) the positive expression of specific surface markers such as CD105, CD90 e CD73, and negative expression of hematopoietic surface markers like CD14, CD34, CD45, HLA-DR, or CD11B, CD79α or CD19; and (3) *in vitro* differentiation into at least osteoblasts, adipocytes, and chondroblasts (Dominici et al., 2006). Friedenstein and colleagues (Friedenstein et al., 1974) were the first to isolate MSCs from bone marrow, describing them as fibroblastoid cells with clonogenic potential and plastic culture adherence. Following these early studies, countless reports have confirmed that in addition to bone marrow, MSCs can also be isolated from various adult and neonatal tissues such as adipose tissue, dental pulp,

amnion, placenta, Wharton jelly of the umbilical cord, and even the brain (Erices et al., 2000; Gronthos et al., 2000; Hass et al., 2011; Paul et al., 2012; Sarugaser et al., 2005; Wang et al., 2004; Zuk et al., 2002). The potential of MSCs has been attributed to their widespread availability throughout the human body, easy isolation and expanding, as well as maintenance of viability and regenerative capacity after cryopreservation (Uccelli et al., 2011a; Uccelli et al., 2011b; Wang et al., 2011). In addition to this, MSCs have also demonstrated low immunogenic properties due to the lack of the major histocompatibility complex class II (MHC-II), making them an attractive cell source for transplantation (Morandi et al., 2008). Furthermore, MSCs have been also described as immunomodulatory agents, being able to interact with different components of the immune system (Wang et al., 2011). For example, it has been described that MSCs are capable to regulate the proliferation, activation and maturation of T and B lymphocytes *in vitro* (Bartholomew et al., 2002), and to induce long-term survival in an allogeneic context (Aggarwal and Pittenger, 2005), which is an important concern for its use in transplantation.

Regarding PD, several reports have already shown that the transplantation of MSCs acts as a promoter of neuroprotection and/or neuronal function (Glavaski-Joksimovic and Bohn, 2013). Hellman and co-workers (Hellmann et al., 2006) demonstrated that after transplantation, bone marrow MSCs (BM-MSCs) were found to be viable and migrate in the brain parenchyma of a 6-OHDA PD rat model. Using the same PD model and the same MSCs population, Danielyan and colleagues (Danielyan et al., 2011) showed neuroprotective effects against nigrostriatal degeneration and improvements in the motor function of the 6-OHDA lesioned rats. Blandini *et al.* (Blandini et al., 2010) also achieved the same outcomes, verifying that although no differentiation of MSCs toward a neuronal (DAergic) phenotype was obtained *in vivo*, the animals that received the striatal MSCs grafts presented an increased survival of both cell bodies and terminals of DAergic neurons. With MSCs derived from adipose tissue (ASCs), Schwerk and colleagues (Schwerk et al., 2015) demonstrated a significant increase in TH-positive expression in transplanted animals when compared to the untransplanted group. The same results were also obtained by Xiong and colleagues (Xiong et al., 2010), which demonstrated neuroprotective and neuroregenerative effects in a rotenone-induced hemiparkinsonian rat model using MSCs isolated from umbilical cord. In patients, Venkataramana and co-workers (Venkataramana et al., 2010) observed that the transplantation of BM-MSCs led to a partial amelioration in the symptomatology and life quality of the patients [measured by Unified Parkinson's disease rating scale (UPDRS)].

The specific mechanism by which MSCs are able to improve the motor performance either in animals or patients remains unclear. It is well studied that MSCs populations can be sub-passaged and differentiate into different cell lineages, however the differentiation into functional neuronal lineages is not likely to happen in such a relevant manner that could impact the recovery of PD animal models or patients (Maltman et al., 2011; Teixeira et al., 2013). Therefore, although some reports suggest the differentiation of MSCs into DAergic neurons or other neuronal lineages as the principal outcome of their therapeutical effects, recent evidences have proposed the secretome of these cells as the main responsible of their therapeutic action (Teixeira et al., 2013).

1.3.3. Stem cells secretome

The therapeutic effects of transplanted stem cells were initially attributed to their differentiation capacity. Indeed, most of the studies emphasize the ability of stem cells to migrate to the sites of injury, integrate the damaged tissue and differentiate into specialized cells (Drago et al., 2013). However, it has also been shown that only a small percentage of cells truly engraft and survive in the damaged host tissue, leading the current body of research to argue that the multipotent differentiation of stem cells, within the CNS, contributes minimally to the observed beneficial effects (Kupcova Skalnikova, 2013; Lavoie and Rosu-Myles, 2013). On the other hand, robust data has recently demonstrated that most of these potential effects, promoted by stem cells, are mainly mediated by the secretion of bioactive molecules (e.g., proteins, cytokines, vesicles), which is defined as secretome (Drago et al., 2013; Salgado et al., 2010; Salgado et al., 2015; Teixeira et al., 2013). The concept of secretome has been described as the proteins released by a cell, tissue or organism, being essential in the regulation of different cell processes (Teixeira et al., 2013). In fact, it has been demonstrated that these secreted molecules by stem cells act as modulators of cell survival, proliferation and differentiation, as well as regulators of inflammatory processes and promoters of angiogenesis (Teixeira et al., 2013). Although most of the secretome studies have been focused in their proteic soluble fraction (e.g. factors, growth factor and cytokines), nowadays it has also been described that stem cells are able to secrete a vesicular fraction that is constituted by microvesicles and exosomes, which involves the transference of proteins and genetic material to neighboring cells (Salgado et al., 2015; Yu et al., 2014).

In 2006, Crigler and colleagues (Crigler et al., 2006) were the first to show that BM-MSCs were able to induce neuronal cell survival and neurite outgrowth in a neuroblastoma cell line and in dorsal root ganglion explants, through the secretion of neurotrophic factors such as brain-derived neurotrophic factor (BDNF) and nerve growth factor (NGF). Further characterization studies have reported that,

14

indeed, these cells are able to secrete a wide panel of growth factors such as glial cell-derived neurotrophic factor (GDNF), FGF-2, insulin-like growth factor 1 (IGF-1), hepatocyte growth factor (HGF), vascular endothelial growth factor (VEGF) and EGF, as well as cytokines like interleukin 6 (IL-6), interleukin-10 (IL-10), transforming growth factor beta (TGF-β), stem cell factor (SCF) and stromal cell-derived factor 1 (SDF-1) (Baraniak and McDevitt, 2010; Meyerrose et al., 2010; Nakano et al., 2010; Ribeiro et al., 2012), which are described as important modulators of neuronal survival/differentiation, neurite outgrowth and glial cells. Cantinieaux and co-workers (Cantinieaux et al., 2013) showed *in vitro* that the BM-MSCs secretome was pro-angiogenic and was able to protect neurons from apoptosis. With ASCs secretome, Lu *et al.* (Lu et al., 2011) demonstrated its potential to protect a PC13 cell line model from glutamate excitotoxicity-induced apoptosis through the secretion of BDNF, VEGF and HGF. Salgado and colleagues (Salgado et al., 2010) revealed that the secretome of human umbilical cord perivascular cells (HUCPVCs) was also a modulator of neuronal viability and cell survival. In the context of PD, Kim and colleagues (Kim et al., 2009), using co-cultures of microglia and mesencephalic neurons together with BM-MSCs, observed that there was a decrease in the microglia activation due to the release of anti-inflammatory molecules such as IL-6 and TGF-β, thereby protecting dopaminergic neurons from death. Similar results were also presented by Wang and colleagues (Wang et al., 2010), which showed that BM-MSCs could exert neuroprotection in 6-OHDA-exposed dopaminergic neurons *in vitro*, through anti-apoptotic mechanisms promoted by the expression of SDF-1. *In vivo*, the secretome of MSCs also plays an important role, either by the active secretion *in situ* (after MSCs transplantation) or by the injection of the secretome itself in the form of conditioned media (CM) (Teixeira et al., 2013). Previous studies from Salgado's lab showed that the injection of MSCs secretome was able to revert the parkinsonian phenotype from both histological and functional outcomes (data not published). This is in line with what has been described in the literature regarding the trophic capability of MSCs in PD. For instance, Sadan and colleagues (Sadan et al., 2009), using human BM-MSCs as neurotrophic factors secreting cells (NTF-SC), observed a remarkable attenuation in the amphetamine-induced rotation and other abnormal behavior, as wells as in the loss of TH immunoreactive nerve terminals when compared to the untreated MSCs group, attributing these effects to the secretion of BDNF and GDNF. Similar observations were also claimed by Cova and co-workers (Cova et al., 2010), which observed that after intrastriatal transplantation of MSCs there was an increase in the preservation of spared DAergic neurons, which was correlated with an increased expression of BDNF by MSCs. Interestingly, in a comparative study reported by Teixeira and colleagues (Teixeira et al., 2015), animals injected just with

the secretome of HUCPVCs into the DG of adult rats, disclosed levels of neuronal survival and differentiation very similar to those observed in cell-transplanted groups.

Neurotrophic growth factors such as NGF, BDNF, GDNF have also been found to be increased after NSCs transplantation (Drago et al., 2013). Likewise MSCs, currently there are no studies regarding the application of NSCs secretome alone in animal models of PD. However, studies have suggested NSCs as neurotrophic-factor secreting cells (Drago et al., 2013). For instance, Yasuhara and co-workers (Yasuhara et al., 2006) showed that after intrastriatal transplantation of NSCs in 6-OHDA PD model, there was an improvement in the behavioral performance of the animals, which was correlated with the increase of TH innervation due to an active expression of SCF. Similar outcomes were also presented by Ourednik and colleagues (Ourednik et al., 2002), which demonstrated, using a MPTP PD model, that after the transplantation of NSCs there was an increased recovery of TH and DAT activity due to an *in situ* expression of GDNF. Moreover, the authors suggest that the NSCs have the capacity to create host environments rich in trophic and neuroprotective support to rescue imperiled host cells (Ourednik et al., 2002). Ebert and colleagues (Ebert et al., 2008) demonstrated that NSCs overexpressing either IGF-1 or GNDF were able to significantly reduce amphetamine-induce rotational behavior and DA neuronal loss in 6-OHDA PD animals, when compared to the untransduced NSCs. Behrstock *et al.* (Behrstock et al., 2006) demonstrated, *in vitro*, that the number of primary neurons staining for TH significantly increased after the addition of NSCs CM. *In vivo*, using NSCs genetically modified to release GDNF, the same authors showed that more TH positive neurons were present in the transplanted rats (partial lesioned with 6-OHDA), verifying fewer rotations compared to the untransplanted group (Behrstock et al., 2006).

Besides the paracrine soluble factors released by stem cells to the extracellular space, intensive research has also been investigating the role of secreted extracellular vesicles (EVs) in the therapeutic potential of stem cells (Drago et al., 2013). Exosomes and microvesicles are the most well studied classes of EVs. These vesicles are involved in cell-to-cell communication, with the ability to transfer proteins and functional genetic material such as micro-RNAs (miRNAs) to other cells, which are implicated in important physiological processes such as antigen presentation, genetic exchange, immune responses and angiogenesis (Lener et al., 2015; Lopez-Verrilli et al., 2016; Xin et al., 2013; Yu et al., 2014). A more detailed characterization of EVs secreted by both MSCs and NSCs is required, in an effort to select and identify the molecules responsible for the therapeutic effects of the secretome (Drago et al., 2013; Lai et al., 2010).

Altogether, these findings strongly suggest that stem cells' secreted factors are the key players on stem cells' mediated effects in models of injury and disease in the CNS. Therefore, the use of secretome as a possible replacement of cell transplantation is of enormous interest and may be a new and important tool for the treatment of PD (Figure 3).
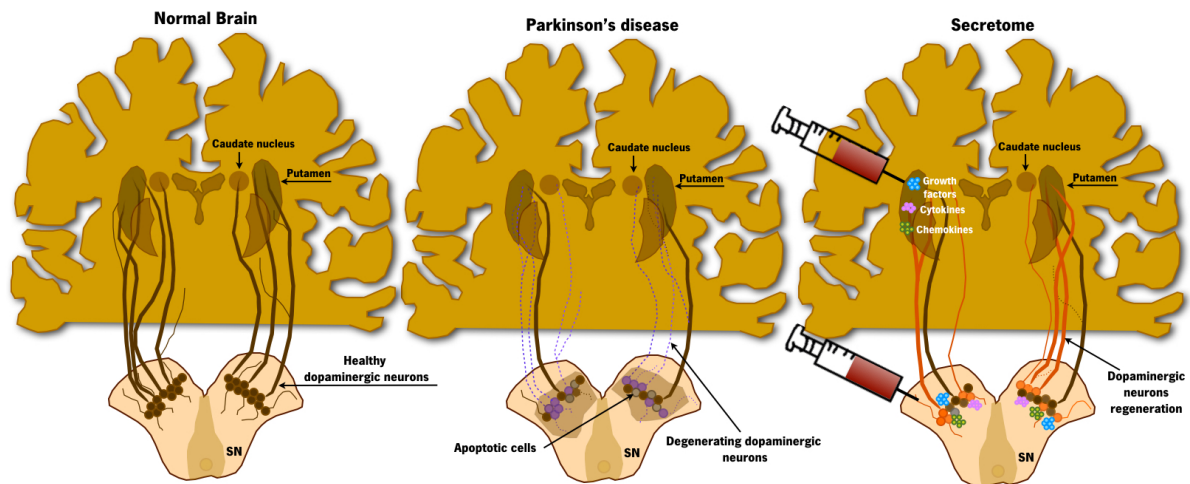
Figure 3. Stem cells secretome-based therapy for Parkinson's disease.

The trophic action of stem cells has been increasingly accepted nowadays as a new concept for the regeneration of the CNS, including PD. The ability to secrete growth factors, cytokines and chemokines seems to be one of the reasons to the contribution to the protection/survival of the preexisting DAergic neurons in lesioned areas, leading to functional amelioration and improvement of motor function. Adapted from (Teixeira et al., 2013).

Stem cells have been on the forefront of new possible therapeutic strategies for CNS regeneration. Recent evidences have indicated that most of the beneficial actions caused by these cells are related with their secretome and its trophic capability. This is extremely important as it should minimize biological variability, allowing precise dosing, and overcome several stem cells related issues including the number of available cells for transplantation and its survival after this procedure. Therefore, the main goal of the present project is to determine the role of secretome as a potential cell-free therapy for PD, when compared to cell-based transplantation approaches. Therefore, the main objectives of the present thesis are:

1. Characterize the secretome of human MSCs (hMSCs) and human NPCs (hNPCs), performing a comparative study through proteomic-based approaches.
2. Determine the impact of hMSCs and hNPCs secretome on the neuronal survival and differentiation of hNPCs *in vitro*.
3. Establish the therapeutic potential of hMSCs secretome in an *in vivo* model of PD (6-OHDA), comparing it to the outputs obtained from animals transplanted with hMSCs, hNPCs and their secretome.

CHAPTER 3

MATERIALS AND METHODS

3. MATERIALS AND METHODS

3.1. Cell Culture

3.1.1. Expansion of hMSCs and collection of conditioned medium

hMSCs derived from bone marrow (Lonza, Switzerland) were thawed and plated into T-75 gelatin (0.1%, Sigma, USA)-coated culture flasks (SPL Life Sciences, Korea) with 12 mL of serum-free growth medium (PPRF-msc6). The formulation and preparation of PPRF-msc6 has previously been described in detail (Jung et al., 2010). The medium was renewed every 3 days and the culture maintained at 37°C in a humidified atmosphere containing 5% CO_2. When the cells reached 80-90% of confluence, they were enzymatically dissociated using 0.05% trypsin-EDTA (Life Technologies, USA) during 5 min at 37°C. Dulbecco's Modified Eagle Medium (DMEM; Life Technologies, USA) supplemented with Fetal bovine serum (FBS, Biochrom, Germany) was then added to stop the reaction. After that, cells were centrifuged at 1200 rpm (4°C) for 5 min. The supernatant was removed and the pellet was resuspended in fresh growth medium, in which a small volume of cells was diluted in Trypan Blue (Life Technologies, USA) to perform cell counts. At last, the cells were plated into new gelatin-coated culture flasks at a density of 5000 cells/cm^2 for experiments, and 12 000 cells/cm^2 for proteomic procedures. At passage 5 (P5), after 72 hours of growth, the medium was removed and the cells were washed twice with Neurobasal A medium (Life Technologies, USA). Following this, Neurobasal-A medium supplemented with 1% kanamycin (Life Technologies, USA) was added to the cells, which were placed at 37°C in a humidified atmosphere containing 5% CO_2. After 24 h, this medium, containing the factors secreted by hMSCs (called conditioned medium (CM)) was collected and centrifuged at 1200 rpm for 10 min to remove any cell debris, and then stored at -80°C until it was required for further experiments.

3.1.2. Expansion of hNPCs and collection of conditioned medium

hNPCs were a kind gift from Prof. Leo A. Behie (University of Calgary, Canada). Cells were isolated from the telencephalon region of a 10 week post-conception fetus according with the protocols and strict ethical guidelines previously established and approved by the Conjoint Health Research Ethics Board (CHREB, University of Calgary, Canada; ID:E-18786) (Baghbaderani et al., 2010; Mendez et al., 2002; Mendez et al., 2005). hNPCs were thawed and the content placed in T-75 culture flasks containing 15 mL of serum-free medium PPRF-h2 (Baghbaderani et al., 2010). After 3 days, the cells were mechanically triturated using a P1000 Pipetman set to 850μL (25-30 times) into a single cell

suspension, being then cultured in fresh growth medium (PPRF-h2). Every 3 days, 40% of spent medium was replaced with fresh growth medium and the culture was maintained at 37°C in a humidified atmosphere containing 5% CO_2. After 10-12 days of growth, hNPCs were centrifuged at 1000 rpm during 6 min and then enzymatically dissociated using 0.05% Trypsin-EDTA (1 mL) during 10 min at 37°C. Afterwards, was added 5 mL of growth medium to the cell suspension to stop trypsin activity. Then, the content were centrifuged at 1000 rpm for 10 min. The supernatant was discard and the pellet was resuspended 25-30 times in fresh growth medium. A small volume of cells was then diluted in Trypan Blue to perform cell counts. Finally, the cells were plated into new tissue culture flasks at a density of 5000 cells/cm² for experiments, and 12 000 cells/cm² for proteomic procedures. At P5, after 10-12 days of growth, the cells were centrifuged at 1000 rpm for 5 min. The supernatant was discard and then Neurobasal A medium supplemented with 1% kanamycin was added to the cells, and these were placed in a humidified incubator, operating at 37°C and 5% CO_2. After 24 h, the medium was removed, centrifuged at 1200 rpm for 10 min to remove any cell debris and then stored at -80°C until it was required for further experiments.

3.2. *In vitro* assay

3.2.1. Growth of hNPCs and incubation with hMSCs and hNPCs conditioned medium

Pre-isolated and cryopreserved hNPCs were thawed at 37°C and placed in T-75 culture flasks with 15 mL of serum-free medium PPRF-h2. After 3 days, the cells were mechanically dissociated into a single cell suspension and cultured in fresh growth medium. Every 4 days, the 40% of the spent medium was replaced with fresh growth medium and the culture as maintained at 37°C in a humidified atmosphere containing 5% CO_2. After 10-15 days of growth, hNPCs were passaged and plated on pre-coated [poly-D-lysine (100 µg/mL, Sigma, USA) and laminin (10 µg/mL, Sigma, USA)] 24-well plates at a density of 50 000 cells per well, for 5 days, with the hMSCs and hNPCs CM and placed at 37°C in a humidified atmosphere containing 5% CO_2. Neurobasal-A medium supplemented with 1% kanamycin was used as control group.

3.2.2. *In vitro* immunostaining of hNPCs

hNPCs were fixed in 4% paraformaldehyde (PFA, Merck, Portugal) for 30 min at room temperature (RT), to retain the antigenicity of the target molecules and preserve cells morphology. Cells were permeabilized in 1X phosphate buffered saline (PBS) with 0.1% Triton X-100 (Sigma, USA) (PBS-T) for 5 min at RT and washed three times with 1X PBS. Blockage of non-specific binding sites was

performed using 1X PBS with 10% newborn calf serum (NBCS; Biochrom, Germany) for 1 h at RT. hNPCs were then incubated with the primary antibodies (Table 1) diluted in 1X PBS with 10% NBCS for 1h at RT, after which they were washed with 1X PBS with 0.5% NBCS and incubated with the secondary antibodies (Table 2) diluted in 1X PBS with 10% NBCS for 1 h at RT. The cells were then incubated with the nuclear counterstain 4-6-diamidino-2-phenylindole-dhydrochloride (DAPI, 1:1000; Life Technologies, USA) for 10 min at RT. Afterwards, coverslips were mounted on glass slides using immu-mount (Thermo Scientific, UK). Finally, for quantification analysis, samples were observed under blind conditions using a fluorescence microscope (BX61, Olympus, Japan). For this purpose, four coverslips per condition and ten representative fields were chosen and analyzed. In order to normalize the data between the different sets, the results are presented in percentage of cells. This was calculated by counting the positive cells for the respective markers (Table 1), dividing this value by the total number of cells/field (DAPI-positive cells).

Table 1. Primary antibodies

Antibody – Specie	Working dilution	Company
Doublecortin (DCX) - Rabbit	1:300	Abcam (UK)
Microtubule associated protein-2 (MAP-2) - Mouse	1:500	Sigma (USA)
Beta III tubulin - Mouse	1:500	Millipore (USA)

Table 2. Secondary antibodies

Antibody – Antigenicity	Working dilution	Company
Alexa Fluor 488 - Goat anti-rabbit		
Alexa Fluor 488 - Goat anti-mouse	1:1000	Life Technologies (USA)
Alexa Fluor 594 - Goat anti-mouse		

3.3. Stereotaxic surgeries

3.3.1. 6-OHDA lesions

All the experiments were done after the consent from the Portuguese national authority for animal research, Direcção Geral de Alimentação e Veterinária (ID: DGAV28421) and Ethical Subcommittee in Life and Health Sciences (SECVS; ID: SECVS-008/2013, University of Minho), conducted in accordance with the local regulations on animal care and experimentation (European Union Directive 2010/63/EU). Eight-weeks old *Wistar-Han* male rats (Charles River, Barcelona) were housed in pairs, in appropriate cages, under standard controlled conditions (12 h light/12 h dark cycles; RT at 22-24°C and 55% humidity; food and water ad libitum). Animals were handled for 1 week

before the beginning of the injections, in order to reduce the stress induced by the surgical procedures. Therefore, for surgical procedures, animals were anesthetized with ketamine (Imalgene, Merial, USA)-medetomidine (Dorbene, Zoetis, Spain) [75 mg/kg; 0.5 mg/kg, intraperitoneally (i.p)], placed on a stereotaxic frame (Stoelting, USA), and unilaterally injected using a 30-gauge needle Hamilton syringe (Hamilton, Switzerland), with either vehicle (Sham group, n=9) or 6-OHDA hydrochloride (Sigma, USA) (6-OHDA group, n=25) directly into the medial forebrain bundle (MFB) [coordinates related to Bregma: AP= -4.4 mm, ML= - 1.0 mm, DV= -7.8 mm; (Paxinos and Watson, 2007)]. At a rate of 1 μl/min, Sham animals received 2 μl of 0.2 mg/ml of ascorbic acid in 0.9% NaCl and the 6-OHDA animals were injected with 2 μl of 6-OHDA hydrochloride (4 μg/μl) with 0.2 mg/ml of ascorbic acid in 0.9% NaCl. After each injection the needle was left in place for 2 min in order to avoid any backflow up the needle tract. Behavioral assessment was performed three weeks after surgery.

3.3.2. Surgical treatment - Injection of hMSCs, hNPCs and CM

Five weeks after the lesion, the animals received cell transplants (hMSCs and hNPCs) and their secretome. As previously described, under ketamine-medetomidine [75 mg/kg; 0.5 mg/kg, i.p.] anesthesia, the animals were placed on a stereotaxic frame, and unilaterally injected, using a 30-gauge needle Hamilton syringe, with either vehicle (Neurobasal A medium: 6-OHDA control group; n=5), hMSCs (n=4), hNPCs (n=5), hMSCs CM (n=6) or hNPCs CM (n=5) directly in the SNpc (coordinates related to Bregma: AP= - 5.3mm, ML= -1.8 mm, DV=-7.4mm) and striatum (coordinates related to Bregma: AP= -1.3 mm, ML= 4.7 mm, DV= -4.5 mm; AP= -0.4 mm, ML= 4.3 mm, DV= -4.5 mm; AP= 0.4 mm, ML= 3.1 mm, DV= -4.5 mm; AP= 1.3 mm, ML= 2.7 mm; DV= -4.5 mm) (Paxinos and Watson, 2007). 6-OHDA-control group received 4 μl of Neurobasal A medium in the SNpc and 2 μl in each coordinate of striatum at a rate of 1 μl/min. Cell transplanted groups received 200 000 cells in SNpc and 50 000 cells in each coordinate of striatum. CM-injected animals received 4 μl in the SNpc and 2 μl in each coordinate of striatum at a rate of 1 μl/min. After each injection the needle was left in place for 2 min in order to avoid any backflow up the needle tract. At one week, four weeks and seven weeks after treatments, behavioral assessment was performed (Figure 4).
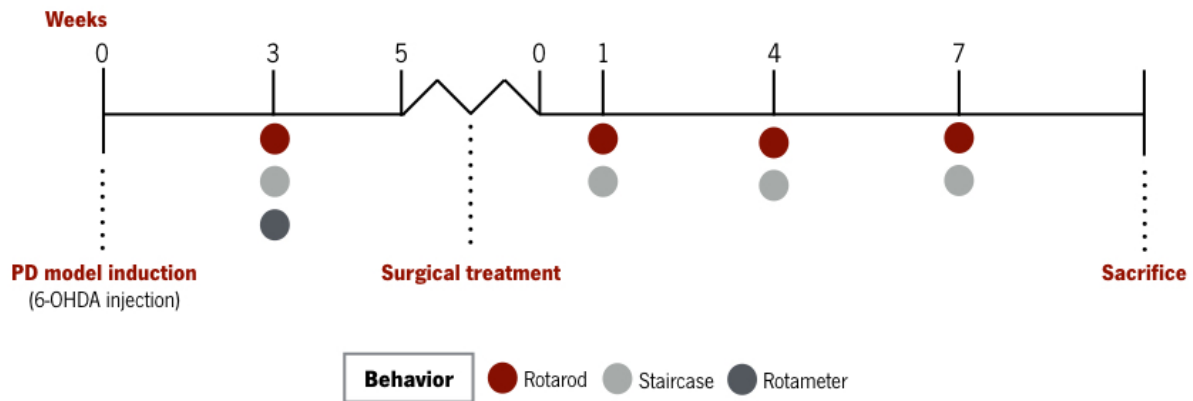
Figure 4. Experimental design.

PD model was induced by a 6-OHDA unilateral injection. 3 weeks later the animals were submitted to a first behavioral analysis to validate the model. Afterwards, the animals were treated with hMSCs, hNPCs and their secretome in the SNPc and striatum. After this, behavioral analysis (1, 4 and 7 weeks after transplantation) was performed, and the animals were posteriorly sacrificed.

3.4. Behavioral assessment

3.4.1. Rotarod

The Rotarod test was used to assess motor coordination and balance of the animals as previously described (Monville et al., 2006). All animals were pre-trained on an automated 4-lane Rotarod unit (3376-4R, TSE systems, USA) with 7 cm diameter drums (which are machined with grooves to improve grip) in order to get a stable performance. The training consisted of four trials during 3 days, under an accelerating protocol starting at 4 rpm and reaching 40 rpm in 5 min. As the speed of rotation is increases, it becomes more difficult for the animal to keep its balance. The animals were allowed to rest at least 20 min between each trial. At the fourth day using the same protocol, the animal latency to fall was recorded.

3.4.2. Skilled paw reaching test (Staircase)

The skilled paw reaching test (also named staircase test) was assessed using double staircase boxes (80300, Campden Instruments Ltd., UK) as previously described (Montoya et al., 1991). This test was developed to provide the basic assessment of the independent forelimb use in skilled reaching and grasping test. Briefly, this type of apparatus consists of a clear chamber with a hinged lid (285 x 90 x 60 mm). A narrow compartment, with a central platform running along its length, is connected to the chamber. The removable double staircase with 7 steps on each side can be inserted in the space between the platform and the box walls. Five pellets were placed into each well of the double staircase

apparatus. In the first day, the rats were familiarized with the test, with the pellets available for 10 min. In the test session, animals were placed inside the box, having 15 min to reach, retrieve and eat the food pellets. All sessions were performed at the same time of the day (during 7 days) and with food deprived animals. After each test period, animals were removed from the staircase boxes and the remaining (left over) pellets were counted. In the last 2 days it was performed a forced-choice task, in which the animals were forced to choose one of the steps-side of the double staircase (left or right), evaluating in this way the motor impairments of the affected side.

3.4.3. Apomorphine turning behavior (Rotameter)

Rotation asymmetry was performed under the influence of the apomorphine in order to obtain an estimate of the extent of DA depletion in each animal as previously described (Carvalho et al., 2013). For this purpose, animals were injected subcutaneously with 0.05 mg/kg apomorphine hydrochloride (Sigma, USA) dissolved in 1% of ascorbic acid in 0.9% NaCl, an then placed on automated metal testing bowls (MED-RSS, Med Associates, USA) during 45 min. Full body turns were counted and data was expressed as net contralateral rotations, with rotation toward the side of the lesion given a positive value. Net rotational behavior represents the number of contralateral turns minus the number of ipsilateral turns. As apomorphine is a strong DA agonist, its repeated use could lead to an overstimulation of the DAergic system, which could impair the adequate interpretation of the impact of the treatments on the functional outcomes of the animals. Therefore, this test was only used to select the animals that were truly injured upon 6-OHDA lesions (Bibbiani et al., 2005; Poewe and Wenning, 2000; Trenkwalder et al., 2015).

3.5. Histological analysis

After 13 weeks (including the development of the lesion and consequent treatment) animals were sacrificed with sodium pentobarbital (Eutasil, 60 mg/kg, i.p., Ceva Saúde Animal, Portugal) and transcardially perfused using 4% paraformaldehyde with 0.1% 1X PBS. Subsequently, the brains were stored in 30% sucrose solution with 0.1% azide before heading to histological processing.

3.5.1. Tyrosine hydroxylase immunohistochemistry

Striatal and mesencephalon coronal sections (including SNpc) were obtained using a vibratome (VT1000S, Leica, Germany) with a thickness of 50 μm and processed as free-floating sections. Four series of consecutive slices were obtained and storage at -20°C in a cryopreservation solution with

ethylene glycol and 30% sucrose.

Initially, the inhibition of endogenous peroxidase activity was performed using a solution of 1X PBS with 3% hydrogen peroxidase (H_2O_2) for 20 min. Then, the slices were permeabilized in 0.1% PBS-T (for 10 min) followed by blockage using a solution of 1X PBS with 5% NBCS during 2 h. After this, slices were incubated overnight at 4°C with rabbit TH primary antibody diluted in 1X PBS with 2% NBCS (TH, 1:2000, Millipore, USA). Afterwards, the slices were washed with 0.1% PBS-T (three times for 10 min). Then, after incubation for 30 min at RT with a biotinylated anti-rabbit secondary antibody (LabVison, USA), the sections were incubated with strepptavidine-peroxidase solution (LabVison, USA) for 30 min at RT. Slices were afterwards immersed in 1X Tris-HCl buffer for 10 min and the antigen visualization was performed using 3,3i-diaminobenzidine tetrahydrocloride (DAB, Sigma, USA) (25 mg of DAB in 50 mL of 1X Tris-HCL with 12.5 µl of H_2O_2). The slices were mounted on superfrost slides and allowed to dry in the dark. After 24 h, thionin counter-coloration was performed and the sections were coverslipped using entellan (Merck KGaA, Germany).

3.5.2. Stereological analysis

In order to have a representative sampling between all the animals, four identical TH-labeled slices covering the entire mesenphalon were chosen, including all the portions of the SNpc. Using a brightfield microscope (BX51, Olympus, Japan) equipped with a digital camera (PixeLINK PL-A622, CANIMPEX Enterprises Ltd., Canada), and with the help of Visiopharm integrator system software (V2.12.3.0, Denmark), the boundaries of SNpc area was drawn. The delineation of this region was performed through identification of anatomic standard reference points and with the help of the rat brain atlas (Paxinos and Watson, 2007). Counting of total TH-immunopositive cells in the SNpc area was performed on both hemispheres (40 x magnification), and the data were presented as the percentage (%) of remaining TH$^+$ cells in the lesioned side compared to the control side. All the counting and analysis was performed under blind conditions.

3.5.3. Striatal fiber density measurement

Total immunoreactivity of TH-positive fibers was measured by densitometry, being this method a gross estimation of the parkinsonian pathology as described by Febbraro *et al.* (Febbraro et al., 2013). For this purpose, TH-immunostained striatal sections (four sections per animal) representing the coordinates of injection sites (within the striatum) were selected and photographed (1 x magnification) under brightfield illumination (SZX16, Olympus, Japan) fitted with a DP-71 digital camera (Olympus,

Japan). All image analysis was completed using the ImageJ software (ImageJ v1.48, National Institute of Health, USA). Micrographs were converted to grey scale and analyzed for grey intensity after calibrating ImageJ program. This was done using the "optical density step tablet" to determine the optical density (O.D.) of the selected sections and performed according to program instructions. From this, striatum O.D. values were determined in both hemispheres using a 1.0 mm^2 rectangular grid, encompassing injection sites, as determined by anatomical references and rat brain atlas (Paxinos and Watson, 2007). Corpus callosum (internal control) O.D. was also measured in both hemisphere sides, to avoid nonspecific background. TH striatal fiber densities were determined by calculating the O.D. difference between the lesioned side and the corpus callosum, as well as, between the intact striatum and corpus callosum. The extent of the immunostaining on lesioned side was expressed as a percentage of the intact side (contralateral striatum).

3.5.4. BrdU administration and *in vivo* immunostaining

Rats were injected daily with 50 mg/kg (i.p.) of 5-bromo-2-deoxyuridine (BrdU; Sigma, USA) during 5 days before the sacrifice. Afterwards, striatal coronal sections were obtained by vibratome with a thickness of 50 μm and processed as described above. As first approach, sections were permeabilized with 0.3% PBS-T (three times for 6 min), and pre-treated with HCl (2M) for 45 min at RT. Then the slices were washed with 1X PBS (three times for 6 min) and incubated in 1X PBS with 10% NBCS during 30 min for endogenous blocking. After that, sections were incubated overnight at 4°C with rat BrdU primary antibody (1:100; Abcam, UK) for proliferation detection and rabbit TH primary antibody for DAergic neurons, diluted in 1X PBS with 2% of FCS. Sections were then washed in 1X PBS (three times for 6 min) and incubated with secondary antibodies: Alexa Fluor 488 goat anti-rat (Life Technologies, USA) and Alexa Fluor 594 goat anti-rabbit (Life Technologies, USA) during 2 h at RT. Then the slices were stained with DAPI, and mounted on slides using immu-mount.

Images were obtained with a confocal microscope (FV1000, Olympus, Japan) using the software FV10-ASW 2.0c (Olympus, Japan), presenting part of SEZ and striatum (five sections per animal were analyzed for a n=3/group).

3.6. Proteomics - Mass Spectrometry and SWATH Acquisition
3.6.1. In gel digestion/Sample preparation

hMSCs and hNPCs CM was firstly concentrated (100X) using a 5 kDA cut-off concentrator (Vivaspin, GE Healthcare, UK) by ultracentrifugation at 3000 g during 45 min. Proteomic analysis of the

hMSCs and hNPCs CM was performed at Dr.Bruno Manadas Laboratory (Proteomic Unit of CNC/Biocant) and the outcomes of this were analysed in our laboratory. For this purpose, the samples were precipitated using the Trichloroacetic acid (TCA, Sigma, USA) – Acetone (Sigma, USA) procedure. TCA was added to each sample to a final concentration of 20% (v/v), followed by 30 minutes of incubation at -80°C and centrifugation at 20 000 g for 20 min. Protein pellets were washed with ice-cold (-20°C) acetone. Briefly, the pellets were solubilized in acetone, aided by ultrasonication, followed by a centrifugation at 20 000 g for 20 min. The washed pellets were ressuspended in 40 μL 2X Laemmli buffer (BioRad, USA), aided by ultrasonication and denaturation at 95°C, and 10 μL of each replicate (in a total of three replicates per condition) were used to create a pooled sample for protein identification.

After denaturation, the replicates and pooled samples were alkylated with acrylamide and subjected in gel digestion by using the short-GeLC approach (Anjo et al., 2014). Briefly, the entire sample was loaded in a "4–20% TGX Stain-Free Gel" (Bio-Rad, USA) and subjected to a partially electrophoretic separation: 15 min at 110 V to allow the samples to enter into the gel. After SDS-PAGE proteins were visualized with Colloidal Coomassie Blue. The staining was performed as previously described (Candiano et al., 2004) with slight modifications (Manadas et al., 2009). The entire lanes were sliced into three parts and each part was sliced in small pieces and processed. Gel pieces were destained using the destaining solution (50 mM ammonium bicarbonate and 30% acetonitrile) following by a washing step with water. Gel pieces were dehydrated on Concentrador Plus/Vacufug Plus (Eppendorf, Germany). Then, were added 75 μL of trypsin (0.01 μg/μL solution in 10 mM ammonium bicarbonate) to the dried gel bands and left for 15 min on ice to rehydrate de gel pieces. After this period, 30 μL of 10 mM ammonium bicarbonate were added and in-gel digestion was performed overnight in the dark at RT. After the digestion, the excess solution from gel pieces were collected to a low binding microcentrifuge tube (LoBind, Eppendorf, Germany) and peptides were extracted from the gel pieces by sequential addition of three solutions of acetonitrile (ACN) in 1% formic acid (FA) (30%, 50%, and 98% of ACN, respectively). After the addition of each solution, the tubes were shaken in the thermomixer (Eppendorf, Germany) at 1050 rpm for 15 min and the solution was collected to the tube containing the previous fraction. At this stage, the peptides extracted from the three fraction of each replicate sample were combined into a single sample for quantitative analysis. All the peptides mixtures were dried (preferentially not completely) by rotary evaporation under vacuum. Before performing the liquid chromatography coupled with tandem mass spectrometry (LC-MS/MS) analysis, the peptide mixtures were subjected to SPE using OMIX tips with C18 stationary phase (Agilent Technologies, USA)

as recommended by the manufacture. Eluates were dried by rotator evaporation, avoiding to totally evaporate the samples and peptides mixtures were ressuspended in 20 µL solution of 2% ACN and 0.1% FA followed by vortex, spin and sonication in water bath [2 min with pulses of 1-1 s sonication followed by 1 s break pulse, at 20% intensity, in a sonicator VibraCell 750 watts (Sonics&Materials, USA)]. In order to remove insoluble material the peptide mixture were then centrifuged for 5 min at 14 000 g and collected into the proper vial for LC-MS injection.

3.6.2. SWATH acquisition

Samples were analyzed on a Triple TOF 5600 System (ABSciex, USA) in two phases: information-dependent acquisition (IDA) of the pooled samples and SWATH (Sequential Windowed data independent Acquisition of the Total High-resolution Mass Spectra) acquisition of each individual sample. Peptides were resolved by LC (nanoLC Ultra 2D, Eksigent, USA) on a Micro LC column ChromXP C18CL (300 µm ID × 15cm length, 3 µm particles, 120 Å pore size, Eksigent, USA) at 5 µL/min with a multistep gradient: 0-2 min linear gradient from 5 to 10 %, 2-45 min linear gradient from 10 % to 30 % and, 45-46 min to 35 % of acetonitrile in 0.1 % FA. Peptides were eluted into the mass spectrometer using an electrospray ionization source (DuoSpray Source, ABSciex, USA) with a 50 µm internal diameter (ID) stainless steel emitter (New Objective, USA).

IDA experiments were performed for each 3 peptides mixtures per samples. The mass spectrometer was set to scanning full spectra of ions (350-1250 m/z range) for 250 ms, followed by up to 100 MS/MS scans (100–1500 m/z from a dynamic accumulation time - minimum 30 ms for precursor above the intensity threshold of 1000, in order to maintain a cycle time of 3.3 s). Candidate ions with a charge state between +2 and +5 and counts above a minimum threshold of 10 counts per second were isolated for fragmentation and one MS/MS spectra was collected before adding those ions to the exclusion list for 25 seconds (mass spectrometer operated by Analyst TF 1.7, ABSciex, USA). Rolling collision was used with a collision energy spread of 5 eV. Peptide identification and library generation were performed with Protein Pilot software (v5.1, ABSciex, USA), using the following parameters: i) search against a database composed by *Homo Sapiens* from SwissProt (release at April 2016), and *malE*-GFP or against a database composed by *Homo Sapiens and Bovine* from SwissProt (release at April 2016), and *malE*-GFP; ii) acrylamide alkylated cysteines as fixed modification and iii) trypsin as digestion type. An independent False Discovery Rate (FDR) analysis using the target-decoy approach provided with Protein Pilot software was used to assess the quality of the identifications and

positive identifications were considered when identified proteins and peptides reached a 5% local FDR (Sennels et al., 2009; Tang et al., 2008).

For SWATH-MS based experiments, the mass spectrometer was operated in a looped product ion mode (Gillet et al., 2012) and the same chromatographic conditions used as in the IDA run described above. The SWATH-MS setup was designed specifically for the samples to be analyzed, in order to adapt the SWATH windows to the complexity of the set of samples to be analyzed. A set of 60 windows of variable width (containing 1 m/z for the window overlap) was constructed covering the precursor mass range of 350-1250 m/z. A 250 ms survey scan (350-1500 m/z) was acquired at the beginning of each cycle for instrument calibration and SWATH-MS spectra were collected from 100–1500 m/z for 50 ms, resulting in a cycle time of 3.25 s from the precursors ranging from 350 to 1250 m/z. The collision energy for each window was determined according to the calculation for a charge +2 ion centered upon the window with variable collision energy spread (CES) according with the window.

A specific library of precursor masses and fragment ions was created by combining all files from the IDA experiments, and used for subsequent SWATH processing. Libraries were obtained using Protein Pilot™ software (v5.1, ABSciex, USA) with the same parameters as described above. Data processing was performed using SWATH processing plug-in for PeakView (v2.0.01, ABSciex, USA). Briefly, peptides were selected automatically from the library using the following criteria: (i) the unique peptides for a specific targeted protein were ranked by the intensity of the precursor ion from the IDA analysis as estimated by the ProteinPilot software and (ii) Peptides that contained biological modifications and/or were shared between different protein entries/isoforms were excluded from selection. Up to 15 peptides were chosen per protein, and SWATH quantitation was attempted for all proteins in library file that were identified below 5% local FDR from ProteinPilot searches. In SWATH acquisition data peptides are confirmed by finding and scoring peak groups, which are a set of fragment ions for the peptide.

Target fragment ions, up to 5, were automatically selected and peak groups were scored following the criteria previously described (Lambert et al., 2013). Peak group confidence threshold was determined based on a FDR analysis using the target-decoy approach and 1% extraction FDR threshold was used for all the analyses. Peptide that met the 1% FDR threshold in at least two of the three biological replicates were retained, and the peak areas of the target fragment ions of those peptides were extracted across the experiments using an extracted-ion chromatogram (XIC) window of 4 min with 100 ppm XIC width. The levels of the human proteins were estimated by summing all the transitions from all the peptides

for a given protein [an adaptation (Collins et al., 2013)] and normalized to the internal standard (*malE*-GFP).

3.7. Data analysis

Statistical analysis was performed using IBM SPSS Statistics ver.22 (IBM Co., USA) and graph's representation using GraphPad Prism ver.6 (GraphPad Software, La Jolla, USA).

For the evaluation of the *in vitro* assay a one-way ANOVA was applied in order to compare the mean values for the three groups. Statistical evaluation for animal behavior tests after 6-OHDA injections was performed using an independent sample t-test, and repeated measures ANOVA if an evaluation along time was desired. After treatments, the behavior and histological data was analyzed using one-way ANOVA in order to compare the mean values for the six groups. If an evaluation along time was required, a mixed design factorial ANOVA was performed. Regarding proteomic analysis, the differences between the two tested conditions were evaluated using an independent sample t-test (for each protein individually).

Normality was measured using the Kolmogorov-Smirnov and Shapiro-Wilk statistical tests and taking into account the respective histograms and measures of skewness and kurtosis. Equality of variances and Sphericity were measured using the Levene's and Mauchly's tests, respectively, and was assumed when p>0.05. Multiple comparisons between groups were accomplished through the Bonferroni statistical test.

Values were accepted as significant if the p-value was higher than 0.05 and all results were expressed as group mean±SEM (standard error of the mean). Effect size was calculated using the Cohen's d or $\eta^2_{partial}$.

4.1. Neuronal differentiation of hNPCs induced by hMSCs and hNPCs conditioned medium

hNPCs grow as neurospheres (Figure 5A) in the presence of PPRF-h2 serum-free medium as previously described (Baghbaderani et al., 2010). Typically, upon removal of PPRF-h2 medium hNPCs lose their neurosphere-like conformation, adhere to tissue culture plastic and spontaneously start to differentiate (Figure 5B).
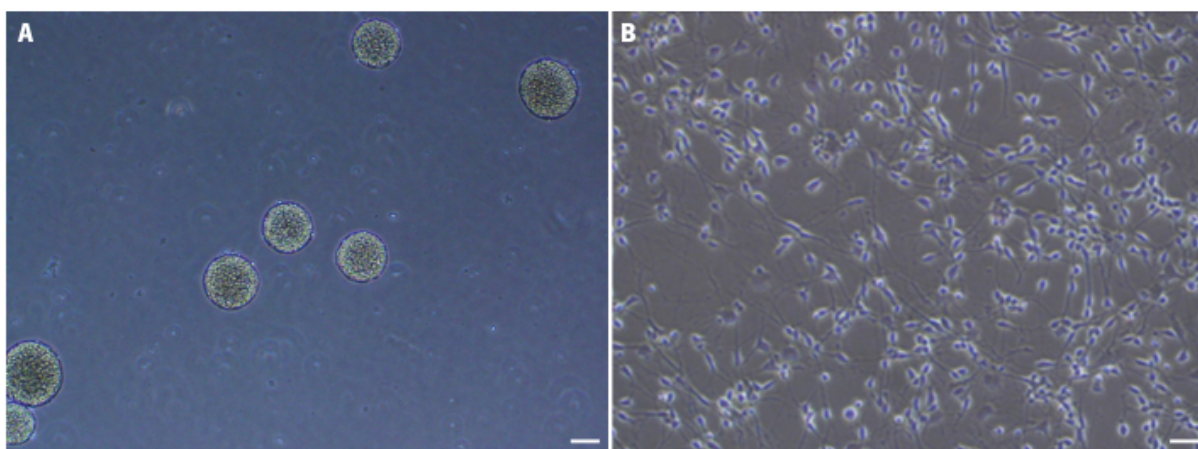
Figure 5. Expansion of hNPCs derived from telencephalon *in vitro*.

(A) In the presence of PPRF-h2 growth medium, continued cell division generates non-adherent neurospheres. (B) Spontaneous differentiation into neural phenotypes upon PPRF-h2 removal. (Scale bar: 100 μm).

Regarding the effects of hMSCs and hNPCs CM on the differentiation of hNPCs, results have revealed distinct trends (Figure 6; Table 3). Indeed, immunocytochemistry analysis revealed that when hNPCs were incubated for 5 days with the hMSCs secretome there was a significant increase in the cell population expressing beta III tubulin (intermediate neuronal state of maturation, Figure 6G) and MAP-2 (mature neurons, Figure 6K) when compared to the control group (incubation with Neurabasal A medium, Figure 6E, H-I, L). Additionally, it was possible to observe that the secretome of hMSCs also induced an increased differentiation of beta III tubulin and MAP-2 positive cells when compared to the secretome of hNPCs (Figure 6F, H, J, L). Regarding the DCX positive cells (immature neurons, Figure 6A-D) no differences were found between groups.

Figure 6. *In vitro* **differentiation of hNPCs.**

hMSCs secretome was able to significantly increase the differentiation of hNPCs into (G) beta III tubulin-positive cells and (K) MAP-2-positive cells when compared to the (F, J) secretome of hNPCs and to the (E, I) control group (H, L). Data presented as mean±SEM. n=3. *p<0.05, ***p<0.001. CTR: control group (Neurobasal A medium); CM_N: hNPCs conditioned medium; CM_M: hMSCs conditioned medium. (Scale bar: 50 μm).

Table 3. Statistical analysis of the in vitro assay (Data presented as mean±SEM)

Markers	Control	hNPCs CM	hMSCs CM	Statistical test, significance, effect size
DCX	19.5±2.7	21.4±7.5	36.8±2.1	$F_{(2,7)}$=5.0, p=0.045, $\eta^2_{partial}$=0.588
Beta III tubulin	18.9±5.7	9.4±8.7	44.6±0.91	$F_{(2,4)}$=15.3, p=0.013, $\eta^2_{partial}$=0.884
MAP-2	19.5±5.3	30.5±7.0	53.3±3.8	$F_{(2,19)}$=10.9, p=0.001, $\eta^2_{partial}$=0.535

4.2. *In vivo* assay

4.2.1. Phenotypic characterization of 6-OHDA lesions

To further evaluate the functional integrity of the DAergic system after the injection of 6-OHDA, and therefore select the animals that were truly injured, the rotameter test was performed at the end of the behavior assessment (rotarod and staircase tests). 3 weeks after the 6-OHDA injections, statistical analysis revealed differences in the apomorphine-induced turning behavior, resulting from a significantly higher number of rotations in the 6-OHDA-injected animals when compared to the Sham group (Figure 7A; Table 4). In addition, also the motor performance of the animals was affected by the 6-OHDA injections. Motor coordination and balance, measured by the rotarod test, was found to be impaired in animals injected with 6-OHDA (Figure 7B; Table 4). In the staircase test, used to assess the forelimb use and skilled motor function, was also observed that the 6-OHDA-injected animals were evidently affected when compared to Sham animals (Figure 7C; Table 4). Furthermore, a significant effect was observed for factor time (days) and interaction between time and group (Table 4). Moreover, in the forced-choice task (in which animals were forced to choose one of the steps-side), the 6-OHDA-injected animals were also found to be significantly impaired in the left side (the affected side) when compared to the Sham animals (Figure 7D; Table 4).
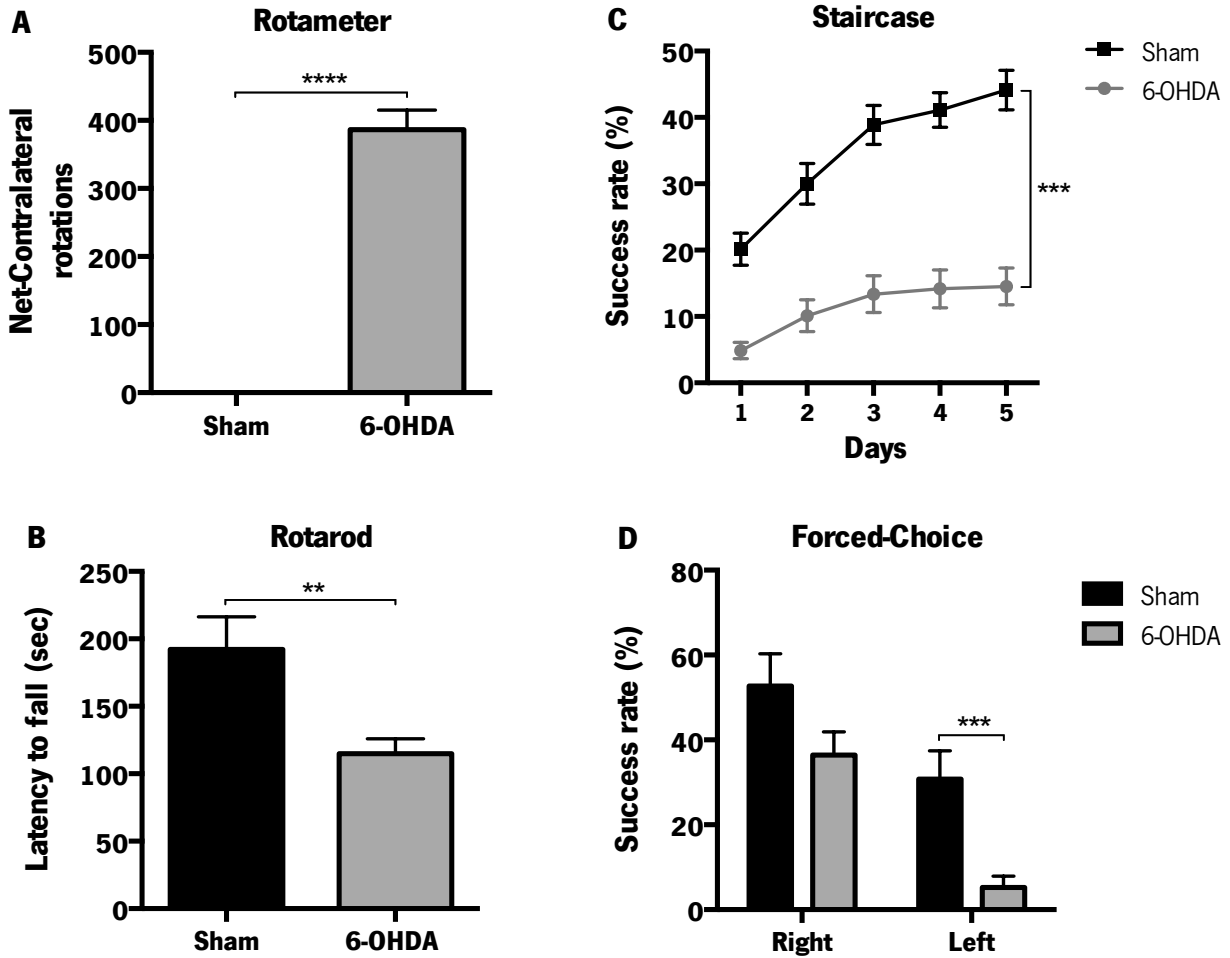
Figure 7. Behavioral characterization of 6-OHDA-induced lesions.

(A) Apomorphine-induced turning behavior (rotameter) revealed that 6-OHDA-injected animals exhibited intense turning behavior when compared to Sham group. 6-OHDA-injected animals also presented significant impairment in motor coordination on the (B) rotarod test and in (C,D) the paw-reaching test performance. Sham: n=9, 6-OHDA: n=25. Data presented as mean±SEM. *p<0.05, **p<0.01, ***p<0.001, ****p<0.0001.

Table 4. Statistical analysis of the phenotypic characterization of the 6-OHDA lesions (Data presented as mean±SEM)

Behavior tests		Sham	6-OHDA	Statistical test, significance, effect size
Rotameter		0±0	386.3±28.9	$t_{(28)}$=8.7, p<0.0001, Cohen's d=0.899
Rotarod		192.3±24.1	114.9±11.1	$t_{(27)}$=3.3, p=0.003, Cohen's d=0.555
Staircase	Day 1	20.2±2.4	4.9±1.2	Treatment effect:
	Day 2	30.0±3.1	10.1±2.4	$F_{(1,32)}$=31.8, p<0.0001, $\eta^2_{partial}$=0.498
	Day 3	38.8±2.9	13.4±2.8	Time effect: $F_{(2.8,90.2)}$=35.4, p<0.0001, $\eta^2_{partial}$=0.525
	Day 4	41.1±2.6	14.2±2.8	
	Day 5	44.1±3.0	14.5±3.1	Interaction time-group: $F_{(2.8,90.2)}$=4.5, p=0.006, $\eta^2_{partial}$=0.124
Forced-choice right		52.7±7.6	36.5±5.4	$t_{(32)}$=1.6, p=0.119, Cohen's d=0.308
Forced-choice left		30.8±6.6	5.3±2.6	$t_{(32)}$=4.4, p<0.001, Cohen's d=0.604

4.2.2. Transplantation of hMSCs, hNPCs and conditioned medium

In order to address the effects of hMSCs and hNPCs transplantation and its CM (i.e. secretome) in 6-OHDA-injected animals, the motor performance was assessed at 1, 4 and 7 weeks after treatments through the rotarod and staircase tests, as previously described.

4.2.2.1. Rotarod

Regarding motor coordination and balance, assessed by the rotarod test, statistical analysis showed a significant effect for the factor treatment and for the factor time (weeks), but no interaction between these factors (Table 5). When we compared the animals injected with cells (hNPCs and hMSCs) and its CM with the untreated group 6-OHDA, the CM injected animals (of both hMSCs and hNPCs) displayed a positive trend on the latency to fall (Figure 8). In addition to this, when we compared CM-injected animals with cells-transplanted animals, we were able to observe a significant improvement of motor coordination performance promoted by the hMSCs and hNPCs CM when compared to hNPCs-injected group ($p < 0.05$, Figure 8).
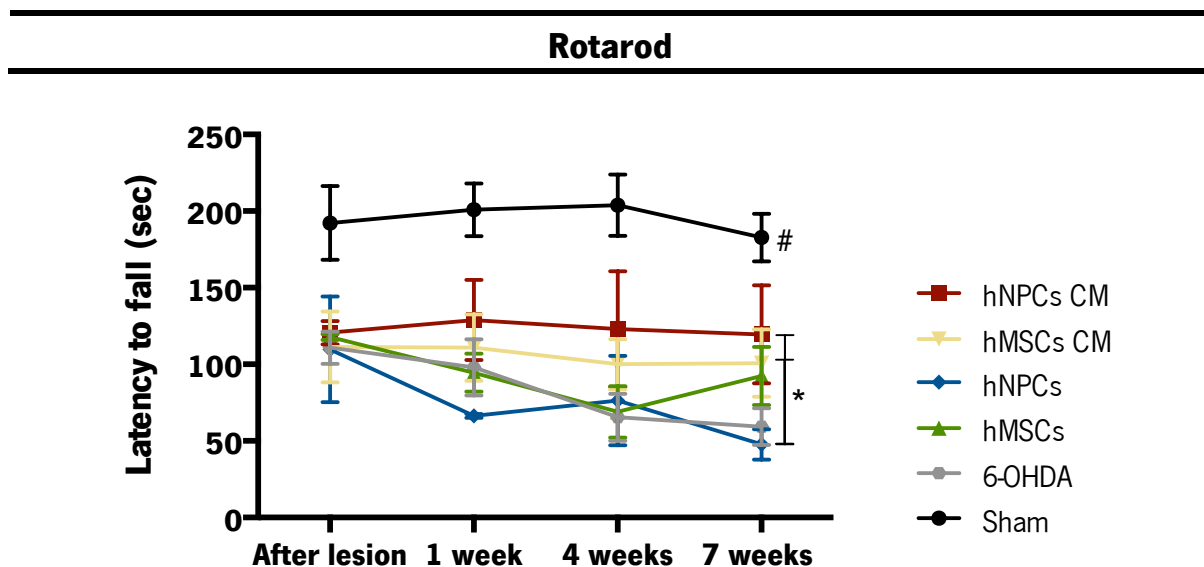
Figure 8. Motor coordination performance 1, 4 and 7 weeks after the transplantation of hMSCs, hNPCs and its CM (i.e. secretome) in the SNpc and striatum.

Latency to fall was measured in the accelerating rotarod test, demonstrating that the hMSCs and hNPCs CM-injected animals had a significant improvement in their motor coordination when compared to the hNPCs-transplanted group. Sham: n=7, 6-OHDA control: n=5, hMSCs: n=4, hNPCs: n=5, hMSCs CM: n=5, hNPCs CM: n=5. Data presented as mean±SEM. *$p < 0.05$. Sham animals statistically different from all the other groups, #$p < 0.001$.

Table 5. Statistical analysis of the rotarod test after treatments (Data presented as mean±SEM)

Group	After lesion	1 week	4 weeks	7 weeks	Statistical test, significance, effect size
Sham	192.3±24.1	200.8±17.1	203.8±20.0	182.8±15.5	Treatment effect:
6-OHDA control	110.9±10.5	98.0±18.3	65.5±15.4	59.3±12.0	$F_{(5,25)}$=15.2, p<0.0001, $\eta^2_{partial}$=0.753
hMSCs	117.7±1.9	94.5±12.41	69.0±16.8	92.5±18.9	Time effect:
hNPCs	109.8±34.5	66.35±1.2	76.4±29.2	47.7±9.9	$F_{(3,75)}$=3.5, p=0.018, $\eta^2_{partial}$=0.124
hMSCs CM	111.35±23.05	111.0±21.7	100.1±16.9	100.8±22.0	Interaction time-group:
hNPCs CM	120.7±7.6	128.9±26.1	123.0±37.8	119.6±32.0	$F_{(15,75)}$=0.8, p=0.669, $\eta^2_{partial}$=0.139

4.2.2.2. Staircase

The skilled paw reaching test was used to assess the forelimb use and the fine motor coordination of the animals. Statistical analysis revealed a significant effect for the factor treatment and for the factor time (weeks), but no interaction between these two factors (Table 6). Comparing the animals injected with CM with the untreated group (6-OHDA), post-hoc analysis revealed that the injection of CM (from both hMSCs and hNPCs) led to a significant improvement on the success rate of eaten pellets (p<0.05, Figure 9A). Moreover, we were also able to observe that hMSCs CM ameliorate the performance in the injected animals when compared to the hNPCs-transplanted group (p<0.05, Figure 9A).

Regarding the forced-choice task, in which the animals were forced to choose one of the steps-side of the double staircase, statistical analysis revealed an effect for the factor treatment and for the factor time (weeks), but no effect in the interaction between these factors (Figure 9B-C; Table 7 and Table 8). Regarding the left side (the affected side), when we compared animals injected with the cells (hNPCs and hMSCs) and its CM with the untreated group 6-OHDA, hMSCs CM-injected animals displayed a positive trend on the success rate of eaten pellets when compared to the untreated group 6-OHDA (Figure 9B).
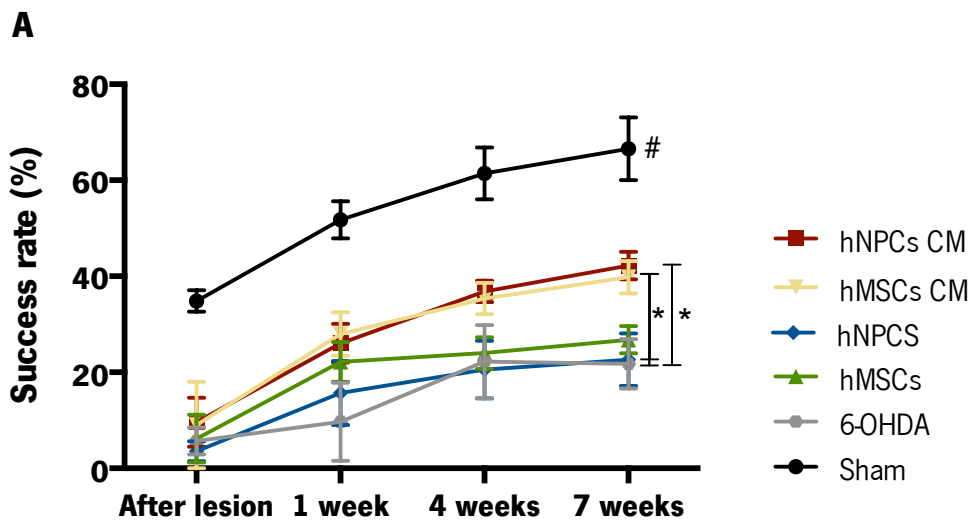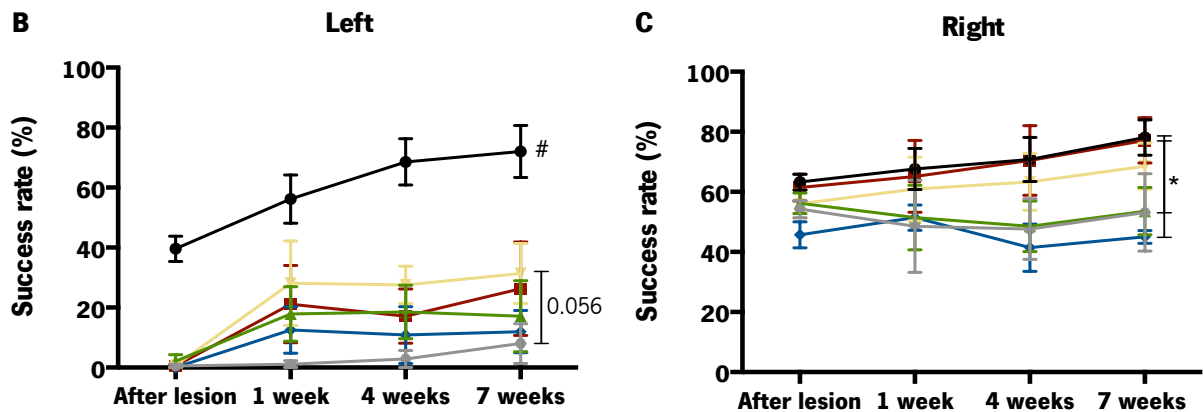
Figure 9. Skilled motor performance 1, 4 and 7 weeks after the transplantation of hMSCs, hNPCs and its CM (i.e. secretome) in the SNpc and striatum.

(A) Paw reaching performance of rats (through staircase test) demonstrated a significant improvement of the forelimb coordination of the hMSCs and hNPCs CM-injected animals when compared to the untreated group 6-OHDA. The animals injected with hMSCs CM also presented significant improvements when compared to the hNPCs-transplanted group. When the animals were submitted to the (B, C) paw reaching forced performance task, the animals injected with hMSCs CM displayed positive trend in skilled motor performance when compared to the untreated group 6-OHDA regarding the left side (the affected side). Performance of rats is expressed as success rate of eaten pellets. Sham: n=9, 6-OHDA control: n=5, hMSCs: n=4, hNPCs: n=5, hMSCs CM: n=6, hNPCs CM: n=5. Data presented as mean±SEM. *p<0.05. Sham animals statistically different from all the other groups, #p<0.001.

Table 6. Statistical analysis of the staircase test after treatments (Data presented as mean±SEM)

Group	After lesion	1 week	4 weeks	7 weeks	Statistical test, significance, effect size
Sham	34.9±2.2	51.7±3.9	61.5±5.4	66.6±6.6	
6-OHDA control	5.7±2.8	9.7±8.1	22.2±7.6	21.8±5.1	Treatment effect: $F_{(5,28)}$=13.9, p<0.0001, $\eta^2_{partial}$=0.712
hMSCs	6.19±5.0	22.14±4.1	24±3.3	26.8±2.8	Time effect:
hNPCs	3.6±2.1	15.7±6.7	20.6±6.0	22.6±5.5	$F_{(1.6,43.7)}$=49.4, p<0.0001, $\eta^2_{partial}$=0.638
hMSCs CM	9±9.0	28.0±4.5	35.4±3.3	39.8±3.4	Interaction time-group:
hNPCs CM	9.62±5.1	26.1±4.0	36.9±2.2	42.2±2.9	$F_{(7.8,43.7)}$=1.2, p=0.305, $\eta^2_{partial}$=0.180

Table 7. Statistical analysis of the forced choice task for the left side after treatments (Data presented as mean±SEM)

| Group	After lesion	1 week	4 weeks	7 weeks	Statistical test, significance, effect size
Sham	39.6±4.2	56.2±8.0	68.6±7.7	77.1±8.7	
6-OHDA control	0.6±0.6	1.1±1.1	2.9±2.9	8±6.7	Treatment effect: $F_{(5,28)}$=8.5, p<0.0001, $\eta^2_{partial}$=0.604
hMSCs	2.1±2.1	17.9±9.1	18.6±8.9	17.4±11.8	Time effect:
hNPCs	0±0	12.6±7.6	10.9±9.4	12.0±7.0	$F_{(3,84)}$=7.1, p<0.001, $\eta^2_{partial}$=0.203
hMSCs CM	0.7±0.7	28.1±14.1	27.6±6.2	31.4±10.0	Interaction time-group:
hNPCs CM	0.6±0.6	21.1±12.9	17.1±9.0	26.3±15.6	$F_{(15,84)}$=1.1, p=0.407, $\eta^2_{partial}$=0.159

Table 8. Statistical analysis of the forced choice task for the right side after treatments (Data presented as mean±SEM)

Group	After lesion	1 week	4 weeks	7 weeks	Statistical test, significance, effect size
Sham	63.3±2.8	67.6±6.9	70.8±7.3	78.1±5.9	
6-OHDA control	54.3±2.9	48.6±15.3	47.6±10.1	53.1±12.9	Treatment effect: $F_{(5,28)}$=3.0, p=0.028, $\eta^2_{partial}$=0.346
hMSCs	56.2±3.4	51.4±9.6	48.6±8.4	53.6±7.9	Time effect:
hNPCs	45.7±4.4	51.4±4.2	41.4±7.9	45.0±2.1	$F_{(1.8,49.9)}$=12.7, p<0.0001, $\eta^2_{partial}$=0.311
hMSCs CM	56±4.7	60.9±10.6	63.3±9.4	68.6±7.7	Interaction time-group:
hNPCs CM	61.4±4.4	65.1±12.0	70.5±11.6	77.1±7.6	$F_{(8.9,49.9)}$=0.6, p=0.778, $\eta^2_{partial}$=0.099

4.3. Assessment of the extension of the lesion

In order to analyze the effects of the 6-OHDA injections as well as the resulting treatments, histological analyses for TH was performed. From the results we observed that there was a significant decrease of DAergic neurons after the injection of 6-OHDA into the MFB (Figure 10A-F; Table 9). Statistical analyses demonstrated that the injection of the hMSCs CM most likely play a role in the survival of DAergic neurons, leading to a significant increase of TH-positive cells in the SNpc when compared to the untreated group 6-OHDA ($p<0.05$, Figure 10G). The same observations were also found in the striatum, by assessing TH-positive fibers through densitometry analysis (Figure 11A-F; Table 10). Comparing the animals injected with cells (hMSCs and hNPCs) and its CM with the untreated group 6-OHDA, statistical analysis revealed that hMSCs CM was able to increase the TH expression levels when compared to the untreated group 6-OHDA ($p<0.05$, Figure 11G).

Table 9. Statistical analysis of the TH-positive cells in the SNpc (Data presented as mean±SEM)

Group	Mean±SEM	Statistical test, significance, effect size
Sham	83.5±3.6	
6-OHDA control	1.8±0.1	
hMSCs	6.7±1.9	$F_{(5,28)}=54.2$, $p<0.0001$, $\eta^2_{partial}=0.906$
hNPCs	6.7±2.8	
hMSCs CM	21.5±8.5	
hNPCs CM	16.2±6.1	

Table 10. Statistical analysis of the TH-positive fibers in the striatum (Data presented as mean±SEM)

Group	Mean±SEM	Statistical test, significance, effect size
Sham	82.9±4.6	
6-OHDA control	12.8±1.3	
hMSCs	18.7±1.6	$F_{(5,25)}=71.6$, $p<0.0001$, $\eta^2_{partial}=0.952$
hNPCs	14.0±1.8	
hMSCs CM	27.5±2.6	
hNPCs CM	24.9±4.7	
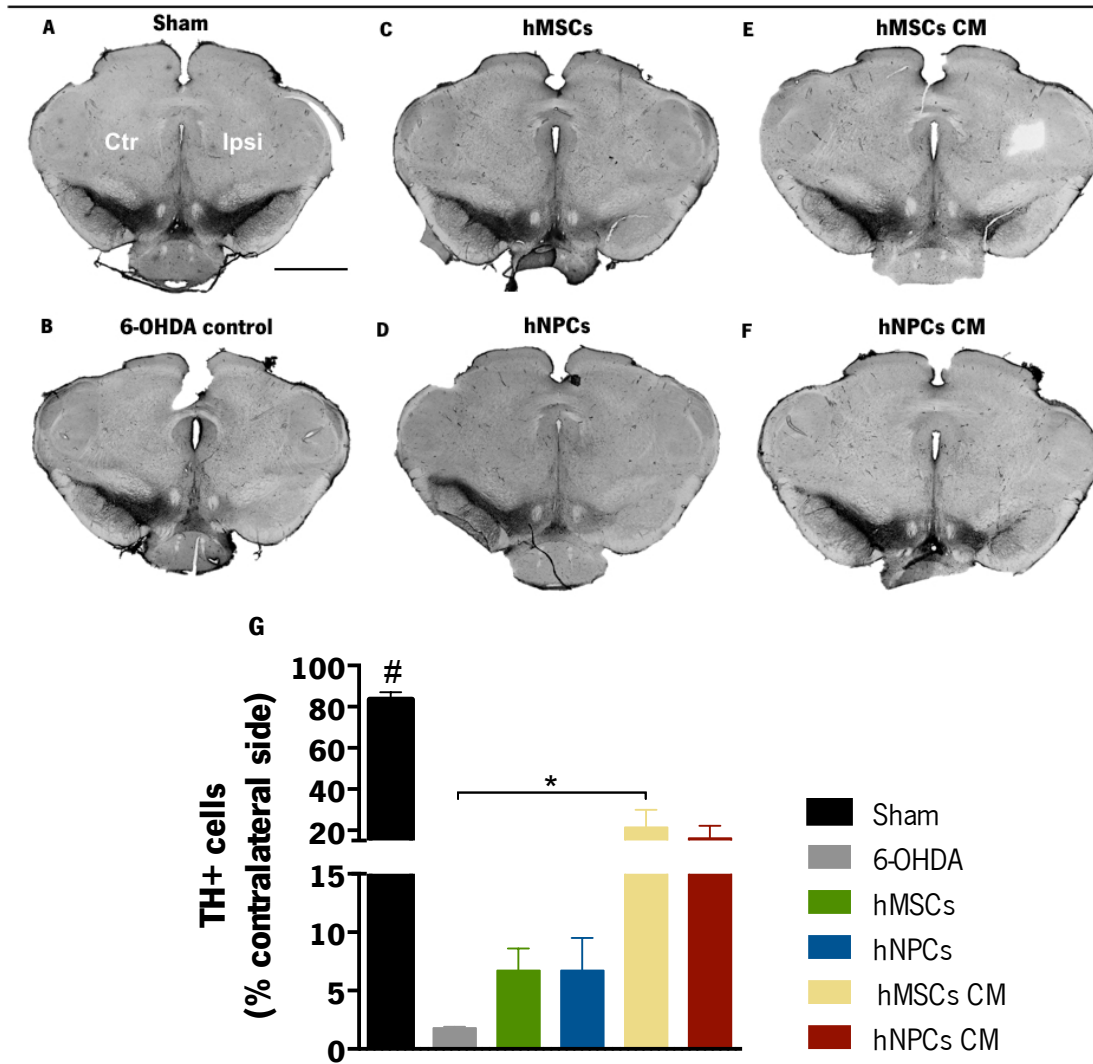
Figure 10. Representative micrographs of SNpc slices stained for TH.

Compared to the (A) Sham group, all the animals that were submitted to 6-OHDA injection presented a reduction of TH cells (B-F). However, animals injected with (E) hMSCs CM presented a significant TH-positive staining cells when compared to (B) 6-OHDA-control group (G). Sham: n=9, 6-OHDA control: n=5, hMSCs: n=4, hNPCs: n=5, hMSCs CM: n=6, hNPCs CM: n=5. Data presented as mean±SEM. *p<0.05. Sham animals statistically different from all the other groups, #p<0.001. (Scale bar: 2000 μm).
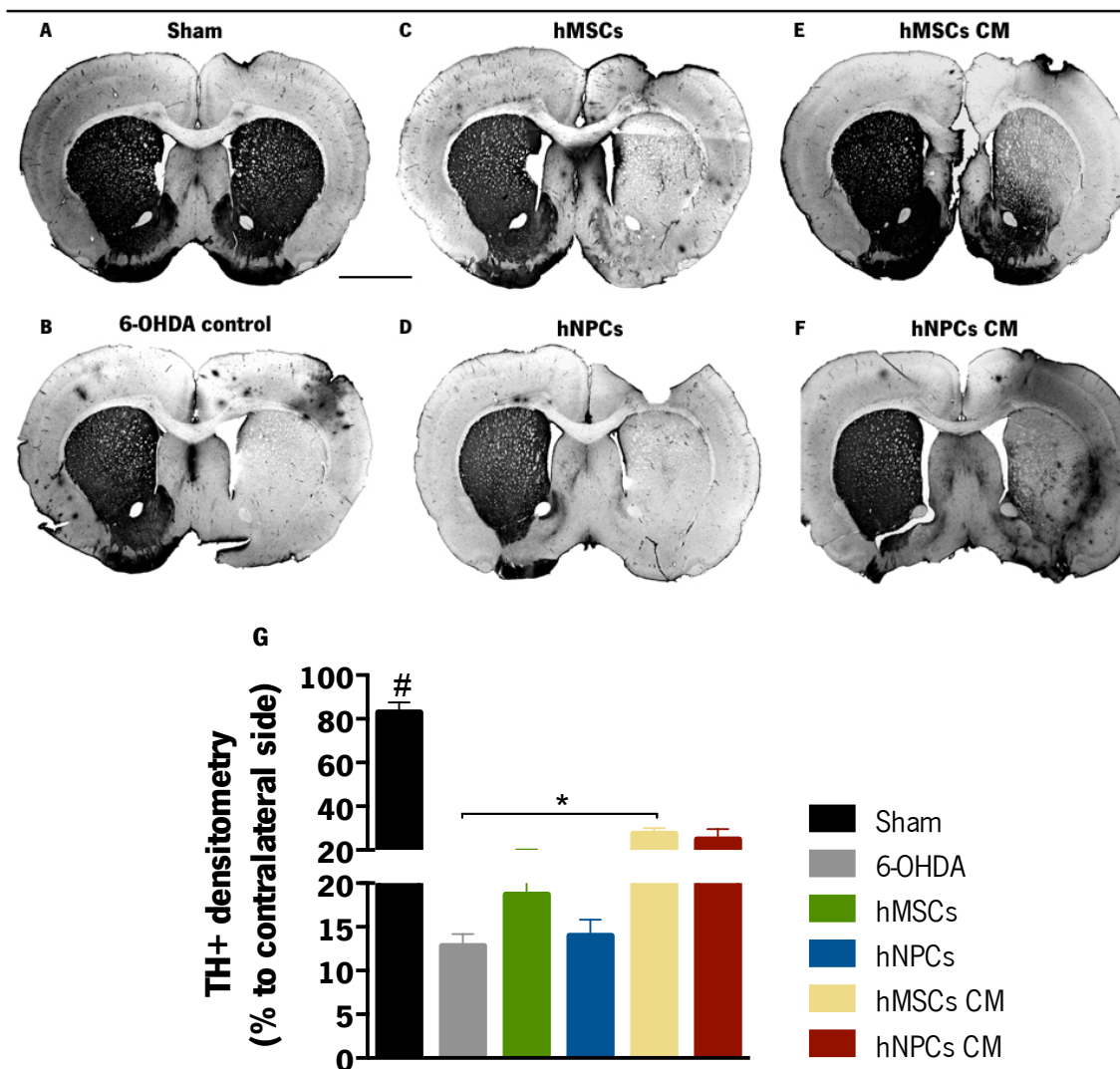
Figure 11. Representative micrographs of striatum slices stained for TH.

Compared to the (A) Sham group, all the animals that were submitted to 6-OHDA injection presented a reduction of the TH positive fibers (B-F). However, animals injected with (E) hMSCs CM presented a significant TH-positive staining when compared to (B) 6-OHDA-control group (G). Sham: n=6, 6-OHDA control: n=5, hMSCs: n=4, hNPCs: n=5, hMSCs CM: n=6, hNPCs CM: n=5. Data presented as mean±SEM. *p<0.05. Sham animals statistically different from all the other groups, #p<0.001. (Scale bar: 2000 μm).

4.4. Secretome of hNPCs and hMSCs increased BrdU and TH-positive cells

Qualitative analysis of the SEZ and striatum (Figure 12) indicates that the secretome of both hMSCs and hNPCs (Figure 12E-F) increased the expression of BrdU and TH-positive cells in the lesion side when compared to the untreated group 6-OHDA (Figure 12B) and to the cell-transplanted groups (Figure 12C-D). Interestingly, we have observed that hMSCs CM seems to be more prone to induce DAergic neuronal differentiation in the lesion side (Figure 12E, BrdU+TH co-localization), although quantitative analysis is further required to ensure this assumption.
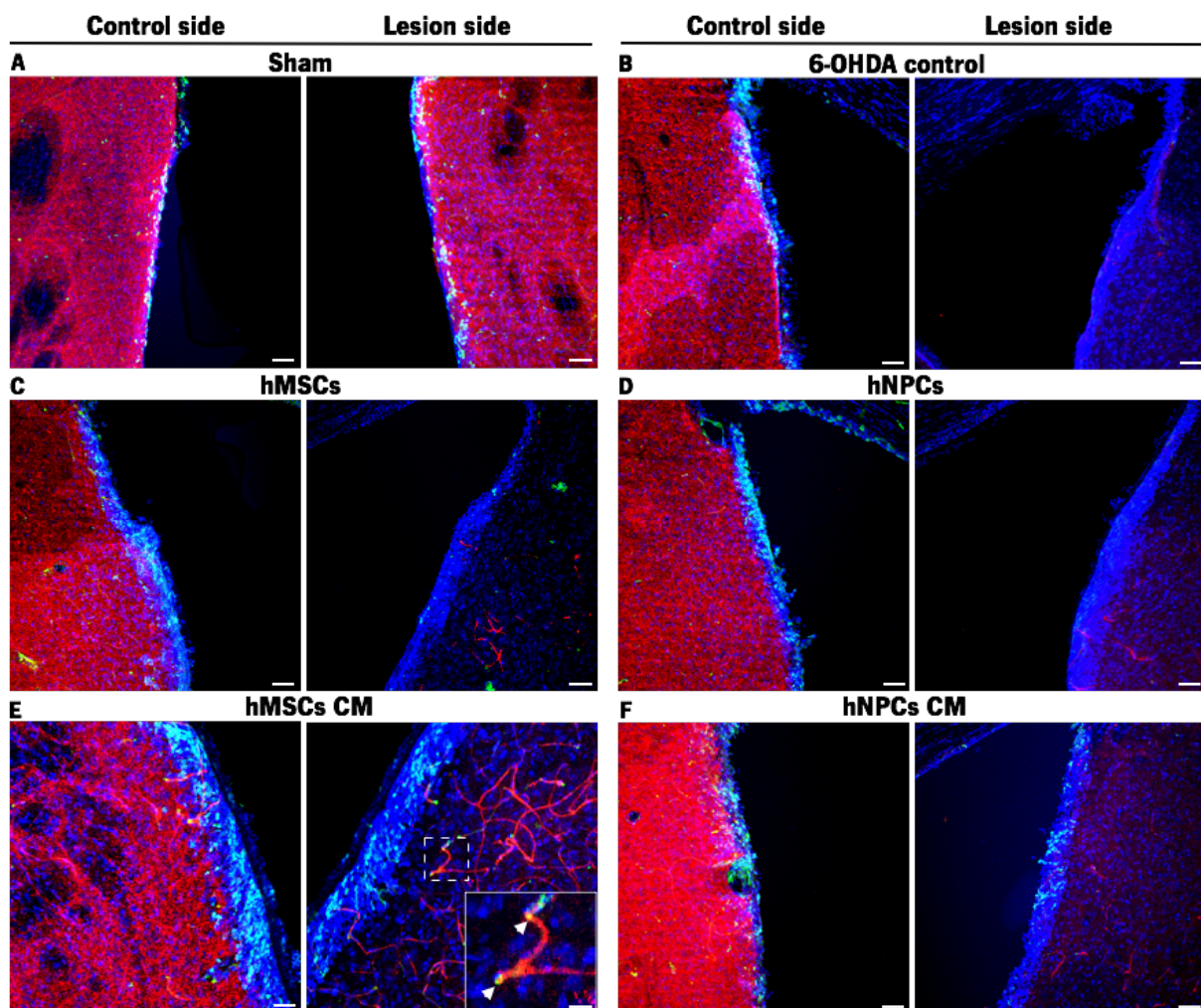
Figure 12. Animals were injected daily with BrdU 5 days before sacrifice.

Histological sections were immunostained for BrdU (green) and TH (red). Nuclei were labeled with DAPI. Qualitative analysis indicates that the secretome of (E) hMSCs is able to induce TH neuronal differentiation (BrdU-positive/TH-positive cells) in 6-OHDA animals, a fact that was not observed in the (B) untreated group (6-OHDA) neither in groups transplanted with (C-D) cells or with (F) hNPCs CM.

4.5. hMSCs and hNPCs secretome proteomic analysis

In order to further understand the differences evidenced on the *in vitro* and *in vivo* studies, the secretome from both hMSCs and hNPCs was characterized through a non-targeted proteomic approach based analysis namely, LS-MS/MS and SWATH acquisition. From proteomic analysis, we observed that the secretome of hMSCs present a different pattern of protein expression when compared to the secretome of hNPCs (Figure 13A-B). In line with this, through the use of the Venn diagram software (http://bioinformatics.psb.ugent.be/webtools/Venn/) we were able to identify 691 proteins in the secretome of hMSCs and 675 proteins in the secretome of hNPCs, in which 633 proteins were common to the two conditions (Figure 13C).
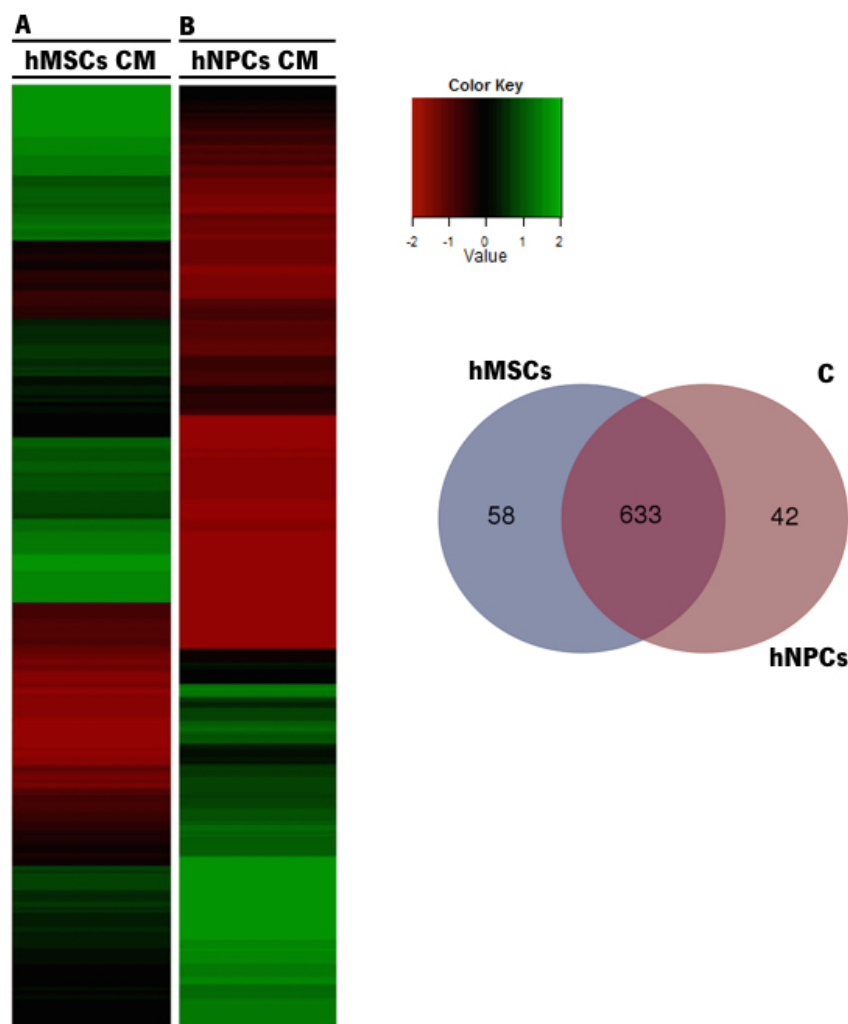
Figure 13. Proteomics - Heatmap and Venn diagram.

Graphical representation of hMSCs and hNPCs CM proteomic analysis by LS-MS/MS and SWATH acquisition. Peaks detected after CM analysis showed that the pattern of protein expression is different between (A) hMSCs CM and (B) hNPCs CM. Proteomic analysis identified more proteins in hMSCs CM (691 proteins) when compared to the hNPCs CM (675 proteins), in which 633 proteins were common to the two conditions (C). n=3.

Among these 633 proteins identified in common in the secretome of hMSCs and hNPCs, 590 were quantified. From these 590 proteins, further analysis revealed that these two cell populations were able to secrete a panel of proteins with neuroregulatory actions on the CNS (Figure 14) such as Ubiquitin carboxyl-terminal hydrolase isozyme L1 (UCHL1), Thioredoxin reductase 1 (TrxR1), 14-3-3 proteins, Macrophage migration inhibitory factor (MIF), Superoxidase dismutase-cytoplasmatic (SODC), Superoxidase dismutase-mitochondrial (SODM), Ezrin, Radixin, Protein deglycase DJ-1 and Peroxiredoxin-1 (Prdx1), which were significantly more expressed in the hMSCs CM (Figure 14). Other important proteins were also expressed in both hMSCs and hNPCs CM such as Clusterin, Pigment epithelium-derived factor (PEDF), Semaphorin-7A (SEM7A), Glia derived nexin (GDN), Dickkopf 3, Galectin-1, Cystatin C (Cys C), Cahdherin-2 and Fibronectin, although no statistical differences were found between the two cell populations (Figure 14).

In addition to this, we have also identified specific proteins that were strictly expressed by each cell population, presenting also important roles in CNS physiology. Regarding hMSCs CM, we were able to identify the presence of Prosaposin, Gremlin, and Beta-1,4-galactosyltransferase 1 whereas, in the hNPCs CM were identified the Interleukin-6 (IL-6) and Prefoldin.

52
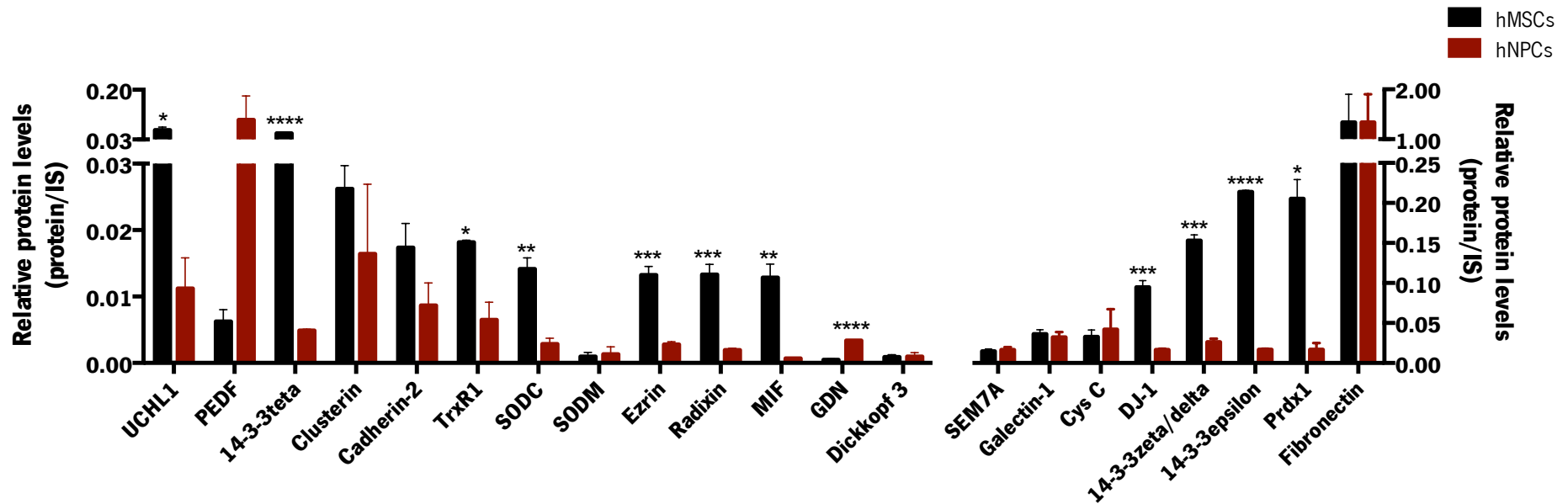
Figure 14. Specific hMSCs and hNPCs CM proteins with neuroregulatory potential in CNS physiology.

Comparative analysis of the secreted paracrine factors collected from the hMSCs and hNPCs CM proteins: UHCL1 (upregulated in hMSCs CM), PEDF, 14-3-3teta (upregulated in hMSCs CM), Clusterin, Cadherin-2, TrxR1 (upregulated in hMSCs CM), SODC (upregulated in hMSCs CM), SODM, Ezrin (upregulated in hMSCs CM), Radixin (upregulated in hMSCs CM), MIF (upregulated in hMSCs CM), GDN (upregulated in hNPCs CM), Dickkopf 3, SEM7A, Galectin-1, Cys C, DJ-1 (upregulated in hMSCs CM), 14-3-3zeta/delta (upregulated in hNPCs CM), 14-3-3- epsilon (upregulated in hMSCs CM), Prdx1 (upregulated in hMSCs CM), and Fibronectin. Data presented as mean±SEM. n=3. *p<0.05, **p<0.01, ***p<0.001, ****p<0.0001. IS: internal standard.

5. DISCUSSION

The limited regeneration capacity of CNS represents a challenge for the development of new therapeutic strategies. Therefore, there as been an increasing interest on the development of cell-based protocols for the treatment of CNS disorders, including PD. Due to their ability of self-renewal and differentiation potential, stem cells have been proposed as promising therapeutic tools (Dantuma et al., 2010). Compelling evidence suggests that adult stem cells, such as hMSCs and hNPCs, are able to exert therapeutical effects when applied in the CNS (Azari et al., 2010; Joyce et al., 2010; Kim et al., 2013; Suksuphew and Noisa, 2015). Throughout the years most of these beneficial effects (after stem cells transplantation) were mainly attributed to their differentiation capacity. However, in recent years there was a paradigm shift, in which different reports have shown that the release of neurotrophic paracrine factors (i.e. secretome) is the main route by which these stem cell populations can mediate improvements in the CNS (Drago et al., 2013; Teixeira et al., 2015). Based on such evidences, the initial *in vitro* experiments performed in the present report focused on exploring the effects of the hMSCs and hNPCs secretome on the neuronal differentiation of hNPCs, revealed that both hMSCs and hNPCs secretome were able to induce the differentiation of human CNS-derived cells. Indeed, as shown in Figure 6, when hNPCs were incubated with the hMSCs secretome an increased differentiation of hNPCs into neuronal lineages - both intermediate mature neurons (beta III tubulin positive cells) and mature neurons (MAP-2 positive cells) - was observed when compared to the control group. This is in line to what Sart and colleagues (Sart et al., 2014) had already reported regarding the effects of hMSCs secretome on hNPCs differentiation and maturation. Moreover, they observed that hMSCs secretome was able to enhance the proliferation, migration and neurite extension of hNPCs, correlating these observations with presence of bioactive molecules in the secretome namely, FGF-2, TGF-β1 and BDNF. Also with HUCPVCs secretome, Teixeira and colleagues (Teixeira et al., 2015) observed an increase in the differentiation of hNPCs into neuronal lineages. In addition to the above-referred results, we also observed that in comparison to the hNPCs secretome, the hMSCs secretome was significantly more efficient in promoting neuronal differentiation of hNPCs (Figure 6F-H and 6J-L). This result was interesting, while simultaneously puzzling, as no references on the literature have mentioned the *in vitro* application of the hNPCs secretome in the modulation of neuronal differentiation. Nonetheless, although the mechanisms by which hMSCs and hNPCs secretome modulates the behavior of neural progenitors still remains unclear, its application in the CNS have already demonstrated therapeutical effects, even in the context of disease as PD (Drago et al., 2013).

In order to further understand which molecules, present in hMSCs and hNPCs secretome, could be involved in observed results, a non-targeted proteomic approach (by LC-MS/MS and SWATH acquisition) was performed. The results revealed that hMSCs and hNPCs produce additional molecules, than those already reported for these kind of studies, with neuroregulatory actions both *in vitro* and *in vivo* CNS models of injury and disease, as wells as other processes such as neurite growth and/or neuronal protection, survival and differentiation (Figure 14). From these, 14-3-3 proteins, UCHL1, MIF, Ezrin and Radixin were found to be upregulated in the secretome of hMSCs CM (Figure 14). For instance, 14-3-3 proteins are known to play crucial roles in several biological processes including cell migration and proliferation, neurite outgrowth, as well as in response to cells damage and prevention of apoptosis, including in CNS-derived cells (Chen et al., 2007; Fraga et al., 2013). Moreover, Ramser and colleagues (Ramser et al., 2010) demonstrated that 14-3-3 zeta protein stimulated the neurite outgrowth from cultures rat hippocampal neurons. On the other hand, UCHL1, an important component of ubiquitin-proteasome system (UPS), as been described as a potential target of some neurodegenerative disorders like PD (Gong and Leznik, 2007). Although the role of the UCHL1 in neurogenesis it is poorly understood, Sakurai and colleagues (Sakurai et al., 2006) showed that this molecule regulated the morphology of NPCs and positively modulated their differentiation. In addition, previous results from our group have also identified the presence of 14-3-3 proteins and UCHL1 in hMSCs secretome, correlating its presence with the increase of neuronal cell densities in cortical and cerebellar primary cultures *in vitro* (Fraga et al., 2013). Regarding MIF, Ohta *et al.* (Ohta et al., 2012) showed that this protein was able to promote the survival and proliferation of NPCs, suggesting that it may be a potential therapeutic factor, capable of activating NPCs, for the treatment of degenerative brain disorders. From the molecular point of view, Zhang and co-workers (Zhang et al., 2013) showed that MIF not only promoted the proliferation but also induced the differentiation of NPCs into neuronal lineages through the modulation of the Wnt/β-Catenin signal pathway. Similarly, Ezrin and Radixin were found to be important mediators of neuritogenesis and regulators of neuronal migration and differentiation, respectively (Matsumoto et al., 2014; Persson et al., 2010; Persson et al., 2013). Interestingly, in addition to the above-referred proteins, we have also identified the presence of specific molecules only in the hMSCs secretome namely, beta-1,4-galactotransferase. According to Huang and colleagues (Huang et al., 1995), beta-1,4-galactotransferase is an important mediator of neurite initiation, neurite formation and elongation. Altogether, these evidences clearly indicates hMSCs secretome as potential modulator of neuronal cell survival and differentiation, and could explain the differences observed between hMSCs and hNPCs in the *in vitro* experiments. Nevertheless, we also

identified in the secretome of hMSCs and hNPCs, other specific proteins with neuroregulatory potential such as GDN, Cys C, Galectin-1, PEDF, Clusterin, SEM7A and Cadherin 2, although no statistical differences were found between the two conditions (Figure 14). For instance, GDN and Cys C are known to play crucial roles in the enhancement of neurite outgrowth and neuroprotection through the prevention of oxidative stress (Farmer et al., 1990; Hoffmann et al., 1992; Nishiyama et al., 2005; Tizon et al., 2010). On the other hand, Galectin-1 and PEDF have been described as important regulators involved in neurogenesis, playing a role on neural stem cells self-renewal and differentiation (Kajitani et al., 2009; Ramirez-Castillejo et al., 2006; Sakaguchi and Okano, 2012; Yabe et al., 2010). Clusterin and SEM7A have also been described as enhancers of neuroprotection, neurogenesis (e.g. neuronal process formation, elongation and plasticity) and axonal outgrowth (Kang et al., 2005; Pasterkamp and Kolodkin, 2003; Pasterkamp et al., 2003; Pucci et al., 2008; Wicher et al., 2008). In the case of Cadherin-2, one of the important molecules for cell to cell interaction in the developing CNS, Gao *et al.* (Gao et al., 2001) suggested that it played a role in neurodifferentiation of P19 cells, possibly through the Wnt signaling pathways (involved in the majority of the processes required to generate fully functional neurons in the CNS) (Munji et al., 2011).

As stated in the introduction, PD is characterized by a progressive and extensive loss of DAergic neurons in the SNpc and their terminals in the striatum, resulting in debilitating motor problems (Mahlknecht and Poewe, 2013). In the *in vivo* experiments of the present study, we used a well-defined rat model of PD, induced by unilateral injection of 6-OHDA into the MFB (Carvalho et al., 2013). This model mimics the progressive nature of DAergic degeneration process in human PD, leading to the appearance of the main motor deficits associated to PD (Carvalho et al., 2013; Simola et al., 2007). Indeed, as shown in the apomorphine-turning behavior (Figure 7A), 6-OHDA-injected animals displayed an intense turning behavior when compared to the Sham group, indicating a clear decline in the functional integrity of the DAergic system. In addition, we verified that the motor function of these animals was also affected, which is in agreement with previous reports (Monville et al., 2006; Truong et al., 2006). In fact, the animals presented impairments in motor coordination and balance, as assessed by the rotarod test, and in the skilled motor function addressed by the staircase test (Figure 7B-D). In the present work, we intended to analyze the effects of secretome derived from hMSCs and hNPCs on the animal motor performance and on the DAergic neuronal survival after 6-OHDA injections, comparing its outputs to the ones obtained from the animals transplanted with cells. Regarding the effects on balance and motor coordination, assessed by the rotarod test, we were able to observe that the CM injection (either from hMSCs and hNPCs) was able to improve the motor performance of the

injected animals when compared to the hNPCs-transplanted group (Figure 8). Although no statistical differences were found, the CM-injected animals also displayed a positive trend on latency to fall when compared to the untreated group 6-OHDA (Figure 8). Similar outcomes were also observed in the staircase test (which assesses the paw reaching motor coordination), in which we verified that the injection of hMSCs and hNPCs CM improved the success rate of eaten pellets in the CM-injected animals when compared to the untreated group 6-OHDA (Figure 9A). In addition to this, we have also observed that the animals injected with hMSCs CM had a significant better performance when compared to the hNPCs-transplanted group (Figure 9A). In the forced-choice task, in the left side (the affected side), we observed a remarkable trend in the animals injected with hMSCs CM when compared to the 6-OHDA group (Figure 9B). After histological analysis, we also observed that the administration of the hMSCs (significantly increase) and hNPCs secretome was able to increase the TH-positive neurons and fibers (Figure 10 and Figure 11) when compared to untreated group 6-OHDA. These histological outcomes nicely correlate with positive functional improvements that we observed for the animals treated with secretome. Similar results, regarding hMSCs secretome, were also observed in previous work from our group, showing that the injection of hMSCs CM in the SNpc and striatum of 6-OHDA-lesioned animals, potentiated the recovery of DAergic neurons (estimated by neuronal densities in SNpc and striatum), thereby supporting the recovery observed in the animals' motor performance outcomes (data not published). Although no reports have been presented with hMSCs secretome in PD animal models to date, the secretion of bioactive factors is known to play a critical role in the mechanisms of action of these cells (Lavoie and Rosu-Myles, 2013). In fact, several studies, using different hMSCs populations, reported that they were able to attenuate the abnormal behavior and the loss TH immunoreactive nerve terminals, to protect spared DAergic neurons as well as display anti-apoptotic effects, attributing these outcomes to the secretion of factors such as BDNF, GDNF and SDF-1α (Cova et al., 2010; Sadan et al., 2009; Wang et al., 2010)

As mentioned earlier, the use of hNPCs CM also led to the enhancement of the motor performance of the animals. In fact, hNPCs have been described as a potential stem cell source for the treatment of neurological disorders, including PD, and their beneficial effects are also attributed to their neurotrophic capability (Ben-Hur, 2008; Drago et al., 2013). Likewise hMSCs, currently, there are no studies regarding the application of hNPCs secretome in animal models of PD. However, different studies have suggested that hNPCs were able to increase the behavioral performance of lesioned animals, TH innervation and DAT activity, as well as the capacity to create host environments rich in trophic and neuroprotective support to rescue imperiled host cells, though the secretion of SCF, IGF-1

and GDNF (Behrstock et al., 2006; Ebert et al., 2008; Ourednik et al., 2002; Yasuhara et al., 2006). The outcomes of the present work show that stem cells secretome could represent a new wave of possible therapeutic strategies for PD. This is extremely important as, instead of transplanting cells, one could envisage therapies where just the secretome could be used. By doing so, we could overcome some of the current limitations of stem cell based therapies namely, the number of available cells for transplantation and cell death after this procedure. Moreover, in a comparative study recently guided by Teixeira and colleagues (Teixeira et al., 2015), it was observed that the animals injected only with the secretome of hMSCs into the hippocampus of adult rats, disclosed similar levels of neuronal survival and differentiation to those observed in cell-transplanted groups.

Also in the context of PD, our proteomic based analysis revealed the secretion of important neuroregulatory candidates both in hMSCs and hNPCs secretome (Figure 14). From these, PEDF was found to have important actions in the migration, differentiation and neuroprotection mechanisms both *in vitro* and *in vivo* (Falk et al., 2010; Yabe et al., 2010). Moreover, as stated by Falk and colleagues (Falk et al., 2010) when comparing with other factors (e.g. GDNF family) PEDF has advantages in the ease of delivery and functional outcomes. Moreover, Falk and collegues (Falk et al., 2009) reported that PEDF is not only neurotrophic but also neuroprotective in both 6-OHDA and rotenone primary midbrain culture model of PD. DJ-1, also identified in the secretome of both hMSCs and hNPCs, it is a multifunctional protein deeply linked to PD. DJ-1 has various functions, including transcriptional regulation, anti-oxidative stress reaction, and chaperone, protease and mitochondrial regulation (Ariga et al., 2013; Miyazaki et al., 2008). The loss of its function is thought to result in the onset of PD (Ariga et al., 2013; Miyazaki et al., 2008). DJ-1 is also a stress sensor and its expression is increased upon various stresses, including oxidative stress (Ariga et al., 2013; Martinat et al., 2004; Yokota et al., 2003), modulating signaling pathways critical to cell survival such as PTEN and AKT (Aleyasin et al., 2010; Kim et al., 2005). Moreover, Inden and colleagues (Inden et al., 2006) showed that the administration of DJ-1 protein prevented DAergic cell death and restored locomotion in a 6-OHDA-rat model of PD, suggesting DJ-1 as a possible pharmaceutical target for PD. Another study conducted by Paterna *et al.* (Paterna et al., 2007) demonstrated that viral overexpression of DJ-1 reduced nigral dopamine neuronal loss in a MPTP mice model of PD. Similarly, it was also possible to identify other proteins known as anti-oxidant factors such as TrxR1, Prdx1, and SOD enzymes (Vlamis-Gardikas and Holmgren, 2002; Zhou et al., 2008; Zhu et al., 2012). For instance, Arodin and colleagues (Arodin et al., 2014) by examining the expression of redox proteins in human postmortem PD brains, found that the levels of Trx1 and TrxR1 were significantly decreased. Using a Caenorhabditis elegans (C.elegans)

model, the authors concluded that in the absence of TrxR1, DAergic neurons were significantly more sensitive to 6-OHDA with significantly increased neuronal degradation, suggesting that this molecule is important for neuronal survival in dopamine-induced cell death (Arodin et al., 2014). Regarding Prdx1, its overexpression in DAergic neuronal cell line has shown to counteract 6-OHDA-induced DAergic cell death by acting as ROS (superoxidase anion and H_2O_2) scavenger (Lee et al., 2008). Among the ROS-scavenging enzymes, SOD enzymes are often regarded as the first line of defense against ROS (Zhou et al., 2008). Indeed, Filograna and co-workers (Filograna et al., 2016), using human SH-SY5Y neuroblastoma cells, tested the beneficial role of SOD enzymes against paraquat-induced toxicity, verifying that both cytosolic (SODC) and mitochondrial (SODM) were effective in protecting cells against superoxide overproduction. Fibronectin, has also been described to exert neuroinflammatory and neuroprotective associated roles (Wang et al., 2013). In fact, evidence showed that Fibronectin could bind integrin and growth factor receptors (such as IGF-1 receptor) to trans-activate intracellular signaling events, such as the phosphatidylinositol 3 kinase/protein kinase B pathway, leading to the increase of growth factor-like neuroprotective actions (Wang et al., 2013). Dickkopf 3, was also identified in the secretome of both hMSCs and hNPCs, and has been described as an important modulator of DAergic neuronal differentiation through the Wnt/β-catenin signaling pathway (Fukusumi et al., 2015).

In addition to this, we discovered specific proteins that were restricted to each condition, presenting also important roles in CNS physiology. In the hMSCs CM, besides the beta-1,4-galactotransferase already mentioned above, we were able to identify the presence of Prosaposin and Gremlin, whereas in the hNPCs CM were identified the IL-6 and Prefoldin. Prosaposin (also known as SGP-1) is an intriguing multifunctional protein that plays roles both intracellularly, as regulator of lysossomal enzyme function, and extracellularly, as a secreted protein with neuroprotective and glioprotective effects (Meyer et al., 2014). For instance, Prosaposin treatment was shown to upregulate the anti-apoptotic factor Bcl-2, and down-regulated the pro-apoptotic factor BAX, inhibiting MPTP-induced toxicity both *in vitro* (in SH-SY5Y cells) and *in vivo* (on DAergic neurons in the PD model mice), suggesting an action on signaling pathways that inhibit apoptosis (Gao et al., 2013). Regarding Gremlin, Phani and collegues (Phani et al., 2013) proposed that Gremlin could be a novel neuroprotective factor for DAergic neurons. In this study, the authors showed that the addition of exogenous Gremlin (transcriptionally increased in the VTA in response to MPTP) was able to significantly protected DAergic neurons against MPTP *in vitro* (using DAergic cell lines and primary SN neuronal cultures). Additionally, it also exhibited neuroprotective ability when used in an MPTP mouse model of PD (TH-positive neuronal survival was significantly increased when compared to controls). Taken together these results

suggest that Gremlin may play an endogenous role in protecting VTA against neurotoxins, but also is capable of protecting DAergic neurons, therefore providing an opportunity for the development of novel PD therapeutic approaches (Phani et al., 2013). On the other hand, IL-6 has been reported to play important roles in scavenging superoxidase radicals by increasing the antioxidant enzyme activity, through STAT pathways, and protect neuronal cells from death (Hirano et al., 2000). Prefoldin was found to be an important protein in the context of PD, as it has been (Takano et al., 2013) suggested as a protective factor in aggregated α-synuclein-induced cell death. Interestingly, in addition to the proteins mentioned above, studies from our group, demonstrated (using targeted proteomic-based approaches) that molecules like VEGF, NGF, BDNF, IL-6 and GDNF, described as stronger modulators neuronal survival and differentiation, as well as modulators of DAergic survival and protection, (Allen et al., 2013; Hirano et al., 2000; Pucci et al., 2008; Xiong et al., 2011) were also present in hMSCs secretome (Teixeira et al., 2016).

In addition to these results, besides the DAergic survival, it has also been described that the modulation of neurogenesis may also play a role in the recovery of PD (Geraerts et al., 2007; Regensburger et al., 2014). Indeed, from a qualitative analysis of SEZ and striatum (Figure 12) also indicates that the secretome of both hMSCs and hNPCs increased the expression of BrdU and TH-positive cells in the lesion side. More intriguing, we have observed that hMSCs CM seems to be more prone to induce DAergic neuronal differentiation in the lesion side. Park *et al.* (Park et al., 2012) demonstrated that hMSCs administration significantly augmented neurogenesis in both the SEZ and SN of MPTP PD animal model, which led to an increase in the differentiation of NPCs into DAergic neurons in the SN. Furthermore, hMSCs-induced EGF modulation appears to be one of underlying contributors to the enhancement of neurogenesis by hMSCs (Park et al., 2012). Similarly, Schwerk and colleagues (Schwerk et al., 2015) verified that ASCs increased neurogenesis in hippocampal and subventricular regions in 6-OHDA-lesioned rat brain, correlating this effect with the *in vivo* BDNF expression. Nevertheless, regarding the present work, quantitative analysis and further studies are required particularly to: 1) understand how stem cells secretome modulates/control neurogenesis and 2) if and how the new differentiated cells integrate into the existing neuronal networks in the context of PD.

In summary, the injection of the hMSCs and hNPCs secretome acts as modulator of neuronal cell survival and differentiation. In the context of disease, we have found that the injection of secretome (regardless the cell populations used) was able to increase the densities and fibers of TH-positive cells, a fact that probably explains the improved behavioral performance of the CM-injected animals. Overall, our results strongly suggest that the use of the secretome *per se* may be considered as a possible cell-

free therapeutic tool for the treatment of PD, since the secretome is able to better modulate the DAergic neuronal survival and animal behavior performance when compared to the transplantation of cells. Thus, we hypothesize that the modulation effect in DAergic neurons triggered by the hMSCs and hNPCs secretome could be related with the presence/expression of specific molecules described throughout this work. Furthermore, our findings suggest that, although there is a different secretion profile between hMSCs and hNPCs secretome, both led to histological and functional improvements, leading to the conclusion that this stimulation by stem cells secretome is not dependent upon the presence of just one secreted factor, but several, demonstrating that different factors (secreted by the two populations) can achieve the same outcomes, as revealed by our proteomic-based analysis. It is also important to note that MSCs are easy to isolate, culture and manipulate in *ex vivo* culture, and when compared to the other sources, such as ESCs or even NSCs, they not imply the ethical and moral questions in their isolation, *in vitro* expansion and further *in vivo* application. Therefore, MSCs can be the most advantageous cell population for the acquisition of the secretome.

CHAPTER 6
CONCLUDING REMARKS

6. CONCLUDING REMARKS

As final remarks it can be stated that the work performed and included in this thesis provided important insights on the potential use of stem cells secretome as a future cell-free therapeutic tool for CNS neurodegenerative disorders, particularly PD. In fact, we observed that the injection of secretome (with no cell transplantation) was able to modulate the DAergic neuronal survival and ameliorate the motor deficits of a 6-OHDA rat model of PD. Proteomic analysis demonstrated that these outcomes are associated with the presence of important neuroregulatory molecules within the secretome, that are involved in a different therapeutic mechanisms spanning from antiapoptotic mechanisms, anti-inflammatory responses, reduction of oxidative stress and endogenous regeneration, stimulation of neurogenesis/gliogenesis, cell survival and differentiation, neurite outgrowth, immunomodulation, among others. In addition to the many important trophic factors that have been described in the literature, PEDF or DJ-1 may be, at least, partly involved on the observed outcomes, which could open novel therapeutic and pharmacological opportunities for PD. Although candidate molecules are under investigation, further detailed studies are needed to carefully define which factors may be responsible for the stem cells secretome-mediated neuroprotective and regenerative properties. Furthermore, it will also be important to understand the mechanisms behind the beneficial effects of the secretome, as the elucidation of activation or inhibition of molecular pathways, as well as its temporal effects. By doing so it could be possible, in a near future, to rationally design new therapeutical strategies for the functional recovery of neurological or neurodegenerative disorders, particularly PD, based on the use of stem cells secretome.

CHAPTER 7
REFERENCES

Aggarwal, S., Pittenger, M.F., 2005. Human mesenchymal stem cells modulate allogeneic immune cell responses. Blood. 105, 1815-22.

Aleyasin, H., et al., 2010. DJ-1 protects the nigrostriatal axis from the neurotoxin MPTP by modulation of the AKT pathway. Proc Natl Acad Sci U S A. 107, 3186-91.

Allen, S.J., et al., 2013. GDNF, NGF and BDNF as therapeutic options for neurodegeneration. Pharmacol Ther. 138, 155-75.

Alvarez-Buylla, A., Garcia-Verdugo, J.M., 2002. Neurogenesis in adult subventricular zone. J Neurosci. 22, 629-34.

Andres, R.H., et al., 2011. Human neural stem cells enhance structural plasticity and axonal transport in the ischaemic brain. Brain. 134, 1777-89.

Anisimov, S.V., 2009. Cell-based therapeutic approaches for Parkinson's disease: progress and perspectives. Rev Neurosci. 20, 347-81.

Anjo, S.I., Santa, C., Manadas, B., 2014. Short GeLC-SWATH: a fast and reliable quantitative approach for proteomic screenings. Proteomics. 15, 757-62.

Ariga, H., et al., 2013. Neuroprotective function of DJ-1 in Parkinson's disease. Oxid Med Cell Longev. 2013, 683920.

Armstrong, R.J., et al., 2002. The potential for circuit reconstruction by expanded neural precursor cells explored through porcine xenografts in a rat model of Parkinson's disease. Exp Neurol. 175, 98-111.

Arodin, L., et al., 2014. Protective effects of the thioredoxin and glutaredoxin systems in dopamine-induced cell death. Free Radic Biol Med. 73, 328-36.

Azari, M.F., et al., 2010. Mesenchymal stem cells for treatment of CNS injury. Curr Neuropharmacol. 8, 316-23.

Baghbaderani, B.A., et al., 2010. Bioreactor expansion of human neural precursor cells in serum-free media retains neurogenic potential. Biotechnol Bioeng. 105, 823-33.

Baraniak, P.R., McDevitt, T.C., 2010. Stem cell paracrine actions and tissue regeneration. Regen Med. 5, 121-43.

Bartholomew, A., et al., 2002. Mesenchymal stem cells suppress lymphocyte proliferation in vitro and prolong skin graft survival in vivo. Exp Hematol. 30, 42-8.

Beach, T.G., et al., 2008. Reduced striatal tyrosine hydroxylase in incidental Lewy body disease. Acta Neuropathol. 115, 445-51.

Behrstock, S., et al., 2006. Human neural progenitors deliver glial cell line-derived neurotrophic factor to parkinsonian rodents and aged primates. Gene Ther. 13, 379-88.

Ben-Hur, T., 2008. Immunomodulation by neural stem cells. J Neurol Sci. 265, 102-4.

Benskey, M.J., Perez, R.G., Manfredsson, F.P., 2016. The contribution of alpha synuclein to neuronal survival and function Implications for Parkinson's Disease. J Neurochem. 3, 331-59.

Bernheimer, H., et al., 1973. Brain dopamine and the syndromes of Parkinson and Huntington. Clinical, morphological and neurochemical correlations. J Neurol Sci. 20, 415-55.

Bezard, E., et al., 1999. Involvement of the subthalamic nucleus in glutamatergic compensatory mechanisms. Eur J Neurosci. 11, 2167-70.

Bezard, E., Gross, C.E., Brotchie, J.M., 2003. Presymptomatic compensation in Parkinson's disease is not dopamine-mediated. Trends Neurosci. 26, 215-21.

Bhat, A.H., et al., 2015. Oxidative stress, mitochondrial dysfunction and neurodegenerative diseases; a mechanistic insight. Biomed Pharmacother. 74, 101-10.

Bibbiani, F., et al., 2005. Continuous dopaminergic stimulation reduces risk of motor complications in parkinsonian primates. Exp Neurol. 192, 73-8.

Blandini, F., et al., 2010. Transplantation of undifferentiated human mesenchymal stem cells protects against 6-hydroxydopamine neurotoxicity in the rat. Cell Transplant. 19, 203-17.

Bonnamain, V., Neveu, I., Naveilhan, P., 2012. Neural stem/progenitor cells as a promising candidate for regenerative therapy of the central nervous system. Front Cell Neurosci. 6, 17.

Braak, H., et al., 2003a. Staging of brain pathology related to sporadic Parkinson's disease. Neurobiol Aging. 24, 197-211.

Braak, H., et al., 2003b. Idiopathic Parkinson's disease: possible routes by which vulnerable neuronal types may be subject to neuroinvasion by an unknown pathogen. J Neural Transm (Vienna). 110, 517-36.

Bras, J.M., Singleton, A., 2009. Genetic susceptibility in Parkinson's disease. Biochim Biophys Acta. 1792, 597-603.

Burke, R.E., O'Malley, K., 2013. Axon degeneration in Parkinson's disease. Exp Neurol. 246, 72-83.

Buzhor, E., et al., 2014. Cell-based therapy approaches: the hope for incurable diseases. Regen Med. 9, 649-72.

Candiano, G., et al., 2004. Blue silver: a very sensitive colloidal Coomassie G-250 staining for proteome analysis. Electrophoresis. 25, 1327-33.

Cantinieaux, D., et al., 2013. Conditioned medium from bone marrow-derived mesenchymal stem cells improves recovery after spinal cord injury in rats: an original strategy to avoid cell transplantation. PLoS One. 8, e69515.

Carvalho, M.M., et al., 2013. Behavioral characterization of the 6-hydroxidopamine model of Parkinson's disease and pharmacological rescuing of non-motor deficits. Mol Neurodegener. 8, 14.

Chaudhuri, K.R., Schapira, A.H., 2009. Non-motor symptoms of Parkinson's disease: dopaminergic pathophysiology and treatment. Lancet Neurol. 8, 464-74.

Chen, J., et al., 2007. Increases in expression of 14-3-3 eta and 14-3-3 zeta transcripts during neuroprotection induced by delta9-tetrahydrocannabinol in AF5 cells. J Neurosci Res. 85, 1724-33.

Chen, J.F., et al., 2001. Neuroprotection by caffeine and A(2A) adenosine receptor inactivation in a model of Parkinson's disease. J Neurosci. 21, RC143.

Cheng, H.C., Ulane, C.M., Burke, R.E., 2010. Clinical progression in Parkinson disease and the neurobiology of axons. Ann Neurol. 67, 715-25.

Chiurchiu, V., Orlacchio, A., Maccarrone, M., 2016. Is Modulation of Oxidative Stress an Answer? The State of the Art of Redox Therapeutic Actions in Neurodegenerative Diseases. Oxid Med Cell Longev. 2016, 7909380.

Chu, Y., et al., 2012. Alterations in axonal transport motor proteins in sporadic and experimental Parkinson's disease. Brain. 135, 2058-73.

Chung, C.Y., et al., 2009. Dynamic changes in presynaptic and axonal transport proteins combined with striatal neuroinflammation precede dopaminergic neuronal loss in a rat model of AAV alpha-synucleinopathy. J Neurosci. 29, 3365-73.

Chung, Y.C., et al., 2010. The role of neuroinflammation on the pathogenesis of Parkinson's disease. BMB Rep. 43, 225-32.

Coleman, M., 2005. Axon degeneration mechanisms: commonality amid diversity. Nat Rev Neurosci. 6, 889-98.

Collins, B.C., et al., 2013. Quantifying protein interaction dynamics by SWATH mass spectrometry: application to the 14-3-3 system. Nature methods. 10, 1246-53.

Cova, L., et al., 2010. Multiple neurogenic and neurorescue effects of human mesenchymal stem cell after transplantation in an experimental model of Parkinson's disease. Brain Res. 1311, 12-27.

Crigler, L., et al., 2006. Human mesenchymal stem cell subpopulations express a variety of neuro-regulatory molecules and promote neuronal cell survival and neuritogenesis. Exp Neurol. 198, 54-64.

Danielyan, L., et al., 2011. Therapeutic efficacy of intranasally delivered mesenchymal stem cells in a rat model of Parkinson disease. Rejuvenation Res. 14, 3-16.

Dantuma, E., Merchant, S., Sugaya, K., 2010. Stem cells for the treatment of neurodegenerative diseases. Stem Cell Res Ther. 1, 37.

Datta, I., Bhonde, R., 2012. Can mesenchymal stem cells reduce vulnerability of dopaminergic neurons in the substantia nigra to oxidative insult in individuals at risk to Parkinson's disease? Cell Biol Int. 36, 617-24.

Dauer, W., Przedborski, S., 2003. Parkinson's disease: mechanisms and models. Neuron. 39, 889-909.

de Lau, L.M., Breteler, M.M., 2006. Epidemiology of Parkinson's disease. Lancet Neurol. 5, 525-35.

deSouza, R.M., et al., 2013. Timing of deep brain stimulation in Parkinson disease: a need for reappraisal? Ann Neurol. 73, 565-75.

Dexter, D.T., Jenner, P., 2013. Parkinson disease: from pathology to molecular disease mechanisms. Free Radic Biol Med. 62, 132-44.

Diack, A.B., et al., 2016. Insights into Mechanisms of Chronic Neurodegeneration. Int J Mol Sci. 17.

Dickson, D.W., et al., 2009. Neuropathological assessment of Parkinson's disease: refining the diagnostic criteria. Lancet Neurol. 8, 1150-7.

Dominici, M., et al., 2006. Minimal criteria for defining multipotent mesenchymal stromal cells. The International Society for Cellular Therapy position statement. Cytotherapy. 8, 315-7.

Drago, D., et al., 2013. The stem cell secretome and its role in brain repair. Biochimie. 95, 2271-85.

Ebert, A.D., et al., 2008. Human neural progenitor cells over-expressing IGF-1 protect dopamine neurons and restore function in a rat model of Parkinson's disease. Exp Neurol. 209, 213-23.

Erices, A., Conget, P., Minguell, J.J., 2000. Mesenchymal progenitor cells in human umbilical cord blood. Br J Haematol. 109, 235-42.

Falk, T., Zhang, S., Sherman, S.J., 2009. Pigment epithelium derived factor (PEDF) is neuroprotective in two in vitro models of Parkinson's disease. Neurosci Lett. 458, 49-52.

Falk, T., Gonzalez, R.T., Sherman, S.J., 2010. The yin and yang of VEGF and PEDF: multifaceted neurotrophic factors and their potential in the treatment of Parkinson's Disease. Int J Mol Sci. 11, 2875-900.

Farmer, L., Sommer, J., Monard, D., 1990. Glia-derived nexin potentiates neurite extension in hippocampal pyramidal cells in vitro. Dev Neurosci. 12, 73-80.

Febbraro, F., et al., 2013. Chronic intranasal deferoxamine ameliorates motor defects and pathology in the alpha-synuclein rAAV Parkinson's model. Exp Neurol. 247, 45-58.

Filograna, R., et al., 2016. Superoxide Dismutase (SOD)-mimetic M40403 Is Protective in Cell and Fly Models of Paraquat Toxicity: IMPLICATIONS FOR PARKINSON DISEASE. J Biol Chem. 291, 9257-67.

Fraga, J.S., et al., 2013. Unveiling the effects of the secretome of mesenchymal progenitors from the umbilical cord in different neuronal cell populations. Biochimie. 95, 2297-303.

Friedenstein, A.J., et al., 1974. Precursors for fibroblasts in different populations of hematopoietic cells as detected by the in vitro colony assay method. Exp Hematol. 2, 83-92.

Fu, M.H., et al., 2015. Stem cell transplantation therapy in Parkinson's disease. Springerplus. 4, 597.

Fukusumi, Y., et al., 2015. Dickkopf 3 Promotes the Differentiation of a Rostrolateral Midbrain Dopaminergic Neuronal Subset In Vivo and from Pluripotent Stem Cells In Vitro in the Mouse. J Neurosci. 35, 13385-401.

Gao, H.L., et al., 2013. Attenuation of MPTP/MPP(+) toxicity in vivo and in vitro by an 18-mer peptide derived from prosaposin. Neuroscience. 236, 373-93.

Gao, X., et al., 2001. A role of N-cadherin in neuronal differentiation of embryonic carcinoma P19 cells. Biochem Biophys Res Commun. 284, 1098-103.

Geraerts, M., et al., 2007. Concise review: therapeutic strategies for Parkinson disease based on the modulation of adult neurogenesis. Stem Cells. 25, 263-70.

Gibb, W.R., Lees, A.J., 1988. The relevance of the Lewy body to the pathogenesis of idiopathic Parkinson's disease. J Neurol Neurosurg Psychiatry. 51, 745-52.

Gillet, L.C., et al., 2012. Targeted data extraction of the MS/MS spectra generated by data-independent acquisition: a new concept for consistent and accurate proteome analysis. Mol Cell Proteomics. 11, O111.016717.

Glavaski-Joksimovic, A., Bohn, M.C., 2013. Mesenchymal stem cells and neuroregeneration in Parkinson's disease. Exp Neurol. 247, 25-38.

Gong, B., Leznik, E., 2007. The role of ubiquitin C-terminal hydrolase L1 in neurodegenerative disorders. Drug News Perspect. 20, 365-70.

Goodarzi, P., et al., 2015. Stem cell-based approach for the treatment of Parkinson's disease. Med J Islam Repub Iran. 29, 168.

Griffiths, P.D., et al., 1999. Iron in the basal ganglia in Parkinson's disease. An in vitro study using extended X-ray absorption fine structure and cryo-electron microscopy. Brain. 122, 667-73.

Gronthos, S., et al., 2000. Postnatal human dental pulp stem cells (DPSCs) in vitro and in vivo. Proc Natl Acad Sci U S A. 97, 13625-30.

Halliday, G.M., Stevens, C.H., 2011. Glia: initiators and progressors of pathology in Parkinson's disease. Mov Disord. 26, 6-17.

Hamani, C., et al., 2004. The subthalamic nucleus in the context of movement disorders. Brain. 127, 4-20.

Hariz, G.M., Limousin, P., Hamberg, K., 2016. "DBS means everything - for some time". Patients' perspectives on daily life with deep brain stimulation for Parkinson's Disease. J Parkinsons Dis. 6, 335-47.

Harrower, T.P., et al., 2006. Long-term survival and integration of porcine expanded neural precursor cell grafts in a rat model of Parkinson's disease. Exp Neurol. 197, 56-69.

Hass, R., et al., 2011. Different populations and sources of human mesenchymal stem cells (MSC): A comparison of adult and neonatal tissue-derived MSC. Cell Commun Signal. 9, 12.

Hellmann, M.A., et al., 2006. Increased survival and migration of engrafted mesenchymal bone marrow stem cells in 6-hydroxydopamine-lesioned rodents. Neurosci Lett. 395, 124-8.

Hirano, T., Ishihara, K., Hibi, M., 2000. Roles of STAT3 in mediating the cell growth, differentiation and survival signals relayed through the IL-6 family of cytokine receptors. Oncogene. 19, 2548-56.

Hoffmann, M.C., et al., 1992. The prolonged presence of glia-derived nexin, an endogenous protease inhibitor, in the hippocampus after ischemia-induced delayed neuronal death. Neuroscience. 49, 397-408.

Holloway, R.G., et al., 2004. Pramipexole vs levodopa as initial treatment for Parkinson disease: a 4-year randomized controlled trial. Arch Neurol. 61, 1044-53.

Huang, Q., Shur, B.D., Begovac, P.C., 1995. Overexpressing cell surface beta 1.4-galactosyltransferase in PC12 cells increases neurite outgrowth on laminin. J Cell Sci. 108, 839-47.

Hutchinson, K., Wick, J.Y., 2016. Deep Brain Stimulation and Medication Management in Parkinson's Disease. Consult Pharm. 31, 73-84.

Inden, M., et al., 2006. PARK7 DJ-1 protects against degeneration of nigral dopaminergic neurons in Parkinson's disease rat model. Neurobiol Dis. 24, 144-58.

Jankovic, J., 2008. Parkinson's disease: clinical features and diagnosis. J Neurol Neurosurg Psychiatry. 79, 368-76.

Jankovic, J., Aguilar, L.G., 2008. Current approaches to the treatment of Parkinson's disease. Neuropsychiatr Dis Treat. 4, 743-57.

Jimenez-Shahed, J., 2016. A review of current and novel levodopa formulations for the treatment of Parkinson's disease. Ther Deliv. 7, 179-91.

Joyce, N., et al., 2010. Mesenchymal stem cells for the treatment of neurodegenerative disease. Regen Med. 5, 933-46.

Jung, S., et al., 2010. Identification of growth and attachment factors for the serum-free isolation and expansion of human mesenchymal stromal cells. Cytotherapy. 12, 637-57.

Kajitani, K., et al., 2009. Galectin-1 promotes basal and kainate-induced proliferation of neural progenitors in the dentate gyrus of adult mouse hippocampus. Cell Death Differ. 16, 417-27.

Kandadai, R.M., et al., 2014. Safinamide for the treatment of Parkinson's disease. Expert Rev Clin Pharmacol. 7, 747-59.

Kang, S.W., et al., 2005. Clusterin interacts with SCLIP (SCG10-like protein) and promotes neurite outgrowth of PC12 cells. Exp Cell Res. 309, 305-15.

Kassem, M., Kristiansen, M., Abdallah, B.M., 2004. Mesenchymal stem cells: cell biology and potential use in therapy. Basic Clin Pharmacol Toxicol. 95**,** 209-14.

Khoo, T.K., et al., 2013. The spectrum of nonmotor symptoms in early Parkinson disease. Neurology. 80**,** 276-81.

Kim, H.J., et al., 2011. Phenotype analysis in patients with early onset Parkinson's disease with and without parkin mutations. J Neurol. 258**,** 2260-7.

Kim, R.H., et al., 2005. DJ-1, a novel regulator of the tumor suppressor PTEN. Cancer Cell. 7**,** 263-73.

Kim, S.U., Lee, H.J., Kim, Y.B., 2013. Neural stem cell-based treatment for neurodegenerative diseases. Neuropathology. 33**,** 491-504.

Kim, Y.J., et al., 2009. Neuroprotective effects of human mesenchymal stem cells on dopaminergic neurons through anti-inflammatory action. Glia. 57**,** 13-23.

Kim-Han, J.S., Antenor-Dorsey, J.A., O'Malley, K.L., 2011. The parkinsonian mimetic, MPP+, specifically impairs mitochondrial transport in dopamine axons. J Neurosci. 31**,** 7212-21.

Kokaia, Z., et al., 2012. Cross-talk between neural stem cells and immune cells: the key to better brain repair? Nat Neurosci. 15**,** 1078-87.

Kupcova Skalnikova, H., 2013. Proteomic techniques for characterisation of mesenchymal stem cell secretome. Biochimie. 95**,** 2196-211.

Lai, R.C., et al., 2010. Exosome secreted by MSC reduces myocardial ischemia/reperfusion injury. Stem Cell Res. 4**,** 214-22.

Lambert, J.-P., et al., 2013. Mapping differential interactomes by affinity purification coupled with data-independent mass spectrometry acquisition. Nature methods. 10**,** 1239-45.

Langston, J.W., 2006. The Parkinson's complex: parkinsonism is just the tip of the iceberg. Ann Neurol. 59**,** 591-6.

Lavoie, J.R., Rosu-Myles, M., 2013. Uncovering the secretes of mesenchymal stem cells. Biochimie. 95**,** 2212-21.

Lee, Y.M., et al., 2008. Oxidative modification of peroxiredoxin is associated with drug-induced apoptotic signaling in experimental models of Parkinson disease. J Biol Chem. 283**,** 9986-98.

Lees, A.J., Hardy, J., Revesz, T., 2009. Parkinson's disease. Lancet. 373**,** 2055-66.

Lener, T., et al., 2015. Applying extracellular vesicles based therapeutics in clinical trials - an ISEV position paper. J Extracell Vesicles. 4**,** 30087.

LeWitt, P.A., Fahn, S., 2016. Levodopa therapy for Parkinson disease: A look backward and forward. Neurology. 86**,** S3-12.

Lindvall, O., et al., 1990. Grafts of fetal dopamine neurons survive and improve motor function in Parkinson's disease. Science. 247**,** 574-7.

Lopez-Verrilli, M.A., et al., 2016. Mesenchymal stem cell-derived exosomes from different sources selectively promote neuritic outgrowth. Neuroscience. 320, 129-39.

Lu, S., et al., 2011. Adipose-derived mesenchymal stem cells protect PC12 cells from glutamate excitotoxicity-induced apoptosis by upregulation of XIAP through PI3-K/Akt activation. Toxicology. 279, 189-95.

Mahlknecht, P., Poewe, W., 2013. Is there a need to redefine Parkinson's disease? J Neural Transm (Vienna). 120, S9-17.

Maltman, D.J., Hardy, S.A., Przyborski, S.A., 2011. Role of mesenchymal stem cells in neurogenesis and nervous system repair. Neurochem Int. 59, 347-56.

Manadas, B., et al., 2009. BDNF-induced changes in the expression of the translation machinery in hippocampal neurons: protein levels and dendritic mRNA. J Proteome Res. 8, 4536-52.

Martinat, C., et al., 2004. Sensitivity to oxidative stress in DJ-1-deficient dopamine neurons: an ES-derived cell model of primary Parkinsonism. PLoS Biol. 2, e327.

Matsumoto, Y., et al., 2014. Ezrin mediates neuritogenesis via down-regulation of RhoA activity in cultured cortical neurons. PLoS One. 9, e105435.

Mendez, I., et al., 2002. Simultaneous intrastriatal and intranigral fetal dopaminergic grafts in patients with Parkinson disease: a pilot study. Report of three cases. J Neurosurg. 96, 589-96.

Mendez, I., et al., 2005. Cell type analysis of functional fetal dopamine cell suspension transplants in the striatum and substantia nigra of patients with Parkinson's disease. Brain. 128, 1498-510.

Meyer, R.C., et al., 2014. The protective role of prosaposin and its receptors in the nervous system. Brain Res. 1585, 1-12.

Meyerrose, T., et al., 2010. Mesenchymal stem cells for the sustained in vivo delivery of bioactive factors. Adv Drug Deliv Rev. 62, 1167-74.

Miyazaki, S., et al., 2008. DJ-1-binding compounds prevent oxidative stress-induced cell death and movement defect in Parkinson's disease model rats. J Neurochem. 105, 2418-34.

Montoya, C.P., et al., 1991. The "staircase test": a measure of independent forelimb reaching and grasping abilities in rats. J Neurosci Methods. 36, 219-28.

Monville, C., Torres, E.M., Dunnett, S.B., 2006. Comparison of incremental and accelerating protocols of the rotarod test for the assessment of motor deficits in the 6-OHDA model. J Neurosci Methods. 158, 219-23.

Moon, H.E., Paek, S.H., 2015. Mitochondrial Dysfunction in Parkinson's Disease. Exp Neurobiol. 24, 103-16.

Morandi, F., et al., 2008. Immunogenicity of human mesenchymal stem cells in HLA-class I-restricted T-cell responses against viral or tumor-associated antigens. Stem Cells. 26, 1275-87.

Munji, R.N., et al., 2011. Wnt signaling regulates neuronal differentiation of cortical intermediate progenitors. J Neurosci. 31, 1676-87.

Nakano, N., et al., 2010. Characterization of conditioned medium of cultured bone marrow stromal cells. Neurosci Lett. 483, 57-61.

Nandhagopal, R., McKeown, M.J., Stoessl, A.J., 2008. Functional imaging in Parkinson disease. Neurology. 70, 1478-88.

Navntoft, C.A., Dreyer, J.K., 2016. How compensation breaks down in Parkinson's disease: Insights from modeling of denervated striatum. Mov Disord. 31, 280-9.

Nishiyama, K., et al., 2005. Expression of cystatin C prevents oxidative stress-induced death in PC12 cells. Brain Res Bull. 67, 94-9.

Noyce, A.J., Lees, A.J., Schrag, A.E., 2016. The prediagnostic phase of Parkinson's disease. J Neurol Neurosurg Psychiatry. DOI: 10.1136/jnnp-2015-311890.

Obeso, J.A., et al., 2004. How does Parkinson's disease begin? The role of compensatory mechanisms. Trends Neurosci. 27, 125-7.

Ogawa, D., et al., 2009. Evaluation of human fetal neural stem/progenitor cells as a source for cell replacement therapy for neurological disorders: properties and tumorigenicity after long-term in vitro maintenance. J Neurosci Res. 87, 307-17.

Ohta, S., et al., 2012. Macrophage migration inhibitory factor (MIF) promotes cell survival and proliferation of neural stem/progenitor cells. J Cell Sci. 125, 3210-20.

Olanow, C.W., Brundin, P., 2013. Parkinson's disease and alpha synuclein: is Parkinson's disease a prion-like disorder? Mov Disord. 28, 31-40.

Onofrj, M., Bonanni, L., Thomas, A., 2008. An expert opinion on safinamide in Parkinson's disease. Expert Opin Investig Drugs. 17, 1115-25.

Ourednik, J., et al., 2002. Neural stem cells display an inherent mechanism for rescuing dysfunctional neurons. Nat Biotechnol. 20, 1103-10.

Pagano, G., et al., 2016. Age at onset and Parkinson disease phenotype. Neurology. 86, 1400-7.

Palmer, T.D., et al., 2001. Cell culture. Progenitor cells from human brain after death. Nature. 411, 42-3.

Pantcheva, P., et al., 2015. Treating non-motor symptoms of Parkinson's disease with transplantation of stem cells. Expert Rev Neurother. 15, 1231-40.

Park, H.J., et al., 2012. Mesenchymal stem cells augment neurogenesis in the subventricular zone and enhance differentiation of neural precursor cells into dopaminergic neurons in the substantia nigra of a parkinsonian model. Cell Transplant. 21, 1629-40.

Parker, W.D., Jr., Boyson, S.J., Parks, J.K., 1989. Abnormalities of the electron transport chain in idiopathic Parkinson's disease. Ann Neurol. 26, 719-23.

Pasterkamp, R.J., Kolodkin, A.L., 2003. Semaphorin junction: making tracks toward neural connectivity. Curr Opin Neurobiol. 13, 79-89.

Pasterkamp, R.J., et al., 2003. Semaphorin 7A promotes axon outgrowth through integrins and MAPKs. Nature. 424, 398-405.

Paterna, J.C., et al., 2007. DJ-1 and Parkin modulate dopamine-dependent behavior and inhibit MPTP-induced nigral dopamine neuron loss in mice. Mol Ther. 15, 698-704.

Paul, G., et al., 2012. The adult human brain harbors multipotent perivascular mesenchymal stem cells. PLoS One. 7, e35577.

Paxinos, G., Watson, C., 2007. The rat brain in stereotaxic coordinates, Vol., Elsevier, Amsterdam; Boston.

Persson, A., et al., 2010. Expression of ezrin radixin moesin proteins in the adult subventricular zone and the rostral migratory stream. Neuroscience. 167, 312-22.

Persson, A., Lindberg, O.R., Kuhn, H.G., 2013. Radixin inhibition decreases adult neural progenitor cell migration and proliferation in vitro and in vivo. Front Cell Neurosci. 7, 161.

Phani, S., et al., 2013. Gremlin is a novel VTA derived neuroprotective factor for dopamine neurons. Brain Res. 1500, 88-98.

Poewe, W., Wenning, G.K., 2000. Apomorphine: an underutilized therapy for Parkinson's disease. Mov Disord. 15, 789-94.

Pringsheim, T., et al., 2014. The prevalence of Parkinson's disease: a systematic review and meta-analysis. Mov Disord. 29, 1583-90.

Privat, A., 2003. Astrocytes as support for axonal regeneration in the central nervous system of mammals. Glia. 43, 91-3.

Pucci, S., et al., 2008. Neuroprotection: VEGF, IL-6, and clusterin: the dark side of the moon. Prog Brain Res. 173, 555-73.

Quik, M., 2004. Smoking, nicotine and Parkinson's disease. Trends Neurosci. 27, 561-8.

Ramirez-Castillejo, C., et al., 2006. Pigment epithelium-derived factor is a niche signal for neural stem cell renewal. Nat Neurosci. 9, 331-9.

Ramser, E.M., et al., 2010. The 14-3-3zeta protein binds to the cell adhesion molecule L1, promotes L1 phosphorylation by CKII and influences L1-dependent neurite outgrowth. PLoS One. 5, e13462.

Rascol, O., et al., 2000. A five-year study of the incidence of dyskinesia in patients with early Parkinson's disease who were treated with ropinirole or levodopa. N Engl J Med. 342, 1484-91.

Rascol, O., et al., 2003. Limitations of current Parkinson's disease therapy. Ann Neurol. 53, S3-15.

Regensburger, M., Prots, I., Winner, B., 2014. Adult hippocampal neurogenesis in Parkinson's disease: impact on neuronal survival and plasticity. Neural Plast. 2014**,** 454696.

Ribeiro, C.A., et al., 2012. The secretome of stem cells isolated from the adipose tissue and Wharton jelly acts differently on central nervous system derived cell populations. Stem Cell Res Ther. 3**,** 18.

Richardson, R.M., et al., 2005. Grafts of adult subependymal zone neuronal progenitor cells rescue hemiparkinsonian behavioral decline. Brain Res. 1032**,** 11-22.

Ross, G.W., et al., 2004. Parkinsonian signs and substantia nigra neuron density in decendents elders without PD. Ann Neurol. 56**,** 532-9.

Ryu, J.K., et al., 2004. Proactive transplantation of human neural stem cells prevents degeneration of striatal neurons in a rat model of Huntington disease. Neurobiol Dis. 16**,** 68-77.

Sadan, O., et al., 2009. Protective effects of neurotrophic factor-secreting cells in a 6-OHDA rat model of Parkinson disease. Stem Cells Dev. 18**,** 1179-90.

Sakaguchi, M., Okano, H., 2012. Neural stem cells, adult neurogenesis, and galectin-1: from bench to bedside. Dev Neurobiol. 72**,** 1059-67.

Sakurai, M., et al., 2006. Ubiquitin C-terminal hydrolase L1 regulates the morphology of neural progenitor cells and modulates their differentiation. J Cell Sci. 119**,** 162-71.

Salgado, A.J., et al., 2010. Role of human umbilical cord mesenchymal progenitors conditioned media in neuronal/glial cell densities, viability, and proliferation. Stem Cells Dev. 19**,** 1067-74.

Salgado, A.J., et al., 2015. Mesenchymal stem cells secretome as a modulator of the neurogenic niche: basic insights and therapeutic opportunities. Front Cell Neurosci. 9**,** 249.

Sart, S., et al., 2014. Microenvironment regulation of pluripotent stem cell-derived neural progenitor aggregates by human mesenchymal stem cell secretome. Tissue Eng Part A. 20**,** 2666-79.

Sarugaser, R., et al., 2005. Human umbilical cord perivascular (HUCPV) cells: a source of mesenchymal progenitors. Stem Cells. 23**,** 220-9.

Sawle, G.V., et al., 1992. Transplantation of fetal dopamine neurons in Parkinson's disease: PET [18F] 6-L-fluorodopa studies in two patients with putaminal implants. Ann Neurol. 31**,** 166-73.

Schwerk, A., et al., 2015. Adipose-derived human mesenchymal stem cells induce long-term neurogenic and anti-inflammatory effects and improve cognitive but not motor performance in a rat model of Parkinson's disease. Regen Med. 10**,** 431-46.

Sennels, L., Bukowski-Wills, J.C., Rappsilber, J., 2009. Improved results in proteomics by use of local and peptide-class specific false discovery rates. BMC Bioinformatics. 10**,** 179.

Shannak, K., et al., 1994. Noradrenaline, dopamine and serotonin levels and metabolism in the human hypothalamus: observations in Parkinson's disease and normal subjects. Brain Res. 639**,** 33-41.

Shokouhi, B.N., et al., 2010. Microglial responses around intrinsic CNS neurons are correlated with axonal regeneration. BMC Neurosci. 11, 13.

Simola, N., Morelli, M., Carta, A.R., 2007. The 6-hydroxydopamine model of Parkinson's disease. Neurotox Res. 11, 151-67.

Singh, N., Pillay, V., Choonara, Y.E., 2007. Advances in the treatment of Parkinson's disease. Prog Neurobiol. 81, 29-44.

Suksuphew, S., Noisa, P., 2015. Neural stem cells could serve as a therapeutic material for age-related neurodegenerative diseases. World J Stem Cells. 7, 502-11.

Takano, M., et al., 2013. Prefoldin prevents aggregation of alpha-synuclein. Brain Res. DOI: 10.1016/j.brainres.2013.10.034.

Tang, W.H., Shilov, I.V., Seymour, S.L., 2008. Nonlinear fitting method for determining local false discovery rates from decoy database searches. J Proteome Res. 7, 3661-7.

Teixeira, F.G., et al., 2013. Mesenchymal stem cells secretome: a new paradigm for central nervous system regeneration? Cell Mol Life Sci. 70, 3871-82.

Teixeira, F.G., et al., 2015. Secretome of mesenchymal progenitors from the umbilical cord acts as modulator of neural/glial proliferation and differentiation. Stem Cell Rev. 11, 288-97.

Teixeira, F.G., et al., 2016. Modulation of the Mesenchymal Stem Cell Secretome Using Computer-Controlled Bioreactors: Impact on Neuronal Cell Proliferation, Survival and Differentiation. Sci Rep. In Press.

Tizon, B., et al., 2010. Induction of autophagy by cystatin C: a mechanism that protects murine primary cortical neurons and neuronal cell lines. PLoS One. 5, e9819.

Toma, J.G., et al., 2001. Isolation of multipotent adult stem cells from the dermis of mammalian skin. Nat Cell Biol. 3, 778-84.

Trenkwalder, C., et al., 2015. Expert Consensus Group report on the use of apomorphine in the treatment of Parkinson's disease–Clinical practice recommendations. Parkinsonism Relat Disord. 21, 1023-30.

Truong, L., et al., 2006. Developing a preclinical model of Parkinson's disease: a study of behaviour in rats with graded 6-OHDA lesions. Behav Brain Res. 169, 1-9.

Tufekci, K.U., et al., 2012. Inflammation in Parkinson's disease. Adv Protein Chem Struct Biol. 88, 69-132.

Uccelli, A., et al., 2011a. Neuroprotective features of mesenchymal stem cells. Best Pract Res Clin Haematol. 24, 59-64.

Uccelli, A., Laroni, A., Freedman, M.S., 2011b. Mesenchymal stem cells for the treatment of multiple sclerosis and other neurological diseases. Lancet Neurol. 10, 649-56.

van der Kooy, D., Weiss, S., 2000. Why stem cells? Science. 287, 1439-41.

Venkataramana, N.K., et al., 2010. Open-labeled study of unilateral autologous bone-marrow-derived mesenchymal stem cell transplantation in Parkinson's disease. Transl Res. 155, 62-70.

Vila, M., et al., 2000. Evolution of changes in neuronal activity in the subthalamic nucleus of rats with unilateral lesion of the substantia nigra assessed by metabolic and electrophysiological measurements. Eur J Neurosci. 12, 337-44.

Vlamis-Gardikas, A., Holmgren, A., 2002. Thioredoxin and glutaredoxin isoforms. Methods Enzymol. 347, 286-96.

Wang, F., et al., 2010. Intravenous administration of mesenchymal stem cells exerts therapeutic effects on parkinsonian model of rats: focusing on neuroprotective effects of stromal cell-derived factor-1alpha. BMC Neurosci. 11, 52.

Wang, H.S., et al., 2004. Mesenchymal stem cells in the Wharton's jelly of the human umbilical cord. Stem Cells. 22, 1330-7.

Wang, J., Yin, L., Chen, Z., 2013. Neuroprotective role of fibronectin in neuron-glial extrasynaptic transmission. Neural Regen Res. 8, 376-82.

Wang, S., Qu, X., Zhao, R.C., 2011. Mesenchymal stem cells hold promise for regenerative medicine. Front Med. 5, 372-8.

Warner, T.T., Schapira, A.H., 2003. Genetic and environmental factors in the cause of Parkinson's disease. Ann Neurol. 53, S16-25.

Wicher, G., et al., 2008. Extracellular clusterin promotes neuronal network complexity in vitro. Neuroreport. 19, 1487-91.

Williams, A., 2014. Central nervous system regeneration–where are we? QJM. 107, 335-9.

Xin, H., et al., 2013. Systemic administration of exosomes released from mesenchymal stromal cells promote functional recovery and neurovascular plasticity after stroke in rats. J Cereb Blood Flow Metab. 33, 1711-5.

Xiong, N., et al., 2010. Long-term efficacy and safety of human umbilical cord mesenchymal stromal cells in rotenone-induced hemiparkinsonian rats. Biol Blood Marrow Transplant. 16, 1519-29.

Xiong, N., et al., 2011. VEGF-expressing human umbilical cord mesenchymal stem cells, an improved therapy strategy for Parkinson's disease. Gene Ther. 18, 394-402.

Xu, L., et al., 2006. Human neural stem cell grafts ameliorate motor neuron disease in SOD-1 transgenic rats. Transplantation. 82, 865-75.

Yabe, T., Sanagi, T., Yamada, H., 2010. The neuroprotective role of PEDF: implication for the therapy of neurological disorders. Curr Mol Med. 10, 259-66.

Yasuhara, T., et al., 2006. Transplantation of human neural stem cells exerts neuroprotection in a rat model of Parkinson's disease. J Neurosci. 26, 12497-511.

Yokota, T., et al., 2003. Down regulation of DJ-1 enhances cell death by oxidative stress, ER stress, and proteasome inhibition. Biochem Biophys Res Commun. 312**,** 1342-8.

Yu, B., Zhang, X., Li, X., 2014. Exosomes derived from mesenchymal stem cells. Int J Mol Sci. 15**,** 4142-57.

Zhang, P., et al., 2009. Transplanted human embryonic neural stem cells survive, migrate, differentiate and increase endogenous nestin expression in adult rat cortical peri-infarction zone. Neuropathology. 29**,** 410-21.

Zhang, X., et al., 2013. Macrophage migration inhibitory factor promotes proliferation and neuronal differentiation of neural stem/precursor cells through Wnt/beta-catenin signal pathway. Int J Biol Sci. 9**,** 1108-20.

Zhou, C., Huang, Y., Przedborski, S., 2008. Oxidative stress in Parkinson's disease: a mechanism of pathogenic and therapeutic significance. Ann N Y Acad Sci. 1147**,** 93-104.

Zhu, H., Santo, A., Li, Y., 2012. The antioxidant enzyme peroxiredoxin and its protective role in neurological disorders. Exp Biol Med (Maywood). 237**,** 143-9.

Zigmond, M.J., et al., 1990. Compensations after lesions of central dopaminergic neurons: some clinical and basic implications. Trends Neurosci. 13**,** 290-6.

Zuk, P.A., et al., 2002. Human adipose tissue is a source of multipotent stem cells. Mol Biol Cell. 13**,** 4279-95.

Table S1. List of proteins identified in both hMSCs and hNPCs secretome

Entry	Entry name	Protein Name_UNIPROT recommended
P02751	FINC_HUMAN	Fibronectin
P12111	CO6A3_HUMAN	Collagen alpha-3(VI) chain
P02768	ALBU_HUMAN	Serum albumin
P08123	CO1A2_HUMAN	Collagen alpha-2(I) chain
P02452	CO1A1_HUMAN	Collagen alpha-1(I) chain
Q99715	COCA1_HUMAN	Collagen alpha-1(XII) chain
P21333	FLNA_HUMAN	Filamin-A
P01023	A2MG_HUMAN	Alpha-2-macroglobulin
P08253	MMP2_HUMAN	72 kDa type IV collagenase
P12109	CO6A1_HUMAN	Collagen alpha-1(VI) chain
P02787	TRFE_HUMAN	Serotransferrin
Q15063	POSTN_HUMAN	Periostin
P08670	VIME_HUMAN	Vimentin
P49327	FAS_HUMAN	Fatty acid synthase
P07996	TSP1_HUMAN	Thrombospondin-1
O43707	ACTN4_HUMAN	Alpha-actinin-4
Q00610	CLH1_HUMAN	Clathrin heavy chain 1
Q15582	BGH3_HUMAN	Transforming growth factor-beta-induced protein ig-h3
P12110	CO6A2_HUMAN	Collagen alpha-2(VI) chain
Q14767	LTBP2_HUMAN	Latent-transforming growth factor beta-binding protein 2
Q16555	DPYL2_HUMAN	Dihydropyrimidinase-related protein 2
P11142	HSP7C_HUMAN	Heat shock cognate 71 kDa protein
P14618	KPYM_HUMAN	Pyruvate kinase PKM
P29401	TKT_HUMAN	Transketolase
P30101	PDIA3_HUMAN	Protein disulfide-isomerase A3
P20908	CO5A1_HUMAN	Collagen alpha-1(V) chain
P13639	EF2_HUMAN	Elongation factor 2
P07437	TBB5_HUMAN	Tubulin beta chain
P05121	PAI1_HUMAN	Plasminogen activator inhibitor 1
P06733	ENOA_HUMAN	Alpha-enolase
P55072	TERA_HUMAN	Transitional endoplasmic reticulum ATPase
P55786	PSA_HUMAN	Puromycin-sensitive aminopeptidase
P26038	MOES_HUMAN	Moesin
P02545	LMNA_HUMAN	Prelamin-A/C
Q71U36	TBA1A_HUMAN	Tubulin alpha-1A chain
P10915	HPLN1_HUMAN	Hyaluronan and proteoglycan link protein 1
P63261	ACTG_HUMAN	Actin, cytoplasmic 2
Q16658	FSCN1_HUMAN	Fascin
Q14766	LTBP1_HUMAN	Latent-transforming growth factor beta-binding protein 1
O75326	SEM7A_HUMAN	Semaphorin-7A
O94985	CSTN1_HUMAN	Calsyntenin-1
P12107	COBA1_HUMAN	Collagen alpha-1(XI) chain
P31150	GDIA_HUMAN	Rab GDP dissociation inhibitor alpha
P07195	LDHB_HUMAN	L-lactate dehydrogenase B chain
P13611	CSPG2_HUMAN	Versican core protein

P08238	HS90B_HUMAN	Heat shock protein HSP 90-beta
P11021	GRP78_HUMAN	78 kDa glucose-regulated protein
P12277	KCRB_HUMAN	Creatine kinase B-type
P22314	UBA1_HUMAN	Ubiquitin-like modifier-activating enzyme 1
O75874	IDHC_HUMAN	Isocitrate dehydrogenase [NADP] cytoplasmic
P00558	PGK1_HUMAN	Phosphoglycerate kinase 1
P07585	PGS2_HUMAN	Decorin
P52209	6PGD_HUMAN	6-phosphogluconate dehydrogenase, decarboxylating
Q15113	PCOC1_HUMAN	Procollagen C-endopeptidase enhancer 1
P36955	PEDF_HUMAN	Pigment epithelium-derived factor
P09486	SPRC_HUMAN	SPARC
P60174	TPIS_HUMAN	Triosephosphate isomerase
P06744	G6PI_HUMAN	Glucose-6-phosphate isomerase
P62258	1433E_HUMAN	14-3-3 protein epsilon
Q16270	IBP7_HUMAN	Insulin-like growth factor-binding protein 7
P04406	G3P_HUMAN	Glyceraldehyde-3-phosphate dehydrogenase
P00338	LDHA_HUMAN	L-lactate dehydrogenase A chain
Q14194	DPYL1_HUMAN	Dihydropyrimidinase-related protein 1
P23471	PTPRZ_HUMAN	Receptor-type tyrosine-protein phosphatase zeta
P04075	ALDOA_HUMAN	Fructose-bisphosphate aldolase A
Q01995	TAGL_HUMAN	Transgelin
P08476	INHBA_HUMAN	Inhibin beta A chain
P08603	CFAH_HUMAN	Complement factor H
P27797	CALR_HUMAN	Calreticulin
P04264	K2C1_HUMAN	Keratin, type II cytoskeletal 1
Q12841	FSTL1_HUMAN	Follistatin-related protein 1
P24821	TENA_HUMAN	Tenascin
Q9Y617	SERC_HUMAN	Phosphoserine aminotransferase
P21810	PGS1_HUMAN	Biglycan
Q14195	DPYL3_HUMAN	Dihydropyrimidinase-related protein 3
P23528	COF1_HUMAN	Cofilin-1
P05997	CO5A2_HUMAN	Collagen alpha-2(V) chain
P37837	TALDO_HUMAN	Transaldolase
P51884	LUM_HUMAN	Lumican
Q9BPU6	DPYL5_HUMAN	Dihydropyrimidinase-related protein 5
Q16610	ECM1_HUMAN	Extracellular matrix protein 1
O00391	QSOX1_HUMAN	Sulfhydryl oxidase 1
P23284	PPIB_HUMAN	Peptidyl-prolyl cis-trans isomerase B
P62937	PPIA_HUMAN	Peptidyl-prolyl cis-trans isomerase A
P07237	PDIA1_HUMAN	Protein disulfide-isomerase
P34932	HSP74_HUMAN	Heat shock 70 kDa protein 4
P0DMV9	HS71B_HUMAN	Heat shock 70 kDa protein 1B
P68104	EF1A1_HUMAN	Elongation factor 1-alpha 1
P13645	K1C10_HUMAN	Keratin, type I cytoskeletal 10
P40926	MDHM_HUMAN	Malate dehydrogenase, mitochondrial
P00738	HPT_HUMAN	Haptoglobin
P02461	CO3A1_HUMAN	Collagen alpha-1(III) chain
Q99497	PARK7_HUMAN	Protein deglycase DJ-1
Q08380	LG3BP_HUMAN	Galectin-3-binding protein
P19022	CADH2_HUMAN	Cadherin-2

P98160	PGBM_HUMAN	Basement membrane-specific heparan sulfate proteoglycan core protein
P50395	GDIB_HUMAN	Rab GDP dissociation inhibitor beta
Q06830	PRDX1_HUMAN	Peroxiredoxin-1
P09211	GSTP1_HUMAN	Glutathione S-transferase P
P61978	HNRPK_HUMAN	Heterogeneous nuclear ribonucleoprotein K
Q13822	ENPP2_HUMAN	Ectonucleotide pyrophosphatase/phosphodiesterase family member 2
P02790	HEMO_HUMAN	Hemopexin
O75083	WDR1_HUMAN	WD repeat-containing protein 1
P08572	CO4A2_HUMAN	Collagen alpha-2(IV) chain
Q14204	DYHC1_HUMAN	Cytoplasmic dynein 1 heavy chain 1
P22626	ROA2_HUMAN	Heterogeneous nuclear ribonucleoproteins A2/B1
P63104	1433Z_HUMAN	14-3-3 protein zeta/delta
P28074	PSB5_HUMAN	Proteasome subunit beta type-5
Q14697	GANAB_HUMAN	Neutral alpha-glucosidase AB
Q96KP4	CNDP2_HUMAN	Cytosolic non-specific dipeptidase
Q02809	PLOD1_HUMAN	Procollagen-lysine,2-oxoglutarate 5-dioxygenase 1
P27695	APEX1_HUMAN	DNA-(apurinic or apyrimidinic site) lyase
P00505	AATM_HUMAN	Aspartate aminotransferase, mitochondrial
P14625	ENPL_HUMAN	Endoplasmin
P18669	PGAM1_HUMAN	Phosphoglycerate mutase 1
P07355	ANXA2_HUMAN	Annexin A2
P35237	SPB6_HUMAN	Serpin B6
P35052	GPC1_HUMAN	Glypican-1
P09936	UCHL1_HUMAN	Ubiquitin carboxyl-terminal hydrolase isozyme L1
P40925	MDHC_HUMAN	Malate dehydrogenase, cytoplasmic
P37802	TAGL2_HUMAN	Transgelin-2
Q13308	PTK7_HUMAN	Inactive tyrosine-protein kinase 7
P09104	ENOG_HUMAN	Gamma-enolase
P16035	TIMP2_HUMAN	Metalloproteinase inhibitor 2
P10809	CH60_HUMAN	60 kDa heat shock protein, mitochondrial
P23142	FBLN1_HUMAN	Fibulin-1
P30041	PRDX6_HUMAN	Peroxiredoxin-6
P09871	C1S_HUMAN	Complement C1s subcomponent
Q16881	TRXR1_HUMAN	Thioredoxin reductase 1, cytoplasmic
Q9Y240	CLC11_HUMAN	C-type lectin domain family 11 member A
P35908	K22E_HUMAN	Keratin, type II cytoskeletal 2 epidermal
O14594	NCAN_HUMAN	Neurocan core protein
P20618	PSB1_HUMAN	Proteasome subunit beta type-1
P12956	XRCC6_HUMAN	X-ray repair cross-complementing protein 6
P60900	PSA6_HUMAN	Proteasome subunit alpha type-6
Q9NY33	DPP3_HUMAN	Dipeptidyl peptidase 3
P32119	PRDX2_HUMAN	Peroxiredoxin-2
P07339	CATD_HUMAN	Cathepsin D
P27348	1433T_HUMAN	14-3-3 protein theta
Q9HC38	GLOD4_HUMAN	Glyoxalase domain-containing protein 4
Q9NRN5	OLFL3_HUMAN	Olfactomedin-like protein 3
Q16531	DDB1_HUMAN	DNA damage-binding protein 1
P22392	NDKB_HUMAN	Nucleoside diphosphate kinase B
P07900	HS90A_HUMAN	Heat shock protein HSP 90-alpha
P17174	AATC_HUMAN	Aspartate aminotransferase, cytoplasmic

O15540	FABP7_HUMAN	Fatty acid-binding protein, brain
Q9BWD1	THIC_HUMAN	Acetyl-CoA acetyltransferase, cytosolic
P11766	ADHX_HUMAN	Alcohol dehydrogenase class-3
P10909	CLUS_HUMAN	Clusterin
O14818	PSA7_HUMAN	Proteasome subunit alpha type-7
O00410	IPO5_HUMAN	Importin-5
Q15907	RB11B_HUMAN	Ras-related protein Rab-11B
P30086	PEBP1_HUMAN	Phosphatidylethanolamine-binding protein 1
P28066	PSA5_HUMAN	Proteasome subunit alpha type-5
Q4ZHG4	FNDC1_HUMAN	Fibronectin type III domain-containing protein 1
Q13838	DX39B_HUMAN	Spliceosome RNA helicase DDX39B
P01034	CYTC_HUMAN	Cystatin-C
P12004	PCNA_HUMAN	Proliferating cell nuclear antigen
P12814	ACTN1_HUMAN	Alpha-actinin-1
P49721	PSB2_HUMAN	Proteasome subunit beta type-2
Q14019	COTL1_HUMAN	Coactosin-like protein
P26022	PTX3_HUMAN	Pentraxin-related protein PTX3
P49321	NASP_HUMAN	Nuclear autoantigenic sperm protein
P01033	TIMP1_HUMAN	Metalloproteinase inhibitor 1
Q14974	IMB1_HUMAN	Importin subunit beta-1
P04792	HSPB1_HUMAN	Heat shock protein beta-1
P02766	TTHY_HUMAN	Transthyretin
P06576	ATPB_HUMAN	ATP synthase subunit beta, mitochondrial
P09651	ROA1_HUMAN	Heterogeneous nuclear ribonucleoprotein A1
P18206	VINC_HUMAN	Vinculin
P07737	PROF1_HUMAN	Profilin-1
Q9BVA1	TBB2B_HUMAN	Tubulin beta-2B chain
P15144	AMPN_HUMAN	Aminopeptidase N
P14314	GLU2B_HUMAN	Glucosidase 2 subunit beta
P09382	LEG1_HUMAN	Galectin-1
O95965	ITGBL_HUMAN	Integrin beta-like protein 1
P25787	PSA2_HUMAN	Proteasome subunit alpha type-2
Q92820	GGH_HUMAN	Gamma-glutamyl hydrolase
O95336	6PGL_HUMAN	6-phosphogluconolactonase
P13010	XRCC5_HUMAN	X-ray repair cross-complementing protein 5
P60842	IF4A1_HUMAN	Eukaryotic initiation factor 4A-I
P08758	ANXA5_HUMAN	Annexin A5
P49419	AL7A1_HUMAN	Alpha-aminoadipic semialdehyde dehydrogenase
P05067	A4_HUMAN	Amyloid beta A4 protein
P35527	K1C9_HUMAN	Keratin, type I cytoskeletal 9
P23246	SFPQ_HUMAN	Splicing factor, proline- and glutamine-rich
P25789	PSA4_HUMAN	Proteasome subunit alpha type-4
P35579	MYH9_HUMAN	Myosin-9
P23526	SAHH_HUMAN	Adenosylhomocysteinase
Q76M96	CCD80_HUMAN	Coiled-coil domain-containing protein 80
P15121	ALDR_HUMAN	Aldose reductase
Q99879	H2B1M_HUMAN	Histone H2B type 1-M
P26641	EF1G_HUMAN	Elongation factor 1-gamma
P46821	MAP1B_HUMAN	Microtubule-associated protein 1B
P14324	FPPS_HUMAN	Farnesyl pyrophosphate synthase

P13667	PDIA4_HUMAN	Protein disulfide-isomerase A4
Q8NBS9	TXND5_HUMAN	Thioredoxin domain-containing protein 5
P23396	RS3_HUMAN	40S ribosomal protein S3
P62987	RL40_HUMAN	Ubiquitin-60S ribosomal protein L40
P07858	CATB_HUMAN	Cathepsin B
Q15019	SEPT2_HUMAN	Septin-2
P25786	PSA1_HUMAN	Proteasome subunit alpha type-1
P62805	H4_HUMAN	Histone H4
Q08629	TICN1_HUMAN	Testican-1
P61981	1433G_HUMAN	14-3-3 protein gamma
Q96CG8	CTHR1_HUMAN	Collagen triple helix repeat-containing protein 1
P84077	ARF1_HUMAN	ADP-ribosylation factor 1
Q01581	HMCS1_HUMAN	Hydroxymethylglutaryl-CoA synthase, cytoplasmic
P30044	PRDX5_HUMAN	Peroxiredoxin-5, mitochondrial
Q01469	FABP5_HUMAN	Fatty acid-binding protein, epidermal
Q9BRK3	MXRA8_HUMAN	Matrix-remodeling-associated protein 8
P39019	RS19_HUMAN	40S ribosomal protein S19
Q14103	HNRPD_HUMAN	Heterogeneous nuclear ribonucleoprotein D0
Q15631	TSN_HUMAN	Translin
Q15084	PDIA6_HUMAN	Protein disulfide-isomerase A6
P61769	B2MG_HUMAN	Beta-2-microglobulin
Q09028	RBBP4_HUMAN	Histone-binding protein RBBP4
O76061	STC2_HUMAN	Stanniocalcin-2
Q68BL8	OLM2B_HUMAN	Olfactomedin-like protein 2B
Q13509	TBB3_HUMAN	Tubulin beta-3 chain
P05155	IC1_HUMAN	Plasma protease C1 inhibitor
O00533	NCHL1_HUMAN	Neural cell adhesion molecule L1-like protein
P68036	UB2L3_HUMAN	Ubiquitin-conjugating enzyme E2 L3
P78371	TCPB_HUMAN	T-complex protein 1 subunit beta
O75368	SH3L1_HUMAN	SH3 domain-binding glutamic acid-rich-like protein
P02792	FRIL_HUMAN	Ferritin light chain
Q01518	CAP1_HUMAN	Adenylyl cyclase-associated protein 1
P11216	PYGB_HUMAN	Glycogen phosphorylase, brain form
Q13263	TIF1B_HUMAN	Transcription intermediary factor 1-beta
P49720	PSB3_HUMAN	Proteasome subunit beta type-3
Q04760	LGUL_HUMAN	Lactoylglutathione lyase
Q92743	HTRA1_HUMAN	Serine protease HTRA1
P52565	GDIR1_HUMAN	Rho GDP-dissociation inhibitor 1
P09493	TPM1_HUMAN	Tropomyosin alpha-1 chain
P62269	RS18_HUMAN	40S ribosomal protein S18
P35442	TSP2_HUMAN	Thrombospondin-2
P05388	RLA0_HUMAN	60S acidic ribosomal protein P0
P07686	HEXB_HUMAN	Beta-hexosaminidase subunit beta
P11047	LAMC1_HUMAN	Laminin subunit gamma-1
Q99832	TCPH_HUMAN	T-complex protein 1 subunit eta
P10155	RO60_HUMAN	60 kDa SS-A/Ro ribonucleoprotein
O00299	CLIC1_HUMAN	Chloride intracellular channel protein 1
Q15149	PLEC_HUMAN	Plectin
P43490	NAMPT_HUMAN	Nicotinamide phosphoribosyltransferase
P50990	TCPQ_HUMAN	T-complex protein 1 subunit theta

O75390	CISY_HUMAN	Citrate synthase, mitochondrial
P61604	CH10_HUMAN	10 kDa heat shock protein, mitochondrial
Q12765	SCRN1_HUMAN	Secernin-1
P14866	HNRPL_HUMAN	Heterogeneous nuclear ribonucleoprotein L
P62081	RS7_HUMAN	40S ribosomal protein S7
Q15181	IPYR_HUMAN	Inorganic pyrophosphatase
Q9Y490	TLN1_HUMAN	Talin-1
P60981	DEST_HUMAN	Destrin
P14550	AK1A1_HUMAN	Alcohol dehydrogenase [NADP(+)]
Q96QV6	H2A1A_HUMAN	Histone H2A type 1-A
P31946	1433B_HUMAN	14-3-3 protein beta/alpha
P50454	SERPH_HUMAN	Serpin H1
P16949	STMN1_HUMAN	Stathmin
P59998	ARPC4_HUMAN	Actin-related protein 2/3 complex subunit 4
P28072	PSB6_HUMAN	Proteasome subunit beta type-6
Q9UBR2	CATZ_HUMAN	Cathepsin Z
P40227	TCPZ_HUMAN	T-complex protein 1 subunit zeta
P25788	PSA3_HUMAN	Proteasome subunit alpha type-3
P00390	GSHR_HUMAN	Glutathione reductase, mitochondrial
P06865	HEXA_HUMAN	Beta-hexosaminidase subunit alpha
P62826	RAN_HUMAN	GTP-binding nuclear protein Ran
P61158	ARP3_HUMAN	Actin-related protein 3
P19338	NUCL_HUMAN	Nucleolin
P06396	GELS_HUMAN	Gelsolin
P13497	BMP1_HUMAN	Bone morphogenetic protein 1
P20700	LMNB1_HUMAN	Lamin-B1
P61088	UBE2N_HUMAN	Ubiquitin-conjugating enzyme E2 N
P30153	2AAA_HUMAN	Serine/threonine-protein phosphatase 2A 65 kDa regulatory subunit A alpha isoform
P02765	FETUA_HUMAN	Alpha-2-HS-glycoprotein
Q16851	UGPA_HUMAN	UTP–glucose-1-phosphate uridylyltransferase
P18065	IBP2_HUMAN	Insulin-like growth factor-binding protein 2
Q04917	1433F_HUMAN	14-3-3 protein eta
P08865	RSSA_HUMAN	40S ribosomal protein SA
P07910	HNRPC_HUMAN	Heterogeneous nuclear ribonucleoproteins C1/C2
Q13907	IDI1_HUMAN	Isopentenyl-diphosphate Delta-isomerase 1
P28838	AMPL_HUMAN	Cytosol aminopeptidase
P53396	ACLY_HUMAN	ATP-citrate synthase
P41222	PTGDS_HUMAN	Prostaglandin-H2 D-isomerase
Q9NVA2	SEP11_HUMAN	Septin-11
Q15691	MARE1_HUMAN	Microtubule-associated protein RP/EB family member 1
P07093	GDN_HUMAN	Glia-derived nexin
Q9UKK9	NUDT5_HUMAN	ADP-sugar pyrophosphatase
P00441	SODC_HUMAN	Superoxide dismutase [Cu-Zn]
Q9BRA2	TXD17_HUMAN	Thioredoxin domain-containing protein 17
P29279	CTGF_HUMAN	Connective tissue growth factor
P46926	GNPI1_HUMAN	Glucosamine-6-phosphate isomerase 1
P13693	TCTP_HUMAN	Translationally-controlled tumor protein
P05455	LA_HUMAN	Lupus La protein
O15067	PUR4_HUMAN	Phosphoribosylformylglycinamidine synthase
P22692	IBP4_HUMAN	Insulin-like growth factor-binding protein 4

Q14011	CIRBP_HUMAN	Cold-inducible RNA-binding protein
Q9Y4K0	LOXL2_HUMAN	Lysyl oxidase homolog 2
P13797	PLST_HUMAN	Plastin-3
P63241	IF5A1_HUMAN	Eukaryotic translation initiation factor 5A-1
Q13404	UB2V1_HUMAN	Ubiquitin-conjugating enzyme E2 variant 1
P63244	RACK1_HUMAN	Receptor of activated protein C kinase 1
P09960	LKHA4_HUMAN	Leukotriene A-4 hydrolase
P62701	RS4X_HUMAN	40S ribosomal protein S4, X isoform
P55060	XPO2_HUMAN	Exportin-2
Q12905	ILF2_HUMAN	Interleukin enhancer-binding factor 2
P30048	PRDX3_HUMAN	Thioredoxin-dependent peroxide reductase, mitochondrial
Q13228	SBP1_HUMAN	Selenium-binding protein 1
P84243	H33_HUMAN	Histone H3.3
P11586	C1TC_HUMAN	C-1-tetrahydrofolate synthase, cytoplasmic
P12955	PEPD_HUMAN	Xaa-Pro dipeptidase
P35241	RADI_HUMAN	Radixin
P04083	ANXA1_HUMAN	Annexin A1
P12081	SYHC_HUMAN	Histidine–tRNA ligase, cytoplasmic
P34897	GLYM_HUMAN	Serine hydroxymethyltransferase, mitochondrial
P60953	CDC42_HUMAN	Cell division control protein 42 homolog
P04217	A1BG_HUMAN	Alpha-1B-glycoprotein
P47756	CAPZB_HUMAN	F-actin-capping protein subunit beta
P54687	BCAT1_HUMAN	Branched-chain-amino-acid aminotransferase, cytosolic
Q15366	PCBP2_HUMAN	Poly(rC)-binding protein 2
P00491	PNPH_HUMAN	Purine nucleoside phosphorylase
P99999	CYC_HUMAN	Cytochrome c
O00154	BACH_HUMAN	Cytosolic acyl coenzyme A thioester hydrolase
P38159	RBMX_HUMAN	RNA-binding motif protein, X chromosome
P10599	THIO_HUMAN	Thioredoxin
P13798	ACPH_HUMAN	Acylamino-acid-releasing enzyme
Q15257	PTPA_HUMAN	Serine/threonine-protein phosphatase 2A activator
O43852	CALU_HUMAN	Calumenin
P15880	RS2_HUMAN	40S ribosomal protein S2
P37108	SRP14_HUMAN	Signal recognition particle 14 kDa protein
Q15417	CNN3_HUMAN	Calponin-3
P15531	NDKA_HUMAN	Nucleoside diphosphate kinase A
Q969H8	MYDGF_HUMAN	Myeloid-derived growth factor
P00367	DHE3_HUMAN	Glutamate dehydrogenase 1, mitochondrial
P78417	GSTO1_HUMAN	Glutathione S-transferase omega-1
P22234	PUR6_HUMAN	Multifunctional protein ADE2
Q99873	ANM1_HUMAN	Protein arginine N-methyltransferase 1
P68366	TBA4A_HUMAN	Tubulin alpha-4A chain
P33993	MCM7_HUMAN	DNA replication licensing factor MCM7
Q16643	DREB_HUMAN	Drebrin
O94760	DDAH1_HUMAN	N(G),N(G)-dimethylarginine dimethylaminohydrolase 1
P14174	MIF_HUMAN	Macrophage migration inhibitory factor
Q8NCW5	NNRE_HUMAN	NAD(P)H-hydrate epimerase
Q15102	PA1B3_HUMAN	Platelet-activating factor acetylhydrolase IB subunit gamma
Q9NTK5	OLA1_HUMAN	Obg-like ATPase 1
P07477	TRY1_HUMAN	Trypsin-1

P42574	CASP3_HUMAN	Caspase-3
P51858	HDGF_HUMAN	Hepatoma-derived growth factor
Q05682	CALD1_HUMAN	Caldesmon
P48637	GSHB_HUMAN	Glutathione synthetase
Q53FA7	QORX_HUMAN	Quinone oxidoreductase PIG3
P08133	ANXA6_HUMAN	Annexin A6
Q9UQ80	PA2G4_HUMAN	Proliferation-associated protein 2G4
P49368	TCPG_HUMAN	T-complex protein 1 subunit gamma
P68871	HBB_HUMAN	Hemoglobin subunit beta
P16403	H12_HUMAN	Histone H1.2
Q99436	PSB7_HUMAN	Proteasome subunit beta type-7
Q15365	PCBP1_HUMAN	Poly(rC)-binding protein 1
P15311	EZRI_HUMAN	Ezrin
P67936	TPM4_HUMAN	Tropomyosin alpha-4 chain
P17987	TCPA_HUMAN	T-complex protein 1 subunit alpha
Q8WX77	IBPL1_HUMAN	Insulin-like growth factor-binding protein-like 1
O95865	DDAH2_HUMAN	N(G),N(G)-dimethylarginine dimethylaminohydrolase 2
P15104	GLNA_HUMAN	Glutamine synthetase
P68371	TBB4B_HUMAN	Tubulin beta-4B chain
Q9UHD8	SEPT9_HUMAN	Septin-9
P29966	MARCS_HUMAN	Myristoylated alanine-rich C-kinase substrate
P46783	RS10_HUMAN	40S ribosomal protein S10
P67775	PP2AA_HUMAN	Serine/threonine-protein phosphatase 2A catalytic subunit alpha isoform
Q9H299	SH3L3_HUMAN	SH3 domain-binding glutamic acid-rich-like protein 3
P62942	FKB1A_HUMAN	Peptidyl-prolyl cis-trans isomerase FKBP1A
P43003	EAA1_HUMAN	Excitatory amino acid transporter 1
Q96A72	MGN2_HUMAN	Protein mago nashi homolog 2
P62244	RS15A_HUMAN	40S ribosomal protein S15a
P13489	RINI_HUMAN	Ribonuclease inhibitor
Q9BUT1	BDH2_HUMAN	3-hydroxybutyrate dehydrogenase type 2
O14531	DPYL4_HUMAN	Dihydropyrimidinase-related protein 4
P49458	SRP09_HUMAN	Signal recognition particle 9 kDa protein
P68402	PA1B2_HUMAN	Platelet-activating factor acetylhydrolase IB subunit beta
P41250	SYG_HUMAN	Glycine–tRNA ligase
P62851	RS25_HUMAN	40S ribosomal protein S25
P31948	STIP1_HUMAN	Stress-induced-phosphoprotein 1
P07108	ACBP_HUMAN	Acyl-CoA-binding protein
P60660	MYL6_HUMAN	Myosin light polypeptide 6
O00468	AGRIN_HUMAN	Agrin
Q9Y266	NUDC_HUMAN	Nuclear migration protein nudC
P28065	PSB9_HUMAN	Proteasome subunit beta type-9
Q9Y281	COF2_HUMAN	Cofilin-2
P35268	RL22_HUMAN	60S ribosomal protein L22
Q92688	AN32B_HUMAN	Acidic leucine-rich nuclear phosphoprotein 32 family member B
P48643	TCPE_HUMAN	T-complex protein 1 subunit epsilon
P62906	RL10A_HUMAN	60S ribosomal protein L10a
P11940	PABP1_HUMAN	Polyadenylate-binding protein 1
O43776	SYNC_HUMAN	Asparagine–tRNA ligase, cytoplasmic
P18085	ARF4_HUMAN	ADP-ribosylation factor 4
P78330	SERB_HUMAN	Phosphoserine phosphatase

Q06323	PSME1_HUMAN	Proteasome activator complex subunit 1
P54578	UBP14_HUMAN	Ubiquitin carboxyl-terminal hydrolase 14
P31153	METK2_HUMAN	S-adenosylmethionine synthase isoform type-2
P23919	KTHY_HUMAN	Thymidylate kinase
O15511	ARPC5_HUMAN	Actin-related protein 2/3 complex subunit 5
P02771	FETA_HUMAN	Alpha-fetoprotein
Q14847	LASP1_HUMAN	LIM and SH3 domain protein 1
P33316	DUT_HUMAN	Deoxyuridine 5'-triphosphate nucleotidohydrolase, mitochondrial
Q13162	PRDX4_HUMAN	Peroxiredoxin-4
P61457	PHS_HUMAN	Pterin-4-alpha-carbinolamine dehydratase
O00231	PSD11_HUMAN	26S proteasome non-ATPase regulatory subunit 11
Q16181	SEPT7_HUMAN	Septin-7
Q9NPH2	INO1_HUMAN	Inositol-3-phosphate synthase 1
Q9UHY7	ENOPH_HUMAN	Enolase-phosphatase E1
Q16778	H2B2E_HUMAN	Histone H2B type 2-E
Q9HAV0	GBB4_HUMAN	Guanine nucleotide-binding protein subunit beta-4
O15144	ARPC2_HUMAN	Actin-related protein 2/3 complex subunit 2
Q14914	PTGR1_HUMAN	Prostaglandin reductase 1
P63279	UBC9_HUMAN	SUMO-conjugating enzyme UBC9
O14979	HNRDL_HUMAN	Heterogeneous nuclear ribonucleoprotein D-like
P61247	RS3A_HUMAN	40S ribosomal protein S3a
Q9UNN8	EPCR_HUMAN	Endothelial protein C receptor
Q96FW1	OTUB1_HUMAN	Ubiquitin thioesterase OTUB1
P27824	CALX_HUMAN	Calnexin
Q86VP6	CAND1_HUMAN	Cullin-associated NEDD8-dissociated protein 1
P35637	FUS_HUMAN	RNA-binding protein FUS
O43175	SERA_HUMAN	D-3-phosphoglycerate dehydrogenase
P28300	LYOX_HUMAN	Protein-lysine 6-oxidase
Q9Y547	IFT25_HUMAN	Intraflagellar transport protein 25 homolog
Q9H0R4	HDHD2_HUMAN	Haloacid dehalogenase-like hydrolase domain-containing protein 2
P28482	MK01_HUMAN	Mitogen-activated protein kinase 1
P16070	CD44_HUMAN	CD44 antigen
P27816	MAP4_HUMAN	Microtubule-associated protein 4
Q13885	TBB2A_HUMAN	Tubulin beta-2A chain
P62140	PP1B_HUMAN	Serine/threonine-protein phosphatase PP1-beta catalytic subunit
P53618	COPB_HUMAN	Coatomer subunit beta
Q9NZL9	MAT2B_HUMAN	Methionine adenosyltransferase 2 subunit beta
P04004	VTNC_HUMAN	Vitronectin
Q9UL46	PSME2_HUMAN	Proteasome activator complex subunit 2
Q9GZT8	NIF3L_HUMAN	NIF3-like protein 1
Q6EEV6	SUMO4_HUMAN	Small ubiquitin-related modifier 4
Q15293	RCN1_HUMAN	Reticulocalbin-1
P62917	RL8_HUMAN	60S ribosomal protein L8
P52888	THOP1_HUMAN	Thimet oligopeptidase
P28799	GRN_HUMAN	Granulins
P62318	SMD3_HUMAN	Small nuclear ribonucleoprotein Sm D3
P01308	INS_HUMAN	Insulin
P18621	RL17_HUMAN	60S ribosomal protein L17
P68032	ACTC_HUMAN	Actin, alpha cardiac muscle 1
Q99523	SORT_HUMAN	Sortilin

Q15819	UB2V2_HUMAN	Ubiquitin-conjugating enzyme E2 variant 2
O43809	CPSF5_HUMAN	Cleavage and polyadenylation specificity factor subunit 5
Q96G03	PGM2_HUMAN	Phosphoglucomutase-2
O76003	GLRX3_HUMAN	Glutaredoxin-3
Q9Y3B8	ORN_HUMAN	Oligoribonuclease, mitochondrial
Q7KZF4	SND1_HUMAN	Staphylococcal nuclease domain-containing protein 1
P35555	FBN1_HUMAN	Fibrillin-1
P14543	NID1_HUMAN	Nidogen-1
Q07954	LRP1_HUMAN	Prolow-density lipoprotein receptor-related protein 1
O14786	NRP1_HUMAN	Neuropilin-1
P03956	MMP1_HUMAN	Interstitial collagenase
P00736	C1R_HUMAN	Complement C1r subcomponent
Q9HCU0	CD248_HUMAN	Endosialin
Q02388	CO7A1_HUMAN	Collagen alpha-1(VII) chain
Q13740	CD166_HUMAN	CD166 antigen
O43854	EDIL3_HUMAN	EGF-like repeat and discoidin I-like domain-containing protein 3
P28070	PSB4_HUMAN	Proteasome subunit beta type-4
Q8IUX7	AEBP1_HUMAN	Adipocyte enhancer-binding protein 1
Q9UBX5	FBLN5_HUMAN	Fibulin-5
P55287	CAD11_HUMAN	Cadherin-11
Q14112	NID2_HUMAN	Nidogen-2
Q96GW7	PGCB_HUMAN	Brevican core protein
P04179	SODM_HUMAN	Superoxide dismutase [Mn], mitochondrial
P61163	ACTZ_HUMAN	Alpha-centractin
Q92626	PXDN_HUMAN	Peroxidasin homolog
Q9BUD6	SPON2_HUMAN	Spondin-2
P19823	ITIH2_HUMAN	Inter-alpha-trypsin inhibitor heavy chain H2
Q7Z7M9	GALT5_HUMAN	Polypeptide N-acetylgalactosaminyltransferase 5
P31949	S10AB_HUMAN	Protein S100-A11
P19105	ML12A_HUMAN	Myosin regulatory light chain 12A
P19367	HXK1_HUMAN	Hexokinase-1
P26599	PTBP1_HUMAN	Polypyrimidine tract-binding protein 1
P62249	RS16_HUMAN	40S ribosomal protein S16
Q01105	SET_HUMAN	Protein SET
P36222	CH3L1_HUMAN	Chitinase-3-like protein 1
Q13813	SPTN1_HUMAN	Spectrin alpha chain, non-erythrocytic 1
Q6EMK4	VASN_HUMAN	Vasorin
Q9UBG0	MRC2_HUMAN	C-type mannose receptor 2
P02794	FRIH_HUMAN	Ferritin heavy chain
Q07020	RL18_HUMAN	60S ribosomal protein L18
O14498	ISLR_HUMAN	Immunoglobulin superfamily containing leucine-rich repeat protein
P78539	SRPX_HUMAN	Sushi repeat-containing protein SRPX
Q15233	NONO_HUMAN	Non-POU domain-containing octamer-binding protein
P51149	RAB7A_HUMAN	Ras-related protein Rab-7a
P62820	RAB1A_HUMAN	Ras-related protein Rab-1A
P10768	ESTD_HUMAN	S-formylglutathione hydrolase
O60506	HNRPQ_HUMAN	Heterogeneous nuclear ribonucleoprotein Q
P30050	RL12_HUMAN	60S ribosomal protein L12
Q96AE4	FUBP1_HUMAN	Far upstream element-binding protein 1
P35080	PROF2_HUMAN	Profilin-2

P02462	CO4A1_HUMAN	Collagen alpha-1(IV) chain
O14980	XPO1_HUMAN	Exportin-1
Q9Y696	CLIC4_HUMAN	Chloride intracellular channel protein 4
O75223	GGCT_HUMAN	Gamma-glutamylcyclotransferase
P31943	HNRH1_HUMAN	Heterogeneous nuclear ribonucleoprotein H
Q07812	BAX_HUMAN	Apoptosis regulator BAX
P28161	GSTM2_HUMAN	Glutathione S-transferase Mu 2
Q92734	TFG_HUMAN	Protein TFG
P07954	FUMH_HUMAN	Fumarate hydratase, mitochondrial
Q29963	1C06_HUMAN	HLA class I histocompatibility antigen, Cw-6 alpha chain
Q9ULV4	COR1C_HUMAN	Coronin-1C
P00568	KAD1_HUMAN	Adenylate kinase isoenzyme 1
P46108	CRK_HUMAN	Adapter molecule crk
P61586	RHOA_HUMAN	Transforming protein RhoA
P62241	RS8_HUMAN	40S ribosomal protein S8
P43121	MUC18_HUMAN	Cell surface glycoprotein MUC18
P26639	SYTC_HUMAN	Threonine–tRNA ligase, cytoplasmic
P50991	TCPD_HUMAN	T-complex protein 1 subunit delta
Q13151	ROA0_HUMAN	Heterogeneous nuclear ribonucleoprotein A0
P62857	RS28_HUMAN	40S ribosomal protein S28
Q15121	PEA15_HUMAN	Astrocytic phosphoprotein PEA-15
P43487	RANG_HUMAN	Ran-specific GTPase-activating protein
O75531	BAF_HUMAN	Barrier-to-autointegration factor
O60888	CUTA_HUMAN	Protein CutA
P42765	THIM_HUMAN	3-ketoacyl-CoA thiolase, mitochondrial
P55263	ADK_HUMAN	Adenosine kinase
P61353	RL27_HUMAN	60S ribosomal protein L27
Q86Y38	XYLT1_HUMAN	Xylosyltransferase 1
P06703	S10A6_HUMAN	Protein S100-A6
O75882	ATRN_HUMAN	Attractin
P01008	ANT3_HUMAN	Antithrombin-III
P48681	NEST_HUMAN	Nestin
P26373	RL13_HUMAN	60S ribosomal protein L13
P50281	MMP14_HUMAN	Matrix metalloproteinase-14
O60462	NRP2_HUMAN	Neuropilin-2
Q6NVV1	R13P3_HUMAN	Putative 60S ribosomal protein L13a protein RPL13AP3
O75367	H2AY_HUMAN	Core histone macro-H2A.1
P55001	MFAP2_HUMAN	Microfibrillar-associated protein 2
P53004	BIEA_HUMAN	Biliverdin reductase A
Q07092	COGA1_HUMAN	Collagen alpha-1(XVI) chain
P49589	SYCC_HUMAN	Cysteine–tRNA ligase, cytoplasmic
Q07666	KHDR1_HUMAN	KH domain-containing, RNA-binding, signal transduction-associated protein 1
Q14764	MVP_HUMAN	Major vault protein
P62854	RS26_HUMAN	40S ribosomal protein S26
P62277	RS13_HUMAN	40S ribosomal protein S13
P43034	LIS1_HUMAN	Platelet-activating factor acetylhydrolase IB subunit alpha
P62304	RUXE_HUMAN	Small nuclear ribonucleoprotein E
P16401	H15_HUMAN	Histone H1.5
P42126	ECI1_HUMAN	Enoyl-CoA delta isomerase 1, mitochondrial
P18124	RL7_HUMAN	60S ribosomal protein L7

P30530	UFO_HUMAN	Tyrosine-protein kinase receptor UFO
Q9UBP4	DKK3_HUMAN	Dickkopf-related protein 3
P10253	LYAG_HUMAN	Lysosomal alpha-glucosidase
P55083	MFAP4_HUMAN	Microfibril-associated glycoprotein 4
Q9UNM6	PSD13_HUMAN	26S proteasome non-ATPase regulatory subunit 13
Q00839	HNRPU_HUMAN	Heterogeneous nuclear ribonucleoprotein U
P16930	FAAA_HUMAN	Fumarylacetoacetase
Q99426	TBCB_HUMAN	Tubulin-folding cofactor B
P02788	TRFL_HUMAN	Lactotransferrin
P52597	HNRPF_HUMAN	Heterogeneous nuclear ribonucleoprotein F
Q00688	FKBP3_HUMAN	Peptidyl-prolyl cis-trans isomerase FKBP3
P42785	PCP_HUMAN	Lysosomal Pro-X carboxypeptidase
Q14315	FLNC_HUMAN	Filamin-C
Q15717	ELAV1_HUMAN	ELAV-like protein 1
P53602	MVD1_HUMAN	Diphosphomevalonate decarboxylase
Q99729	ROAA_HUMAN	Heterogeneous nuclear ribonucleoprotein A/B
P56537	IF6_HUMAN	Eukaryotic translation initiation factor 6
O00469	PLOD2_HUMAN	Procollagen-lysine,2-oxoglutarate 5-dioxygenase 2
Q15436	SC23A_HUMAN	Protein transport protein Sec23A
P98179	RBM3_HUMAN	RNA-binding protein 3
P69905	HBA_HUMAN	Hemoglobin subunit alpha
Q9NR12	PDLI7_HUMAN	PDZ and LIM domain protein 7
Q14566	MCM6_HUMAN	DNA replication licensing factor MCM6
P32969	RL9_HUMAN	60S ribosomal protein L9
P02774	VTDB_HUMAN	Vitamin D-binding protein
P01344	IGF2_HUMAN	Insulin-like growth factor II
P02753	RET4_HUMAN	Retinol-binding protein 4
P06748	NPM_HUMAN	Nucleophosmin
P29218	IMPA1_HUMAN	Inositol monophosphatase 1
Q9BZM5	N2DL2_HUMAN	NKG2D ligand 2
O00487	PSDE_HUMAN	26S proteasome non-ATPase regulatory subunit 14
P06493	CDK1_HUMAN	Cyclin-dependent kinase 1
P62753	RS6_HUMAN	40S ribosomal protein S6
P05386	RLA1_HUMAN	60S acidic ribosomal protein P1
P09341	GROA_HUMAN	Growth-regulated alpha protein
Q9UMY4	SNX12_HUMAN	Sorting nexin-12
P62829	RL23_HUMAN	60S ribosomal protein L23
P62314	SMD1_HUMAN	Small nuclear ribonucleoprotein Sm D1
P67809	YBOX1_HUMAN	Nuclease-sensitive element-binding protein 1
Q6YP21	KAT3_HUMAN	Kynurenine–oxoglutarate transaminase 3
P42766	RL35_HUMAN	60S ribosomal protein L35
P09874	PARP1_HUMAN	Poly [ADP-ribose] polymerase 1
Q9NR31	SAR1A_HUMAN	GTP-binding protein SAR1a
Q9Y5S9	RBM8A_HUMAN	RNA-binding protein 8A
P16152	CBR1_HUMAN	Carbonyl reductase [NADPH] 1

Table S2. List of proteins identified in the hMSCs secretome

Entry	Entry name	Protein Name_UNIPROT recommended
P35555	FBN1_HUMAN	Fibrillin 1
O14672	ADA10_HUMAN	Disintegrin and metalloproteinase domain-containg protein 10
P19652	A1AG2_HUMAN	Alpha-1-acid glycoprotein 2
P15291	B4GT1_HUMAN	Beta-1,4-galactosyltransferase 1
O60869	EDF1_HUMAN	Endothelial differentiation-related factor 1
Q7Z7G0	TARSH_HUMAN	Target of Nesh-SH3
P05556	ITB1_HUMAN	Integrin beta-1
P07602	SAP_HUMAN	Prosaposin
P07942	LAMB1_HUMAN	Laminin subunit beta-1
P17936	IBP3_HUMAN	Insulin-like growth factor-binding protein 3
P69905	HBA_HUMAN	Hemoglobin subunit alpha
Q8NBJ4	GOLM1_HUMAN	Golgi membrane protein 1
P58397	ATS12_HUMAN	A desintegrin and metalloproteinase with thrombospondin motifs 12
P43681	ACHA4_HUMAN	Neuronal acetylcholine receptor subunit alfa-4
A1L4H1	SRCRL_HUMAN	Soluble scavenger receptor cysteines-rich domain-containing protein SSC5D
P55001	MFAP2_HUMAN	Microfibrillar-associated protein 2
O00244	ATOX1_HUMAN	Copper transport protein ATOX1
P02749	APOH_HUMAN	Beta-2-glycoprotein 1
O60687	SRPX2_HUMAN	Sushi repeat-containing protein SRPX2
P27658	CO8A1_HUMAN	Collagen alpha-1 (VIII) chain
Q92626	PXDN_HUMAN	Peroxidasin homolog
Q08431	MFGM_HUMAN	Lactadherin
Q9H3R0	KDM4C_HUMAN	Lysine-specific demethylase 4C
P61916	NPC2_HUMAN	Epididymal secretor protein E1
Q9Y6C2	EMIL1_HUMAN	Emilin-1
O75821	EIF3G_HUMAN	Eukaryotic translation initiation factor 3 subunit G
Q07507	DERM_HUMAN	Dermatopontin
P30040	ERP29_HUMAN	Endoplasmatic reticulum residente protein 29
Q07954	LRP1_HUMAN	Prolow-density lipoprotein
Q12884	SEPR_HUMAN	Prolyl endopeptidase FAP
P02763	A1AG1_HUMAN	Alpha-1-acid glycoprotein 1
O00622	CYR61_HUMAN	Protein CYR61
O95967	FBLN4_HUMAN	EGF-containing fibulin-like extracelular matrix protein 2
Q9BTY2	FUCO2_HUMAN	Plasma alfa-L-fucosidase
P17050	NAGAB_HUMAN	Alpha-N-acetylgalactosaminidase
Q6YHK3	CD109_HUMAN	CD109 antigen
Q6UVK1	CSPG4_HUMAN	Chondroitin sulfate proteoglycan 4
P02647	APOA1_HUMAN	Apolipoprotein A-I
Q06481	APLP2_HUMAN	Amyloid-like protein 2
Q9Y2B0	CNPY2_HUMAN	Protein canopy homolog 2
P43251	BTD_HUMAN	Biotinidase
Q10471	GALT2_HUMAN	Polypeptide N-acetylgalactosaminyltransferase 2
Q96S86	HPLN3_HUMAN	Hyaluronan and proteoglycan link protein 3
Q02818	NUCB1_HUMAN	Nucleobindin-1
O14950	ML12B_HUMAN	Myosin regulatory Light chain 12B
P39060	COIA1_HUMAN	Collagen alpha-1 (XVIII) chain
P26885	FKBP2_HUMAN	Peptidyl-prolyl cis-trans isomerase FKBP2
Q13162	PRDX4_HUMAN	Peroxiredoxin-4

99

Entry	Entry name	Protein Name_UNIPROT recommended
P48444	COPD_HUMAN	Coatomer subunit delta
O14817	TSN4_HUMAN	Tetraspanin-4
P56537	IF6_HUMAN	Eukaryotic translation initiation factor 6
P22413	ENPP1_HUMAN	Ectonucleotoide pyrophosphatase/phosphodiesterase family member 1
O00462	MANBA_HUMAN	Beta-mannosidase
P07711	CATL1_HUMAN	Cathepsin L1
O60565	GREM1_HUMAN	Gremlin-1
P45877	PPIC_HUMAN	Peptidyl-prolyl cis-trans isomerase C
P33908	MA1A1_HUMAN	Mannosyl-oligosaccharide 1,2-alpha-mannosidase IA
Q9BRF8	CPPED_HUMAN	Serine/threonine-protein phosphatase CPPED1

Table S3. List of proteins identified in the hNPCs secretome

Entry	Entry name	Protein Name_UNIPROT recommended
P41219	PERI_HUMAN	Peripherin
P30464	1B15_HUMAN	HLA class I histocompatibility antigen, B-15 alpha chain
Q99536	VAT1_HUMAN	Synaptic vesicle membrane protein VAT-1 homolog
Q86XF0	DYRL1_HUMAN	Dihydrofolate reductase, mitochondrial
P21695	GPDA_HUMAN	Glycerol-3-phosphate dehydrogenase [NAD(+)], cytoplasmatic
Q6GMV3	PTRD1_HUMAN	Putative peptidyl-tRNA hydrolase PTRHD1
P30685	1B35_HUMAN	HLA class I histocompatibility antigen, B-35 alpha chain
P30495	1B56_HUMAN	HLA class I histocompatibility antigen, B-56 alpha chain
P30484	1B46_HUMAN	HLA class I histocompatibility antigen, B-46 alpha chain
Q29960	1C16_HUMAN	HLA class I histocompatibility antigen, Cw-16 alpha chain
P30498	1B78_HUMAN	HLA class I histocompatibility antigen, B-78 alpha chain
P35749	MYH11_HUMAN	Myosin-11
A6NCE7	MP3B2_HUMAN	Microtubule-associated proteins 1A/1B light chain 3 beta 2
P05231	IL6_HUMAN	Interleukin-6
Q13630	FCL_HUMAN	GDP-L-fucose synthase
P0CG48	UBC_HUMAN	Polyubiquitin-C
P30492	1B54_HUMAN	HLA class I histocompatibility antigen, B-54 alpha chain
P60709	ACTB_HUMAN	Actin, cytoplasmic 1
P60983	GMFB_HUMAN	Glia maturation factor beta
P00374	DYR_HUMAN	Dihydrofolate reductase
Q15843	NEDD8_HUMAN	NEDD8
Q9H492	MLP3A_HUMAN	Microtubule-associated proteins 1A/1B light chain 3A
P30493	1B55_HUMAN	HLA class I histocompatibility antigen, B-55 alpha chain
P61758	PFD3_HUMAN	Prefoldin
P18465	1B57_HUMAN	HLA class I histocompatibility antigen, B-57 alpha chain
Q9GZQ8	MLP3B_HUMAN	Microtubule-associated proteins 1A/1B light chain 3B
Q9Y3C6	PPIL1_HUMAN	Peptidyl-prolyl cis-trans isomerase-like 1
P52758	UK114_HUMAN	Ribonuclease UK114
Q6S8J3	POTEE_HUMAN	Pote ankyrin domain family member E
Q9UNZ2	NSF1C_HUMAN	NSFL1 cofactor p47
Q15185	TEBP_HUMAN	Prostaglandin E synthase 3
P28062	PSB8_HUMAN	Proteasome subunit beta type-8
P10319	1B58_HUMAN	HLA class I histocompatibility antigen, B-58 alpha chain
P30490	1B52_HUMAN	HLA class I histocompatibility antigen, B-52 alpha chain
Q04837	SSBP_HUMAN	Single-stranded DNA-binding protein, mitochondrial
P18464	1B51_HUMAN	HLA class I histocompatibility antigen, B-51 alpha chain

P30491	1B53_HUMAN	HLA class I histocompatibility antigen, B-53 alpha chain
P63010	AP2B1_HUMAN	AP-2 complex subunit beta
O43242	PSMD3_HUMAN	26S proteasome non-ATPase regulatory subunit 3
P06753	TPM3_HUMAN	Tropomyosin alpha-3 chain
Q29940	1B59_HUMAN	HLA class I histocompatibility antigen, B-59 alpha chain